NTNU
Norwegian University of
Science and Technology

Synthesis of building blocks for (*S*)-pindolol and vitamin K_2 by use of lipase catalysis

Sigrid Sløgedal Løvland

Chemistry
Submission date: August 2018
Supervisor: Elisabeth Egholm Jacobsen, IKJ

Norwegian University of Science and Technology
Department of Chemistry

Preface

This thesis has been composed at the Department of Chemistry at the Norwegian University of Science and Technology in Trondheim. The project has lasted from August 2016 until August 2018 and has been supervised by associate professor Elisabeth Egholm Jacobsen. The thesis is part of my education in the Master of Science in Chemistry program.

Most importantly, I would like to thank my supervisor, Associate Professor Elisabeth Egholm Jacobsen, for advice, helpful discussions and for the supportive atmosphere that she creates in our research group.

I would also like to thank PhD candidate Fredrik Heen Blindheim for help on analyses and for motivation. Further, I wish to thank everyone that has worked with me in the lab and in our research group. Thank you for the encouragement, the advice, the scientific discussions and for always keeping my spirits up.

Also, my gratitude goes out to Staff Engineer Roger Aarvik for always providing equipment and chemicals, to Senior Engineer Susana Villa Gonzalez for help and training in different MS analyses, to Senior Engineer Julie Aasmussen for help and training in GC and HPLC analysis and to Senior Engineer Torun Melø for help and training in NMR analysis.

Lastly, I wish to thank my friends and family for continuous support and encouragement. A big thanks to the residents of Gården for making home a fun place to be these last years. Tarjei Nesbø Skreien deserves a special thanks, for always listening to me, supporting me and for helping me organize my thoughts so that I found feasible solutions to unmanageable problems. Thank you.

Abstract

The objective of this thesis has been to synthesize an enantiopure building block of β-blocker (*S*)-pindolol. This has been attempted by organic synthesis followed by lipase catalysis using *candida antarctica* lipase B (CALB) in kinetic resolutions. Experiments have also been performed concerning the biocatalytic hydrolysis of **9**, a possible precursor in the synthesis of vitamin K_2.

In the synthesis of 1-((1H-indol-4-yl)oxy)-3-chloropropan-2-ol (**5**) and by-product 4-(oxiran-2-ylmethoxy)-1H-indole (**4**) from starting material 1H-indol-4-ol (**3**) (Scheme 1) a yield of 52% was achieved. It was also found that by extracting with dichloromethane and washing with both water and ethyl acetate simultaneously, a high degree of purity for the products was achieved.

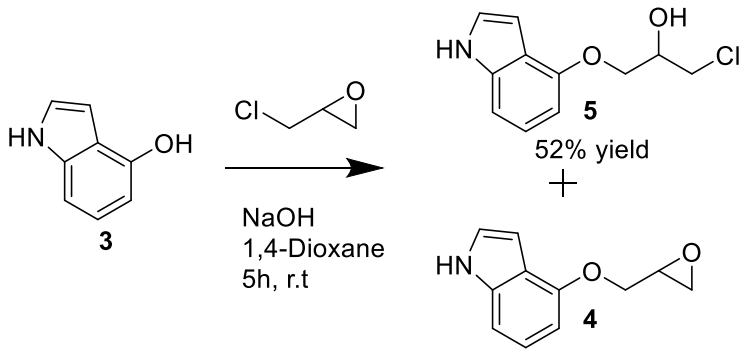

Scheme 1: Synthesis of 1-((1H-indol-4-yl)oxy)-3-chloropropan-2-ol (**5**) and by-product 4-(oxiran-2-ylmethoxy)-1H-indole (**4**) from 1H-indol-4-ol (**3**)

In order to increase the yield of **5**, by-product **4** was reacted with LiCl and acetic acid (Scheme 2) giving an overall yield of 59% after two steps.

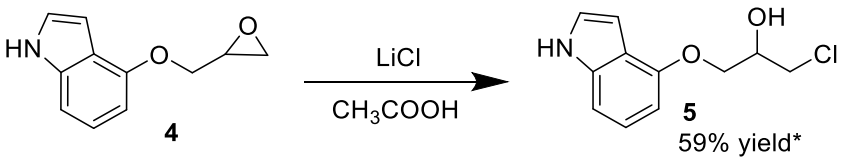

*calculated over two synthesis steps

Scheme 2: Opening of epoxide on 4-(oxiran-2-ylmethoxy)-1H-indole (**4**) forming 1-((1H-indol-4-yl)oxy)-3-chloropropan-2-ol (**5**), using LiCl in acetic acid.

In the kinetic resolution of **5** using CALB in acylation (Scheme 3) an E-value of 66 was achieved, and at 53% conversion ee_s and ee_p values were at 92% and 81% respectively. However, these results are uncertain because the enantiomers of product **6** were not successfully separated in chiral HPLC, resulting in incorrect integration of peaks in HPLC chromatograms.

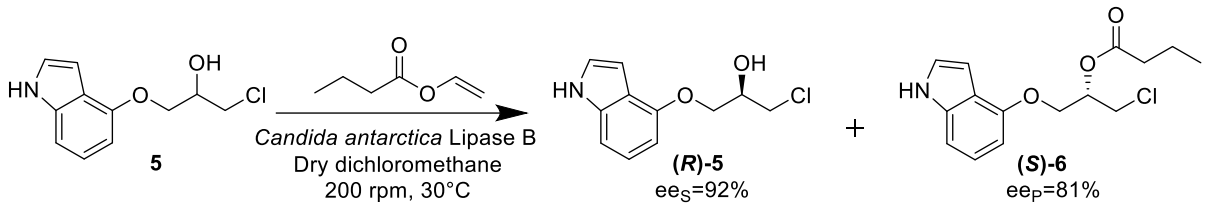

Scheme 3: Kinetic resolution of **5** forming **(*S*)-6** and **(*R*)-5** using CALB and vinyl butyrate in dry dichloromethane.

The hydrolysis of **9** using different co-solvents and enzymes was attempted. None of the reactions performed resulted in the formation of the expected products **10**, **11** and **12** (Scheme 4).

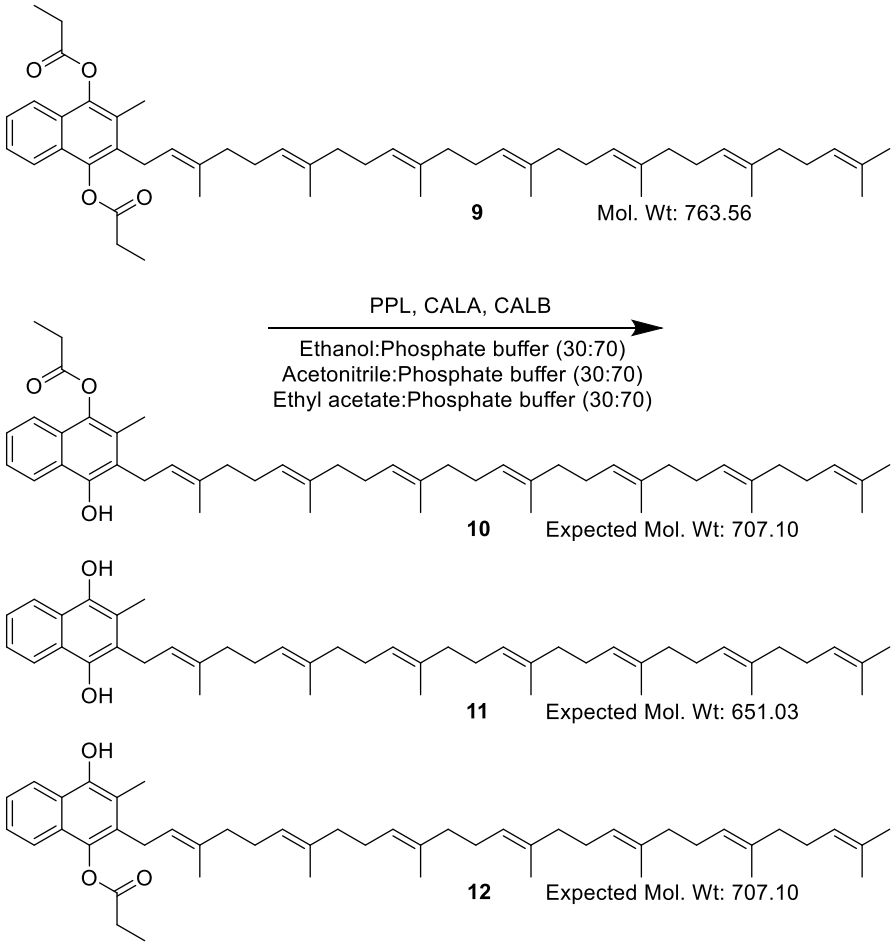

Scheme 4: Enzymes and solvent systems tested in the hydrolysis of **9** with the possible products **10**, **11** and **12**.

In the attempted hydrolysis of **9** using CALB and ethyl acetate as co-solvent, colourless crystals were produced. MS analysis of the crystals showed a mass of 663 g/mol, which did not fit with any of the expected products. Solubility test of the crystals have been performed, and the crystals were found to dissolve in water. However, NMR analysis of the crystals using D_2O as solvent gave no proton or carbon peaks in ^{1}H and ^{13}C analysis.

Sammendrag

Målet med denne masteroppgaven har vært å syntetisere en enantiomert ren byggestein for beta-blokker (*S*)-pindolol. Dette har blitt forsøkt ved organisk syntese fulgt av lipase katalyse med *candida antarctica* lipase B (CALB) i kinetiske oppløsninger. Det har også blitt gjort undersøkelser rundt biokatalytisk hydrolyse av **9**, et mulig forprodukt i syntesen av vitamin K_2.

Syntesen av 1-((1H-indol-4-yl)oksy)-3-kloropropan-2-ol (**5**) og biproduktet 4-(oksiran-2-ylmetoksi)-1H-indol (**4**) fra startmaterialet 1H-indol-4-ol (**3**) (Skjema 1) gav et utbytte på 52%. Det ble også oppnådd høy grad av renhet i produktene ved å ekstrahere med diklormetan og vaske med både vann og etylacetat samtidig.

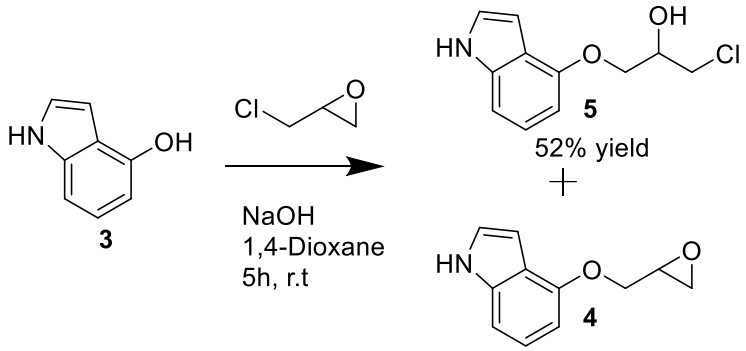

Skjema 1: Syntese av 1-((1H-indol-4-yl)oksy)-3-kloropropan-2-ol (**5**) and by-product 4-(oksiran-2-ylmetoksi)-1H-indole (**4**) fra 1H-Indol-4-ol (**3**).

For å øke utbyttet av **5** ble biproduktet **4** reagert med LiCL og eddiksyre (Skjema 2). Dette gav et totalt utbytte på 59% etter to syntesesteg.

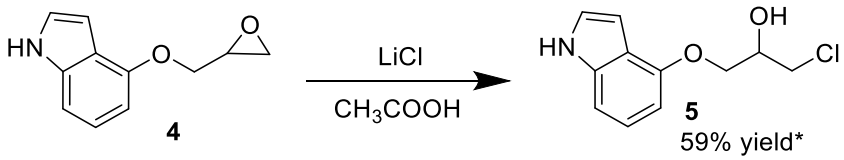

*calculated over two synthesis steps

Skjema 2: Åpning av epoksid på 4-(oksiran-2-ylmetoksi)-1H-indole (**4**) ved bruk av AcOH og LiCL, som resulterte i produktet 1-((1H-indol-4-yl)oksy)-3-kloropropan-2-ol (**5**).

Kinetisk oppløsning av **5** med CALB i acylering (Skjema 3) resulterte i en E-verdi på 66. Ved 53% konversjon ble ee_s og ee_p verdier på henholdsvis 92% og 81% oppnådd. Disse

resultatene er unøyaktige fordi enantiomerene av produktet **6** ikke ble separert på kolonne ved kiral-HPLC analyse. Dette førte til feil i integreringen av toppene, som igjen gir usikkerhet i resultatene.

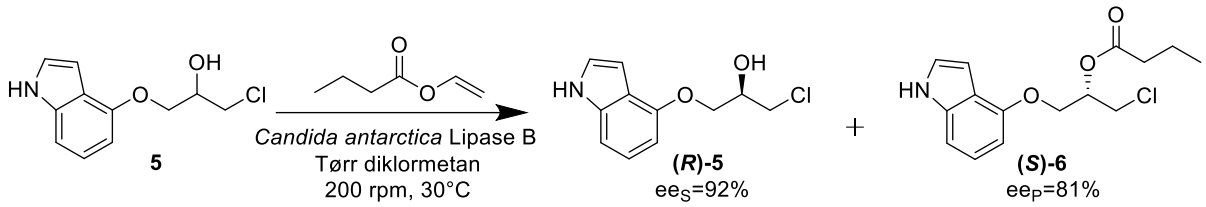

Skjema 3: Kinetisk oppløsning av **5** som resulterte i **(*S*)-6** og **(*R*)-5**, ved bruk av CALB og vinyl butyrat som acyldonor i tørr diklormetan.

I hydrolysen av **9** ble forskjellige ko-solventer testet sammen med forskjellige lipaser. Ingen av reaksjonene resulterte i de forventede produktene **10**, **11** og **12** (Skjema 4).

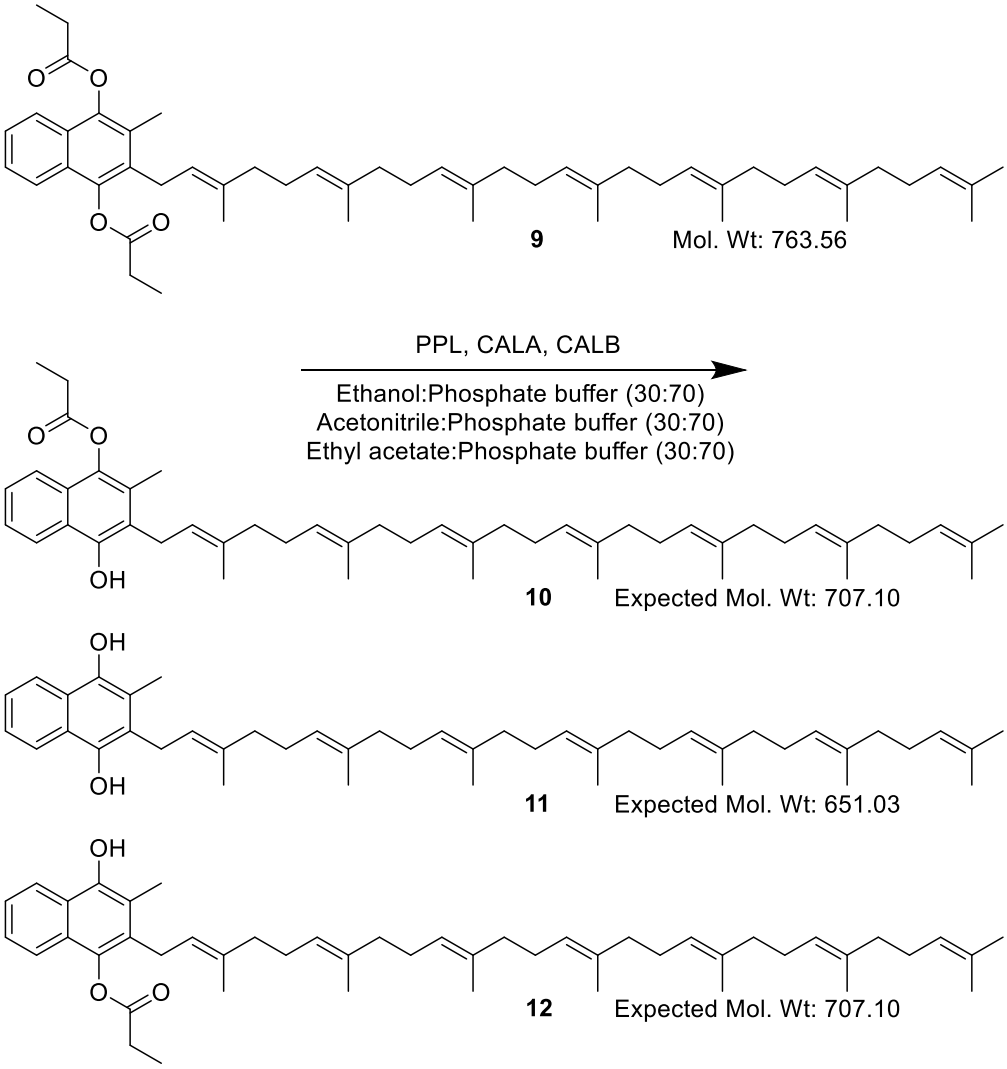

Skjema 4: Enzymer og solventblandinger testet i hydrolysen av **9**, sammen med forventede produkter **10**, **11** og **12**.

I forsøkte hydrolyser av **9** der CALB ble brukt sammen med etylacetat som ko-solvent ble fargeløse krystaller produsert. MS analyse av krystallene gav en masse på 663 g/mol, som ikke stemmer overens med noen av de forventede produktene. Løselighetstester av krystallene ble utført, og det ble funnet at krystallene løste seg i vann. NMR med D_2O som solvent ble forsøkt, men både proton- og karbonspekter viste ingen signaler.

Compounds featured in this thesis

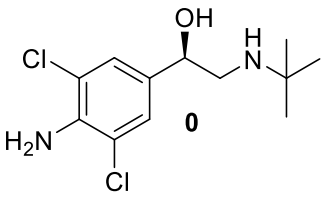

0

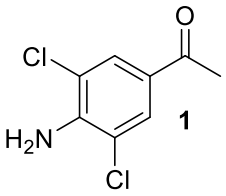

1

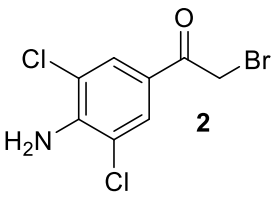

2

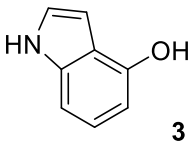

3

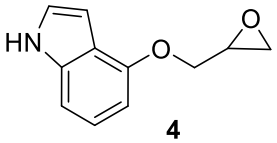

4

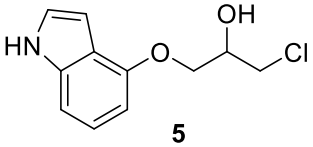

5

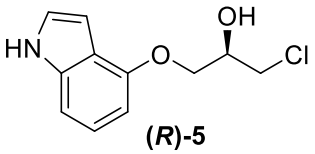

(*R*)-5

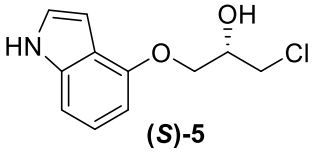

(*S*)-5

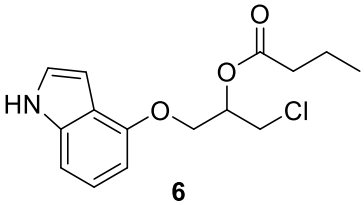

6

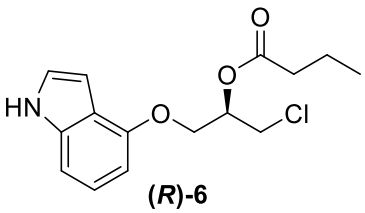

(*R*)-6

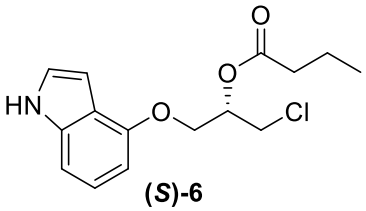

(*S*)-6

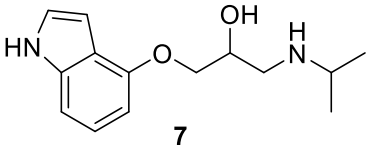

7

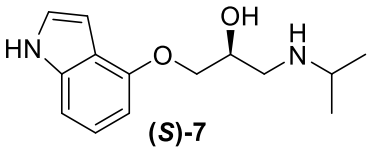

(*S*)-7

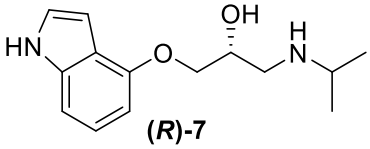

(*R*)-7

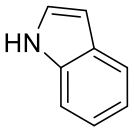

8

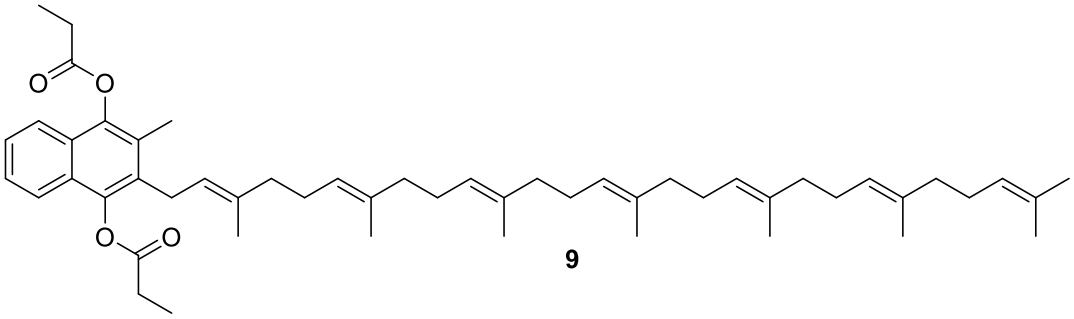

9

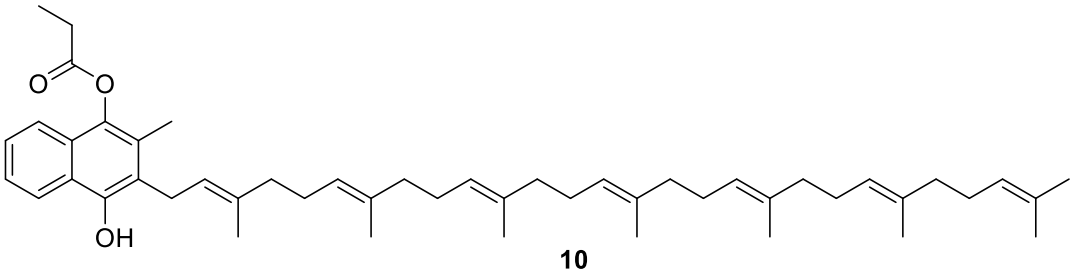

10

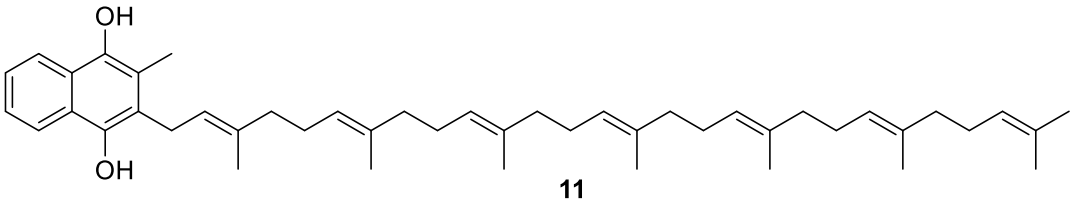

11

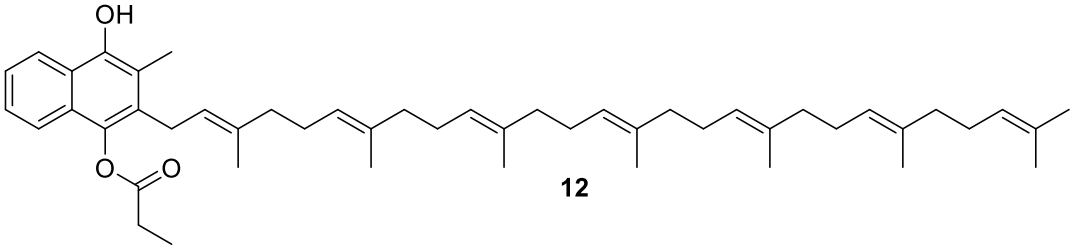

12

Abbreviations and symbols

α	Optical rotation
δ	Chemical shift in NMR spectrums
λ	Wavelength in nanomillimetres
API	Active pharmaceutical ingredient
c	Conversion
c	Concentration (calculating [α])
CALA	*Candida Antarctica* Lipase A
CALB	*Candida Antarctica* Lipase B
DMSO	Dimethyl sulfoxide
%ee	Enantiomeric excess
$\%ee_p$	Enantiomeric excess of product
$\%ee_s$	Enantiomeric excess of substrate
E	Enantiomeric ratio
EtOAc	Ethyl acetate
EtOH	Ethanol
FDA	Food and drug administration
FID	Flame ionizing detector
GC	Gas chromatography
GC-MS	Gas chromatography with subsequent mass spectroscopy
HPLC	High performance liquid chromatography
Hz	Hertz
IR	Infrared
J	Coupling constant
l	Length (calculating [α])
MeCN	Acetonitrile
MeOH	Methanol
NBS	N-bromosuccinimide
NMR	Nuclear magnetic resonance spectroscopy
PPL	Porcine pancreas lipase
R_f	Retention factor
R_s	Resolution in chromatography
T	Temperature (calculating [α])
t_R	Retention time
USA	United states of america
UV	Ultra violet
Vit-K	Vitamin K
W	Width of peaks measured at half height in chromatograms

Table of contents

1. Introduction

1.1 Background for the thesis

In 1992, the United States of America's (USA) Food and Drug Administration (FDA) issued a new policy statement regarding the development of new stereoisomeric drugs.[1] The statement gave two main points to be considered in future drug development. Firstly, appropriate procedures in manufacturing should be implemented to ensure the correct stereoisomeric composition of a product. Secondly, drugs that exists as stereoisomers should be studied individually when considering their pharmacological effects. This was implemented to ensure increased control on the pharmacological effects of different stereoisomers, and to possibly eliminate unwanted side-effects caused by other stereoisomers. Drugs with pure enantiomers as active pharmaceutical ingredient (API) fall within the group of stereoisomeric drugs, together with diastereomers and geometrical isomers.

In line with the policies issued by the FDA, one objective of this thesis has been to synthesize an enantiopure building block of β-blocker (*S*)-pindolol, by use of lipase catalysis. In addition, using enzymes is considered a "greener" form of chemistry, and more environmental friendly methods for producing chemicals should be sought after.[2] Therefore, a second objective has been to investigate the biocatalytic hydrolysis of **9**, a possible precursor in the synthesis of vitamin K_2.

1.2 Stereochemistry

Chirality is a steric property possessed by many compounds and it is an important concept to understand before discussing enantiomeric drugs. The word chiral is derived from the Greek word *cheir*, which means "handedness". The right and left hand are mirror images of each other and therefore they are not superimposable on each other. A chiral compound is one that has a non-superimposable mirror image. This occurs when the structure has one or several chirality centres. A chiral centre is commonly found on a carbon atom that is connected to four different atoms or groups, though this may also occur on other atoms such as sulphur or phosphorous (Figure 1.2.1).[3]

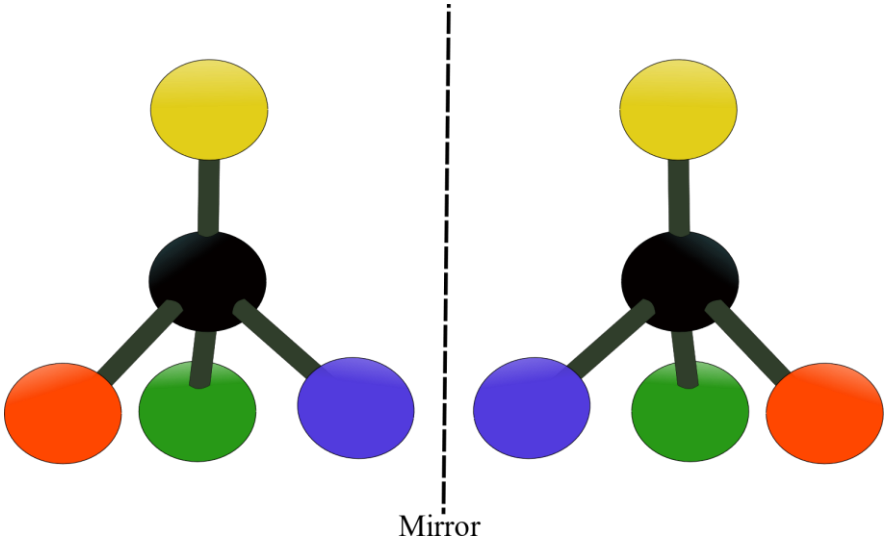

Figure 1.2.1: A chiral compound with its non-superimposable mirror image. The chiral centre is illustrated by four different groups (coloured) connected to a central atom (black).

Two compounds that are non-superimposable mirror images of each other are called enantiomers. They will share the same physical and chemical properties such as melting point and solubility, but they will differ in the direction in which they rotate plane-polarized light and in how they interact with other chiral substances.[4]

To differentiate between two enantiomers, which will share the same chemical formula and constitution, several nomenclature systems exist. In this thesis, the Cahn-Ingold-Prelog system will be used. It is also called the *R*,*S*-system, where *R* and *S* is derived from *rectus* and *sinister*; the Greek words for right and left. Using this system, the two enantiomers will be designated with the prefix *R*- or *S*- depending on the spatial arrangement of the groups connected to the chiral centre. Each group is given a priority based on their atomic number, where the highest atomic number has the highest priority. If the molecule is placed so that the group with the lowest priority is directed away from the viewer, the three remaining groups will be used to determine the prefix. If the path traced from the group with the highest priority to the group with the second-lowest priority is a clockwise path, the enantiomer is given the prefix *R*-. If the path traced is a counter-clockwise path, the enantiomer is given the prefix *S*- (Figure 1.2.2).[3]

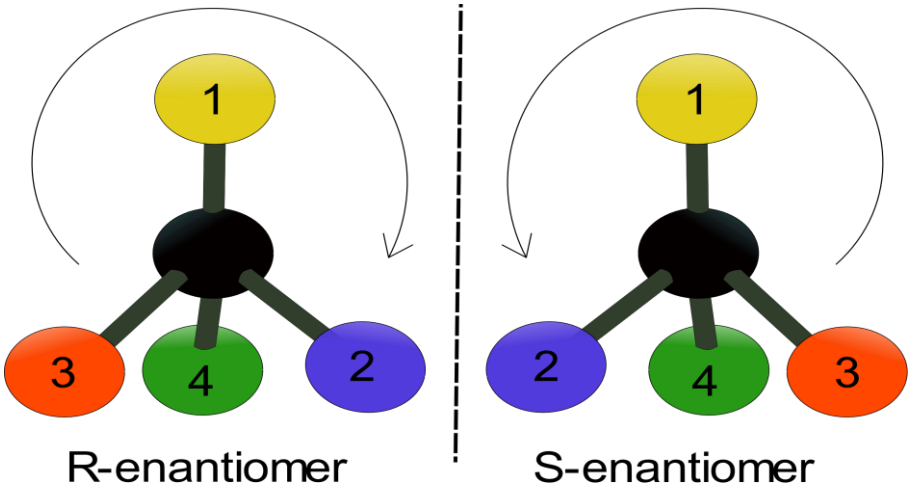

Figure 1.2.2: A pair of enantiomers with group priorities given, showing how a clockwise priority path gives the *R*-prefix and a counter-clockwise path gives the *S*-prefix.

Another way to distinguish between two enantiomers is by using their optical rotation α. If the enantiomer rotates the plane of polarized light to the right it will be given the prefix (+) and the other enantiomer will be given the prefix (-). The prefixes *d* and *l* have also been used for the (+) and (-) enantiomers, where *d* stands for dextrorotatory and *l* for levorotatory. Dextro and Levo are derived from the Latin words *dexter* and *laevus*, meaning right and left respectively.[4]

1.3 Enantiomeric drugs

As mentioned above, enantiomers will interact differently with other chiral molecules. This is the reason why different enantiomers of a drug may display different effects in the body. Drugs exert their effects by interaction with molecules in the body. These molecules can be proteins, for example signal receptors, which are made up of amino acids. In proteins, amino acids only exist in one enantiomeric form, the *l*-form. Receptors may display complex three-dimensional structures that will determine the affinity of a drug molecule depending on its spatial arrangement. Because of this, the biological or pharmaceutical effects of enantiomers of a chiral drug may be quite different.[4]

A classic example of the difference in biological effects of two enantiomers is thalidomide. The drug was used for morning sickness in pregnant women in Canada and Europe in the late 1950s to early 60s. Thalidomide was withdrawn from the marked when teratogenic effects were observed in babies whose mothers had used the drug. It was discovered that the drug caused abnormalities in the physiological development of the foetuses, and as a result several

thousand babies had been born with various deformities.[5,6] Further, it was shown that only the *S*-(-)-enantiomer of thalidomide had teratogenic effects in mice and rats, leading to the speculation that the birth defects might have been avoided if only the *R*-(+)-enantiomer had been used.[7] However, it was later shown that thalidomide racemizes *in vivo* and that both enantiomers have desirable and undesirable effects. The story of thalidomide is one that has had a great impact on the development of chiral drugs.[4,5]

Even though the case of thalidomide proved to be false regarding the effects of the different enantiomers, there are several different examples of how enantiomeric drugs give different pharmacological results. If two enantiomers show different complementarity with a receptor, the one with the highest complementarity is called the eutomer and the other is called the distomer. A measure of stereoselectivity of a receptor is the eudismic ratio, which increases when the eutomer is highly active and the distomer is correspondingly low in activity.[8]

If the eutomer possesses the wanted therapeutic action of the drug, the distomer may act in different ways. The distomer may contribute to, or even be responsible for the side-effects, as is the case of ketamine. Ketamine is an anaesthetic drug that produces a profound analgesic effect, meaning relief from pain. Because of its chiral centre, ketamine exists as two enantiomers where the (+)-isomer has been shown to be approximately 3.4 times more potent than the distomer. Furthermore, (+)-ketamine was shown to produce less stimulation of the heart rate and less spontaneous motor activity than its counterpart (-)-ketamine or the racemate. (-)-Ketamine also showed significantly more psychic reactions in the postanaesthetic period, such as vivid illusions, sensations of drunkenness or delirium.[9]

Considering the diversity shown in the effects from different enantiomers of a drug, it is crucial to produce enantiopure drugs so that their individual pharmacological effects can be studied.

1.4 Beta-adrenoceptor antagonists

Beta(β)-adrenoceptor antagonists are commonly known as β-blockers, the class of drugs is so named because they have β-receptors as their target. They represent a group of drugs that treat many cardiovascular disorders. Precursors of the well-known β-blockers pindolol and clenbuterol (Figure 1.4.1) have been synthetized in this project. The neurotransmitters that normally stimulate these receptors are the catecholamines, including dopamine, epinephrine

and norepinephrine (Figure 1.4.1), which mediate a large number of responses in the cardiovascular system.[10]

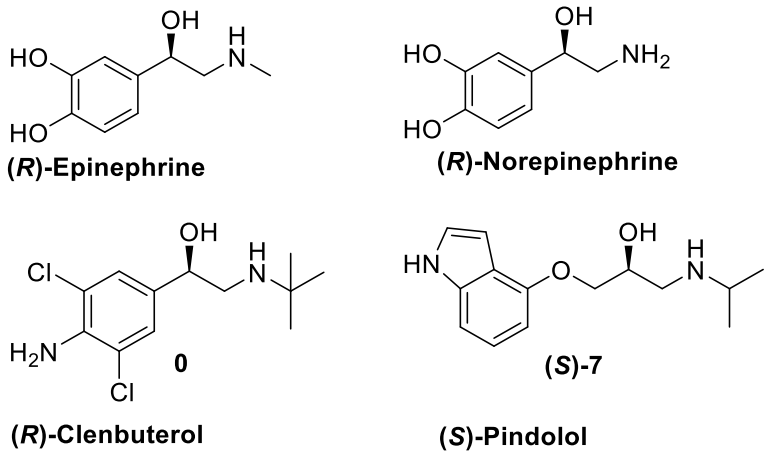

Figure 1.4.1: Structure of β-blockers (*S*)-pindolol (S-**7**) and (*R*)-clenbuterol (**0**), and neurotransmitters (*R*)-epinephrine and (*R*)-norepinephrine.

Adrenergic receptors are found throughout the body and are classified into two groups, namely alfa(α)- and β-receptors. These are further classified as either subtype 1 or 2. This thesis focuses on the β-receptors, but a mentioning of the alfa receptors is expedient to understand the nuances in pharmacological effects of the β-blockers. The α-adrenergic receptors are mostly found in blood vessels of the heart, skin, lungs, muscles and kidneys. The stimulation of these receptors leads to responses like breakdown of glycolysis and constriction of blood vessels. The β_1-adrenergic receptors are primarily found in the heart, but also in the kidneys. Stimulation of β_1-receptors increases the heart rate, the heart's ability to contract and renin secretion in the kidneys. The β_2-adrenergic receptors are located in smooth muscle of arteries and arterioles, in visceral organs such as the heart, liver and kidneys, and in the bronchioles. When the β_2-receptors are stimulated, both the bronchi and the arteries are dilated, which increases airflow to the lungs and blood flow respectively.[10,11]

β-blockers are drugs that interact with the β-adrenoceptors in such a way that the interaction between neurotransmitters and the receptors are blocked. β-blockers that are selective for β_1-receptors, called β_1-blockers, are used in treatment of heart disease. β-blockers selective for β_2-receptors, called β_2-blockers, are used in treatment of the respiratory system.[10,12] A β-blocker may be further categorized as either an agonist or an antagonist depending on its function as it binds to the receptor. If the drug promotes the process that is stimulated by the original neurotransmitter it is said to be an agonist, while a drug that blocks the action of the original neurotransmitter is called an antagonist.[13] Some drugs may also display what is

called an intrinsic sympathomimetic activity; a partial agonist activity. These drugs will still possess a high affinity for the receptor and effectively block the active site of the receptor from the original neurotransmitters, the catecholamines, but at the same time they will cause a slight activation of the receptor. This may result in a smaller reduction of the heart rate which may be more tolerable for patients suffering from bradycardia - an uncommonly low heart rate.[11]

1.4.1 Pindolol

Racemic pindolol, 1-(1H-indol-4-yloxy)-3-(isopropylamino)-2-propanol (**7**) (Figure 1.4.2), was first released for clinical use in USA in 1982. It is a non-selective β-blocker, used in the treatment of high blood pressure, chest pain and irregular heartbeat. Pindolol has its substituents on the aromatic ring in the ortho- and meta-position, which is common for non-selective β-blockers. Selective β-blockers usually have a substituent in the para-position on the aromatic ring.[14] Pindolol is also a partial agonist and will therefore slow the resting heart rate less than other β-blockers like atenolol or metoprolol.[15] Pindolol is usually sold under the brand names Visken or Barbloc and is often used to treat high blood pressure during pregnancy because it does not affect the foetal heart function or blood flow. Although pindolol is a non-selective β-blocker, other uses for the drug have been reported. It has been tested in the treatment of fibromyalgia and related fatigue diseases, as well as in the treatment of depression in combination with selective serotonin reuptake inhibitors.[16,17] Pindolol is a rapidly absorbed drug, and after oral ingestion it can be detected in the blood after 30 minutes. In patients with normal renal function pindolol has a plasma half-life of three to four hours. The drug is also lipophilic and enters the central nervous system rapidly. Reported side effects include unwanted lowering of heart function or changes in the respiratory system. These side effects are related to its β-adrenergic blocking activity, other side effects have also been reported, such as dizziness, vivid dreams, feeling of weakness or fatigue, muscle cramps as well as nausea.[15]

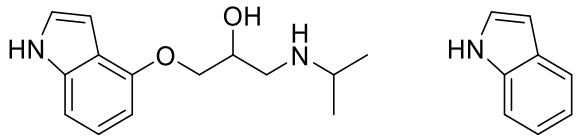

7 **8**

Figure **1.4.2**: The structure of pindolol (**7**) and its backbone structure indole (**8**).

In 2017, Lima *et al.* reported the successful synthesis of (*S*)-pindolol using different lipases in hydrolytic processes and esterifications,[16] the results of which has been attempted improved in this thesis.

1.4.1.1 The indole structure

As can be seen in Figure 1.4.2, the backbone structure of pindolol is the indole skeleton. The indole structure is commonly found in a wide variety of compounds. Most importantly it is a part of tryptophan (Figure 1.4.3), one of the essential amino acids. Tryptophan is also an important precursor for serotonin which is known as the "happiness hormone".[18]

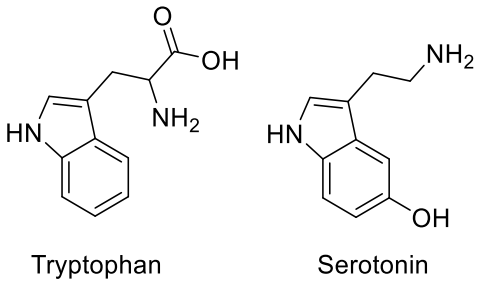

Figure 1.4.3: The structure of essential amino acid tryptophan and neurotransmitter serotonin.

Indole is also a common structure in alkaloids, a class of biologically active basic nitrogenous heterocycles. A well-known compound from the indole-alkaloid group is psilocybin, a natural product from *psilocybe carpophores*, also known as "magic mushrooms". Fricke *et al.* reported the enzymatic synthesis of psilocybin from tryptophan using several different enzymes.[19]

1.4.2 Clenbuterol

In this thesis, 4-amino-3,5-dichlorobenzoyl bromide (**2**) (Figure 1.4.4), a building block of the β-blocker clenbuterol, has been synthesized. Clenbuterol, sold under the brand name Ventipulmin, is a selective β_2-agonist used in the treatment of respiratory diseases. The drug is not approved by the FDA for human use, but it is used to treat airway obstructions diseases

in horses.[20,21,22] Clenbuterol is listed on the World Anti-Doping Agency's prohibition list but is still abused by body-builders and athletes because of its reported body-fat reduction effects.[23] The drug is also one where the two enantiomers have shown different properties. It has been reported, by examination of human urine, that the (*S*)-enantiomer is more retained in the body than its counterpart.[24] It has also been reported that only the (*S*)-enantiomer causes reduced blood pressure and enhanced blood glucose levels in rats, and that only the (*R*)-enantiomer causes decreased motor activity, tremors or head twitching.[25,26]

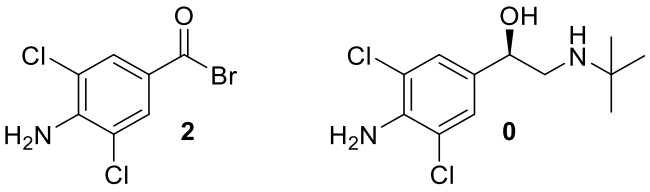

Figure 1.4.4: The structure of (*R*)-clenbuterol (**0**) and its building block 4-amino-3,5-dichlorobenzoyl bromide (**2**).

1.5 Vitamin K

Vitamin K (vit-K) is a fat-soluble vitamin that is involved in blood coagulation and bone metabolism. Different types of vit-K are found in nature and they are divided into types K_1 and K_2. Vitamin K_1, or phylloquinone, is the dominant form found in our diet, and it is synthesized in plants (Figure 1.5.1).

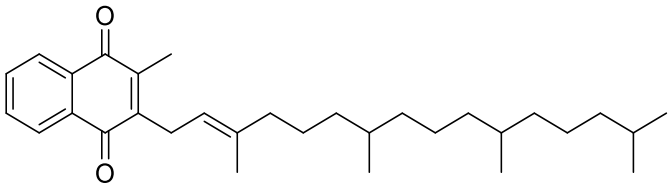

Figure 1.5.1: Structure of vitamin K_1, also known as phylloquinone.

Vitamin K_2 includes a range of different structures called menaquinones. The different forms are designated MK-n, where n gives the number of 5-carbon units found in the side chain of the molecule. Examples are shown in Figure 1.5.2. Menaquinones are mostly found in animal products, they are synthesized in the human intestine and also produced in different fermentations.

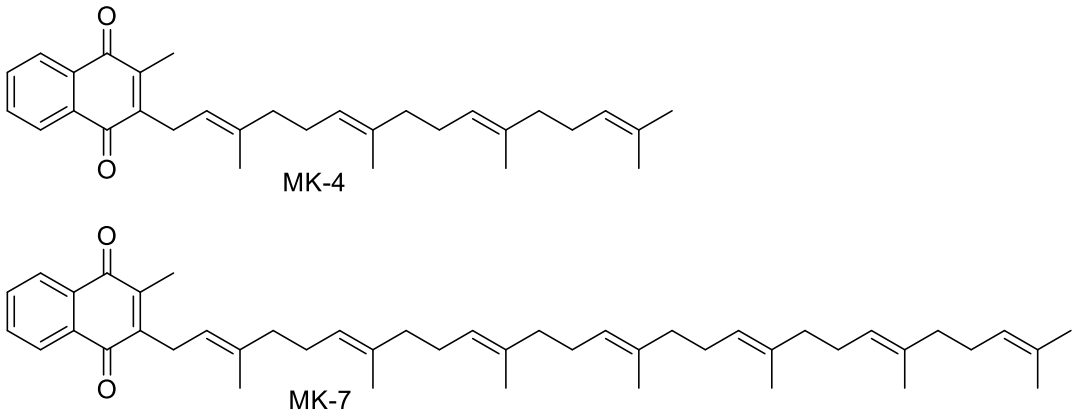

Figure 1.5.2: Examples of menaquinones MK-4 and MK-7, two different types of vitamin K_2.

Even though vit-K is a fat-soluble vitamin, only small amounts are stored in the human body. This might be why the body reuses a small amount of vit-K through the vit-K epoxide cycle. Here, the reduced form of vit-K is oxidized to an epoxide form and later reduced back to its original form. A vit-K deficiency often manifests as nosebleeds, blood in urine, bleeding gums or very heavy menstrual bleeding. A person with this deficiency may also bruise very easily. Still, vit-K deficiency is uncommon with a healthy diet.[27] However, it has been shown that individuals with cystic fibrosis have a higher risk of developing a vit-K deficiency.[28]

People who are at risk of forming blood clots may use anticoagulants to prevent this. Anticoagulants are often vit-K antagonists that counteract the effects of vit-K. This can be done by preventing the recycling of vit-K, or by interfering with the coagulation cascade which will hinder the formation of blood clots. People taking vit-K antagonists are at risk of developing a deficiency.[27] It has been speculated that diets low in vit-K may be associated with osteoporosis, osteoarthritis and bone fractures, especially in postmenopausal women. However, currently there is not strong enough evidence that vit-K supplements will prevent fractures, osteoporosis or osteoarthritis. Smaller trials have been done, but improvements in bone density have not been statistically significant. For individuals with cystic fibrosis, the same conclusions have been drawn, and it has been recommended that larger trials should be performed.[28-30]

Kappa Bioscience is a company currently selling vitamin K_2 in the form of MK-7 (Figure 1.5.2), under the brand name K2VITAL®. In 2016, they patented a synthetic route to preparation of MK-7.[31] MK-7 was chosen as the optimal form of dietary supplementation because it has a half-life of about 72 hours. Unlike MK-4, used for treatment of osteoporosis in Japan, which only has a half-life of about 1.5 hours.[32,33]

The possibility of producing MK-7 by use of enzymes has been investigated in this thesis. Even though the need for vit-K as a supplement is disputed, the argument for finding more environmentally friendly methods of producing chemicals is strong.

1.6 Biocatalysis in organic synthesis

The use of enzymes as catalysts in chemical synthesis is called biocatalysis. Using enzymes as catalysts has many advantages, such as faster reaction rates and low mole percentages of catalysts needed. An enzyme-mediated process may proceed at rates 10^{8}-10^{10} times faster than the non-catalysed reactions which means that the mole percentage of an enzyme needed for a bio-catalysed reaction can be as low as 10^{-3}-10^{-4}%, while chemical catalysts are often needed in mole percentages around 0.1-1%.[34]

There are also other advantages to using enzymes as catalysts, they are not restricted to their original substrates and can be used for a large number of reactions. Enzymes are also better for the environment, they can facilitate reactions under mild conditions and they can display different types of selectivities.[34,2] Chemo-selectivity is the ability of an enzyme to discriminate between functional groups of a substrate, and regioselectivity is the discrimination of identical functional groups that hold different positions on a molecule. Finally, there is enantioselectivity, where enzymes interact differently with two enantiomers because of their spatial arrangement. Because enzymes are proteins consisting of chiral amino acids, the enzymes themselves are also chiral and will therefore interact differently with a pair of enantiomers. When an enantioselective enzyme is used to catalyse the conversion of a racemic substrate, one of the enantiomers will fit better with the active site of the enzyme and therefore be converted to the product at a higher rate than the other enantiomer. This is called a kinetic resolution.[34]

1.6.1 Enzymes

Enzymes are divided into six categories depending on which reactions they mediate. The six categories are presented in Table 1.6.1.[34] In this thesis, enzymes from the 3rd class, hydrolases, have been used in attempted hydrolyses and ester formations of different substrates.

Table 1.6.1: List of enzyme categories with the reactions they facilitate.[34]

No.	Enzyme class	Reaction type
1	Oxidoreductases	Oxidations and reductions. For example: oxygenation of C-H, C-C, or C=C bonds or addition or removal of hydrogen atoms.
2	Transferases	Transfer of groups: aldo-, keto- and/or acyl-groups, as well as sugar-, phosphoryl-, methyl- or NH_3-groups.
3	Hydrolases	Hydrolysis, esterification, amides, lactones, lactams, epoxides, nitriles, anhydrides, glycosides, organohalides.
4	Lyases	Addition-elimination of small molecules on C=C, C=N, C=O bonds.
5	Isomerases	Isomerization, such as racemisation, epimerisation, rearrangement.
6	Ligases	Formation-cleavage of, C-O, C-S, C-N, C-C bonds with concomitant triphosphate cleavage.

1.6.2 Kinetic resolution

In a kinetic resolution with a racemic substrate, an enantioselective enzyme will convert one enantiomer to the product faster than its counterpart. This means that during the course of an enzyme-mediated reaction there will be different ratios of the enantiomers present in both the substrate and the product. To measure this ratio the enantiomeric exess (%ee) is used. It is most commonly calculated by using equation 1. Subtracting the area of the minor peak (Q) in a chromatogram from the area of the major one (P) and dividing by the sum of both areas gives %ee.[34]

$$\%ee = \frac{P-Q}{P+Q} * 100\% \qquad (1)$$

The %ee can be calculated for both the products and the substrates, and the ratios are then called $\%ee_p$ and $\%ee_s$ respectively. If an enzyme is so selective that it will only convert one enantiomer to its product and not convert the other enantiomer at all, it is called a specific enzyme. In such a scenario, both the product and the substrate will be enantiopure and have $\%ee_p$ and $\%ee_s$ of 100%.

Further, to quantify the selectivity of the enzyme towards one substrate, the enantiomeric ratio E can be calculated. A higher E-value means that the enzyme is more selective towards one enantiomer, while a lower E-value indicates a less selective enzyme. In general, pure enantiomeric products can be synthesized through a kinetic resolution with an E-value of 200

or above. The E-value can be calculated using $\%ee_p$ and $\%ee_s$, as shown in equation 2.[34]

$$E = \frac{\ln \frac{[\%ee_p(1 - \%ee_s)]}{(\%ee_p + \%ee_s)}}{ln \frac{[\%ee_p(1 + \%ee_s)]}{(\%ee_p + \%ee_s)}} \quad (2)$$

Enzymes will catalyse an equilibrium in both directions, and therefore it is important to control reaction parameters to optimize for an irreversible reaction. In this thesis, vinyl butanoate was used as acyl donor for acylation reactions. After donating an acyl group the remaining ethenol is so volatile that it will evaporate from the solution. This hinders the reaction from reversing, and the product will not be converted back to the original substrate. In an irreversible kinetic resolution, the enantiomeric excess will start at zero for the racemate substrate and, depending on the E-value, it will increase in value as more and more of one enantiomer is converted to its product. The enantiomeric excess of the product also depends on the selectivity, but it will have the opposite development through the resolution. This is illustrated in Figure 1.6.1, showing the development of the %ee values of both substrate and product in two irreversible kinetic resolutions with different E-values.[34]

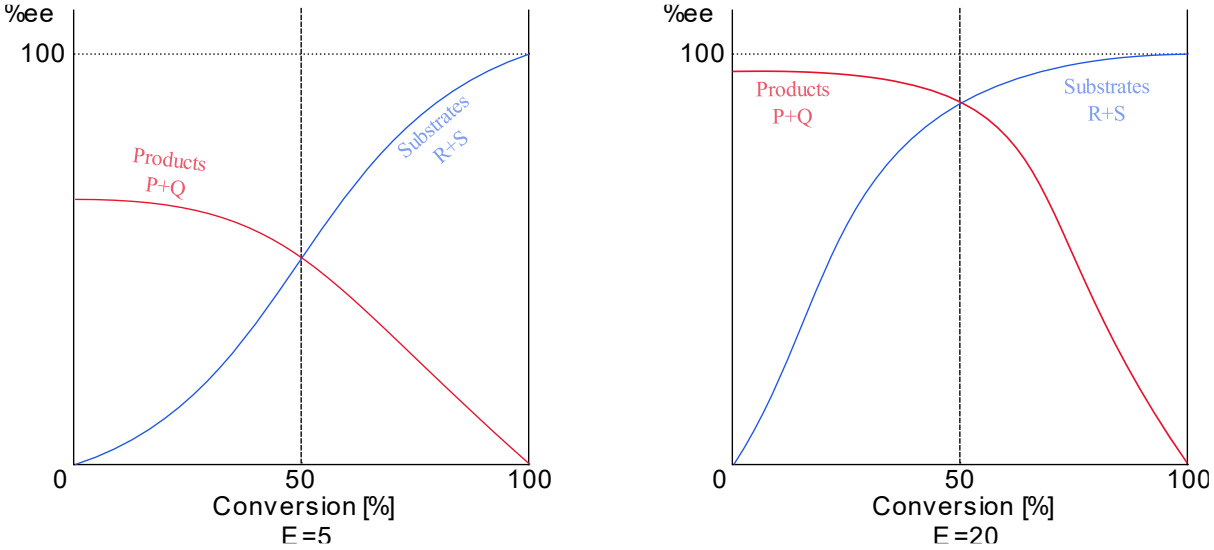

Figure 1.6.1: Illustrates how the %ee values changes for both the products and the substrates during two irreversible kinetic resolutions with E-values of 5 (left) and 20 (right).[34]

In earlier works in our research group, E-values for different kinetic resolutions of precursors of different β-blockers have been reported. In 2016, P. Bøckmann reported the kinetic resolution of 1-chloro-3-(4-(2-methoxyethyl)phenoxy)propan-2-ol, precursor of metoprolol, using *Candida antarctica* lipase B (CALB) in hexane with vinyl butanoate as the acyl donor. This produced the (*S*)-butanoate ester in 54%ee, leaving the (*R*)-alcohol in 99%ee. Further hydrolysis of the (*S*)-ester, using CALB in buffer at pH 7, gave (*S*)-1-chloro-3-(4-(2-methoxyethyl)phenoxy)-propan-2-ol in 99%ee. This kinetic resolution had an E-value calculated to be $E > 200$.[35] Lund *et al.* reported the successful synthesis of enantiopure (*R*)-1-phenoxy-3-chloro-2-propanol by kinetic resolution of racemic 1-phenoxy-3-chloro-2-propanol. CALB was used, and the resolution had an E-value > 200.[36] F. H. Blindheim reported the kinetic resolution of 2-(4-(3-chloro-2-hydroxypropoxy)phenyl)-acetamide, a precursor of atenolol, using CALB in an esterification with vinyl butanoate in acetonitrile. Resulting in (*R*)- 2-(4-(3-chloro-2-hydroxypropoxy)-phenyl)acetamide in >99 %ee.[37]

Precursors of β-blocker pindolol were reported synthesized by biocatalysis in 2017 by Lima *et al.* The hydrolysis of precursor rac-2-acetoxy-1-(1H-indol-4-yloxy)-3-chloropropane using lipase from *Pseudomonas fluorescens* yielded (2S)-1-(1H-indol-4-yloxy)-3-chloro-2-propanol in 96 %ee and (2R)-2-acetoxy-1-(1H-indol-4-yloxy)-3-chloropropane in 97 %ee.[16]

1.6.3 *Candida antarctica* lipases

Candida antarctica lipase A (CALA) and CALB are enzymes from the antarctic yeast *Candida antarctica*. They are lipases, which is a group of enzymes in the 3rd category – hydrolases.[38] Lipases are widely used in biocatalysis, especially in kinetic resolutions of alcohols and amines.[16] Further, lipases are commercially available as immobilized preparations that do not require co-factors, and are therefore easy to both handle and reuse. The lipases are also preferred for their high regio- and enantioselectivity, and they show relatively high stability in organic solvents.[38] Both CALA and CALB are serine hydrolases, meaning that they mediate conversions at the active site through their catalytic triade of three amino acids; serine – histidine – aspartate (Figure 1.6.2).[39]

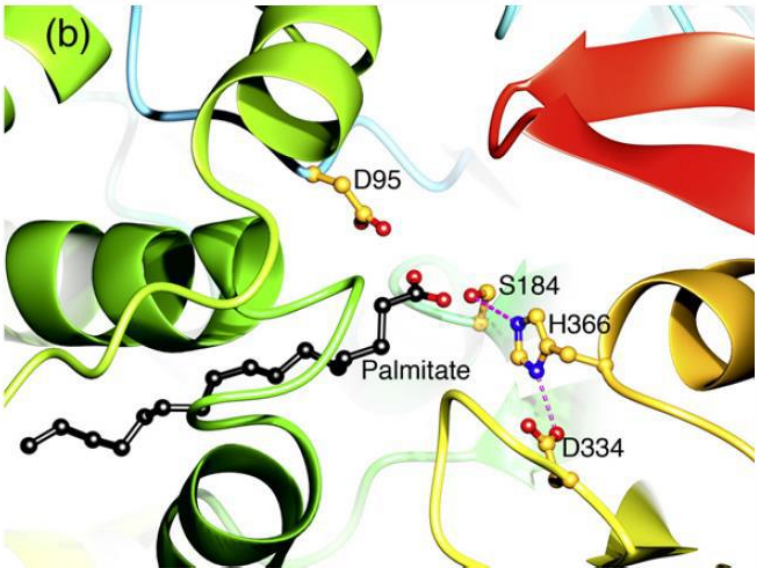

Figure 1.6.2: The catalytic triade of the serine hydrolase mechanism, located at the active site of *candida antarctica* lipase A, containing amino acids serine 184 (S184), histidine 366 (H366) and aspartate 334 (D334).[39]

CALB is the more commonly used lipase of the two, and it has been reported to catalyse depolymerizations,[40] transesterifications[41] as well as the synthesis of peroxy acids.[42] In kinetic resolutions of secondary alcohols CALB is selective towards the (*R*)-configuration of the alcohol, unless the smallest group on the secondary alcohol is a halogen, then the selectivity is towards the (*S*)-configuration.[34]

1.6.4 Porcine pancreas lipase

The crude fraction that is isolated from the porcine pancreas contains the cheapest and also the most widely used lipase. The crude contains a vast number of other hydrolases, as well as the lipase that is called the "true" porcine pancreas lipase (PPL). The crude is often called pancreatin or steapsin, and contains other enzymes such as cholesterol esterase, carboxypeptidase B, phospholipases and probably other unknown hydrolases. It is therefore important to be cautious when using crude PPL as a biocatalyst, as any observed transformation may be the result of any of the hydrolases present in the crude. However, it is possible to obtain PPL in a purified form, in which it shows selective transformation of esters of primary alcohols.[34,43]

1.6.5 Influencing factors on biocatalysis

When enzymes are to be used as catalysts in organic chemistry, there are many factors that may influence the results. The natural environment for enzymes is water, therefore enzymes show higher conversion rates when water is used as a solvent. Enzymes may still catalyse reactions successfully in other solvents, but with slower rates. To increase conversion rates in other solvents, the control of water activity is essential. This can be done by using mixtures of solvents or adding pairs of salt hydrates. [34] Anthonsen *et al.* has reported the effects on E-values by adding 10% of different co-solvents to the hydrolysis of the butanoate of 3-methoxy-1-(phenylmethoxy)-2-propanol using CALB. The results show that adding co-solvent can both decrease and increase the E-value.[44] In nature, it is common for enzymes to have environments with a neutral pH and therefore the highest conversion rates are also displayed at neutral pH. In this regard, using buffers can be helpful in keeping a stable pH range for the reaction.[34]

Further, the structure of the substrate is important to the success of an enzyme-catalysed reaction. Many enzymes will catalyse the conversion of other substrates than their natural one, but small changes in substrate structure may influence the conversion rate and the selectivity greatly.[34] This has been reported by Jacobsen *et al.*, showing that the extension of the ”small group” by one carbon unit greatly affects the conversion rate.[45]

1.7 Theory on relevant organic synthesis

In this thesis, several organic synthetic steps were performed before the racemic mixtures were subjected to kinetic resolutions. The theoretical basis for these synthetic steps is presented here.

1.7.1 α-Bromination of ketones

The halogenation of ketones is a common way of enabling the molecule for nucleophilic attack. In this project, the α-bromination of 1-(4-amino-3,5-dichlorophenyl)ethan-1-one (**1**) to 4-amino-3,5-dichlorobenzoyl bromide (**2**) was attempted (Scheme 1.7.1).

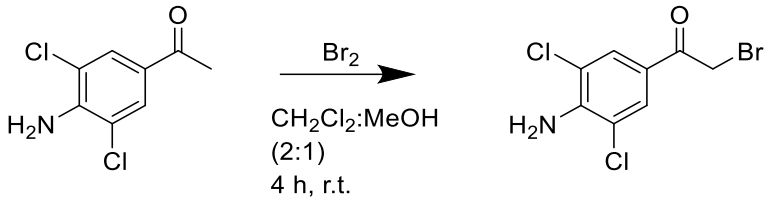

Scheme 1.7.1: α-Bromination of 1-(4-amino-3,5-dichlorophenyl)ethan-1-one (**1**) to 4-amino-3,5-dichlorobenzoyl bromide (**2**), using bromine as reagent and dichloromethane and methanol (MeOH) as solvents.

Bromine (Br_2) and N-bromosuccinimide (NBS) are two common reagents used in bromination. When bromine is used there are several challenges. Br_2 is a toxic substance with corrosive properties and it is also highly reactive. Therefore, it is less attractive for industry. It is a challenge to limit the number of bromines incorporated in a structure, because the product will be more reactive than the substrate and might react with another bromine, forming by-products. To avoid this the reactions are often performed in acidic environments where the product is less likely to tautomerize.[3] NBS is a less hazardous reagent used for bromination. The ketone tautomerizes to its enol form, which then undergoes a nucleophilic attack on the bromine atom on NBS.[46] In this thesis, bromine was used as reagent based on the results reported by Blindheim *et al.* in 2017.[37]

1.7.2 Base-catalysed S_N2 addition of epichlorohydrin to secondary alcohols

In the synthesis of **5** from 1H -indol-4-ol (**3**), the first synthetic step was the reaction of **3** with NaOH and 2-(chloromethyl)oxirane (epichlorohydrin). This reaction is an S_N2 reaction and it is shown in Scheme 1.7.2.

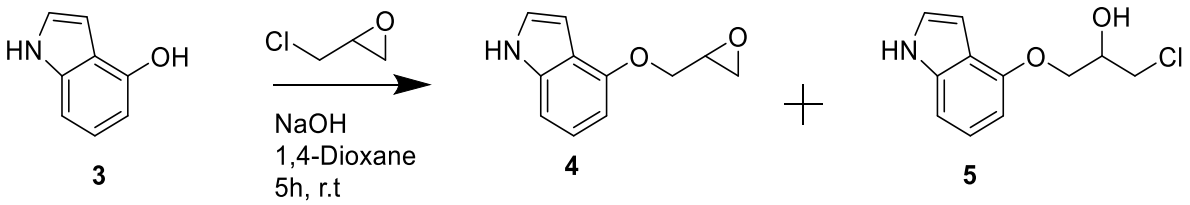

Scheme 1.7.2: S_N2 reaction with 1H-indol-4-ol (**3**) as starting material, using NaOH as a base and 2-(chloromethyl)oxirane as reagent.

In this reaction, the base will deprotonate the alcohol group on the starting material **3**. The resulting anion then undergoes a nucleophilic attack on epichlorohydrin. There are several carbons available for attack on epichlorohydrin, which is why both **4** and **5** are products of

this reaction. There is also the possibility of an internal reaction on the wanted product **5** because of the basic environment, which would result in the by-product **4**. Therefore, a short reaction time is desired, to decrease the production of the by-product **4**. Different bases have been used in similar reactions in the synthesis of β-blockers, Austli reported using NaOH and K_2CO_3 as bases in the synthesis of precursors of (*S*)-practolol, where the use of NaOH gave the highest purity of the wanted halohydrin.[47] Lima *et al.* reported the use of NaOH in the synthesis of **5** using **3** as starting material.[16] In addition, Austli also reported the production of a by-product in the form of a dimer, possibly formed by the deprotonated starting material, reacting with the halohydrin product.[47]

1.7.3 Acid-catalysed opening of epoxide-function on **4** using a halogen donor

In order to increase the yield of halohydrin **5** formed from the starting material **3**, a ring-opening of the epoxide on **4** was performed. This can be seen in Scheme 1.7.3.

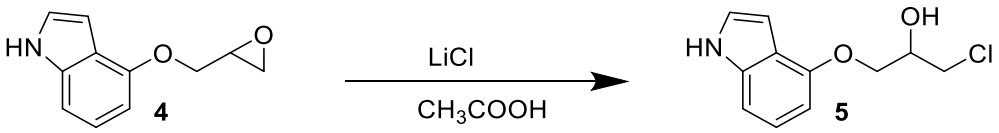

Scheme 1.7.3: Opening of the epoxide on **4**, resulting in the halohydrin **5**, using LiCl and acetic acid.

Lima *et al.* reported the successful ring opening of **4** using concentrated hydrochloric acid in dichloromethane.[16] Earlier work in our research group has been performed using different halogen donors in the ring-opening of similar structures, such as lithium chloride,[47] lithium bromide,[35] and Li_2CuCl_4.[48]

1.7.4 Amination of halohydrin **5** forming pindolol **7**

After the kinetic resolution of racemic **5**, the enantiopure (*R*)-**5** could be subject to amination, yielding the wanted enantiopure (*S*)-pindolol ((***S***)-**7**) (Scheme 1.7.4).

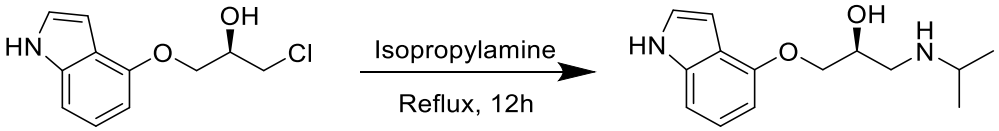

Scheme 1.7.4: The formation of (S)-pindolol from enantiopure chlorohydrin (R)-**5** by amination as reported by Lima *et al.*[16]

Depending on their structure and their environments, amines can act as both bases and nucleophiles. In general, the bulkier amines act as bases, while less sterically hindered amines also act as nucleophiles. In order for the amines to act as bases, the environment must be polar enough, if not, the protons will not dissociate.[49] The formation of (*S*)-pindolol from enantiopure chlorohydrin (*R*)-**5** by amination, has been reported by Lima *et al*. using isopropylamine.[16]

1.8 Methods of analysis on chiral compounds

When analysing chiral compounds, the fact that chiral compounds will interact differently with other chiral substances must be utilized. Many regular methods of analysis will not be able to distinguish between enantiomers, and therefore chirality must be introduced to the analytical method. This can be done by using chiral stationary phases, chiral additives or by studying optical rotations of the compounds.

1.8.1 Chiral chromatography

In chiral chromatography, chirality can be introduced to the system in two ways, either by being part of the stationary phase or as an additive to the mobile phase. The chiral substance that is added is called a chiral selector, and separation of enantiomers occurs because one of the enantiomers will interact stronger with the chiral selector. The interactions between enantiomers and the chiral selector is often described by using a three-point model, where the three different groups on the enantiomer corresponds to three groups on the chiral selector. Because of the different spatial arrangement of the enantiomers, one of them will form a more stable complex with the selector. This is illustrated in Figure 1.8.1. Interactions that may occur between groups include hydrogen-bonding, non-bonding-/polarizable pi-interactions, regular pi-interactions, as well as electrostatic-, Van der Waals-, and hydrophobic-interactions.[50]

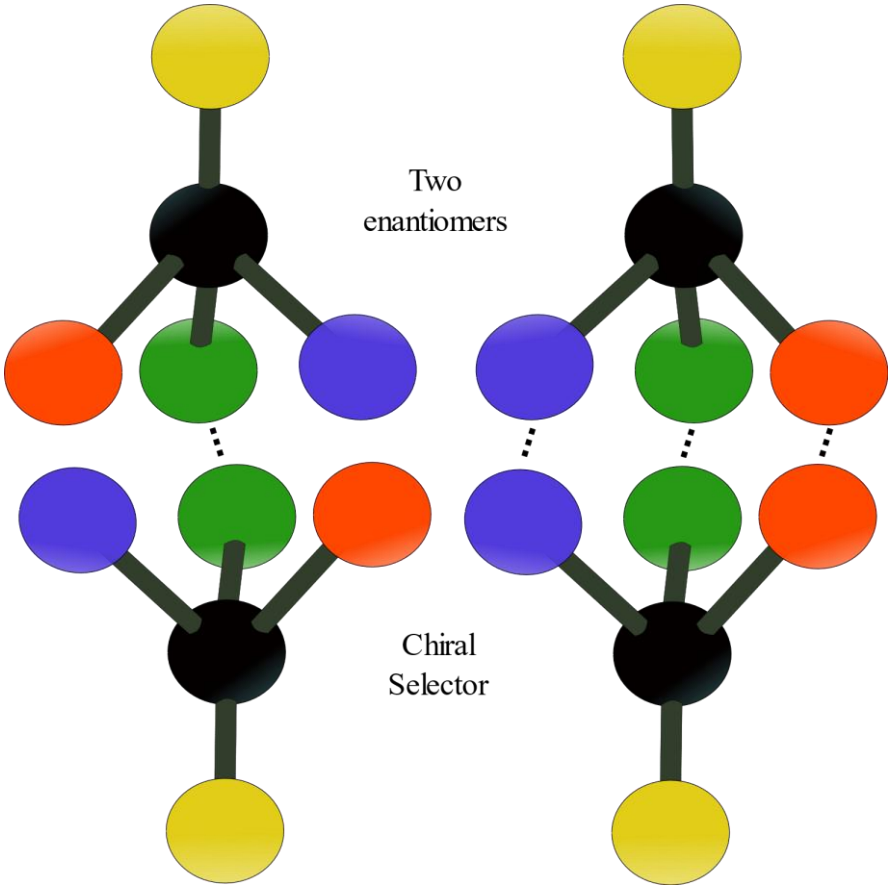

Figure 1.8.1: Two enantiomers forming complexes of different stabilities with chiral selectors in the three-point model.

In order to calculate the %ee from a chromatogram of two enantiomers, it is important that the separation of the two peaks is sufficient. For two peaks to be considered fully separated, they must have a resolution (R_s) value of at least 1.5. To calculate the resolution of two peaks, equation 3 is used.

$$R_S = \frac{1.77(t_2 - t_1)}{W_1 + W_2} \quad (3)$$

Here, t_1 and t_2 are the retention times of the two peaks, and W_1 and W_2 are the width of the two peaks measured at half height.[50]

1.8.1.1 Chiral high-performance liquid chromatography (HPLC)

In high-performance liquid chromatography (HPLC), separation of analytes occurs when analytes are moved through a column containing a stationary phase by use of a liquid mobile phase. In order to separate chiral analytes, the chiral selector can be added to either the stationary phase or the mobile phase. Common stationary phases include cellulose

derivatives, cyclodextrins, metal chelates or proteins. Cyclodextrins, metal chelates and proteins are also common additives to chiral mobile phases. When using a Daicel Chiralcel OD-H column, Lystvet *et al.* reported that the (*R*)-enantiomers of different halogenated 1-(4-benzyloxy)phenyl)ethanols were the most retained.[51] Lima *et al.* reported the chiral separation of enantiomers in racemic 2-acetoxy-1-(1H-indole-4-yloxy)-3-chloropropane (**6**) and the enantiomers in 1-(1H-indole-4-yloxy)-3-chloro-2-propanol (**5**). The column used was a Chiracel® OD-H and for both the ester and the alcohol the (*R*)-enantiomers were the most retained.[16]

1.8.1.2 Chiral gas chromatography (GC)

In gas chromatography (GC), separation occurs when analytes are moved through a heated column with a stationary phase by use of carrier gas. Often, a temperature gradient is used to achieve sufficient separation of analytes. In chiral GC, the stationary phase contains the chiral selector, and often they will not endure as high temperatures as the achiral stationary phases. CP-Chirasil-DEX DB stationary phase is commonly used in chiral GC. It has been reported by Lystvet *et al.* that the (*S*)-enantiomer is the most retained on this stationary phase when separating 1-(4-benzyloxy)phenyl)ethanols and that the (*R*)-enantiomer is the most retained when separating esters derived from the alcohol.[51] Uray *et al.* separated 17 enantiomers of substituted 1-phenylethanols by use of the same column and found that the (*S*)-enantiomers were most retained except for the ortho-methyl-substituted 1-phenyethanol.[52]

1.8.2 Nuclear magnetic resonance spectroscopy (NMR)

Nuclear magnetic resonance spectroscopy (NMR) is one of the most important techniques for determining structures in organic chemistry. It is a spectroscopic method based on the different angular momentums (spin) of nuclei. The angular momentum quantum number, *I*, can have half-integer numbers between zero and six, and all atoms that have a non-zero nuclear spin number can be detected by NMR. Protons fall within this group and have I = ½ and two allowed angular momentum states +½ and -½ (often called spin up and spin down). When a sample is placed in an external magnetic field B_0, nuclei with non-zero nuclear spin numbers will align their angular momentum states with the external magnetic field B_0. For protons, the spin states will align so that they are parallel or antiparallel to the direction of B_0. Protons that are parallel with the magnetic field have lower energy than the ones that are oriented antiparallel. A radio frequency pulse is then used to irradiate the sample, in order to

“flip” the parallel magnetic moments of the nuclei to the higher energy level. The amount of energy needed to bring the magnetic moment to a higher energy level is influenced by the electron density around the nuclei.

The electrons around the nuclei also create a small local magnetic field around the nuclei, this will partially shield it from B_0. Because of this, the experienced magnetic field will be different for each nucleus. This allows the different chemical environments of the nuclei to be determined. For example, a nucleus that is close to an electronegative atom will experience less shielding and therefore have a higher shift. Further, when the nuclei undergo relaxation after the irradiation by the radio frequency pulse, it is possible to detect the free induction decay, which in turn can be converted by fourier transformation to the peaks in an NMR spectrum.[53]

To differentiate between two enantiomers, a chiral additive must be used, otherwise the NMR spectra for two enantiomers will look identical. If a chiral derivatization additive is included in the sample, NMR spectra can be used to calculate %ee by integrating peaks.[53]

1.8.3 Polarimetry

To measure the optical rotation (α) of an enantiomer, a polarimeter is used. This device usually consists of a light source, a polarizer, a cell to hold the sample, an analyzer and a scale to measure the degree of rotation, see Figure 1.8.2. When light is passed through a polarizer the electric field of the light will no longer oscillate in all planes perpendicular to the direction of propagation. Instead, the light that emerges from the polarizer will only be oscillating in one plane. This is called plane-polarized light. If the plane-polarized light passes through the cell containing an optically active substance, such as an enantiomer, the plane will be rotated to some degree. The analyzer used in this device is simply another polarizer; this polarizer will hold a parallel position to the first one when the process is started. If the cell is empty or contains an optically inactive substance, the plane-polarized beam will pass through the cell with no change in its rotation. Then it will pass through the parallel analyzer to the scale where the maximum amount of light will be detected, and the degree of rotation will be 0°. However, if the cell contains an optically active substance, such as an enantiomer, the plane of polarized light will be rotated to some degree in either a clockwise or counter-clockwise direction. For the maximum amount of light to be detected

after passing through the cell, the analyzer must be rotated either clockwise or counter-clockwise until it matches the beam and the plane-polarized light is let through.[3]

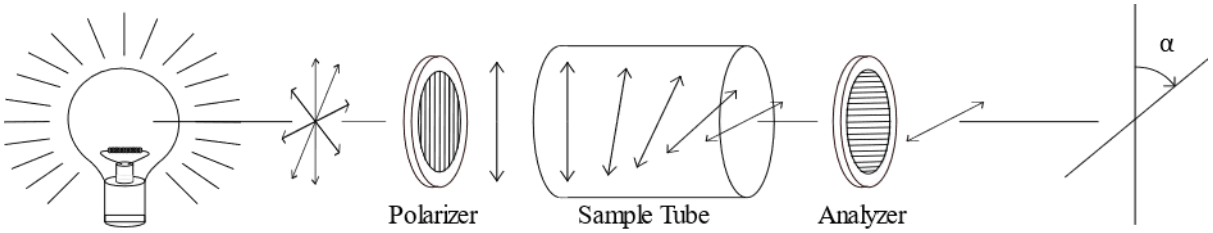

Figure 1.8.2: From left to right, a beam of light can be followed from the light source through all components of a polarimeter. After passing through a polarizer, only one plane of light will continue through the sample tube. Here the plane may be rotated by a chiral sample, and the degree of rotation, α, is measured by the analyzer.

The degrees that the plane is rotated by the optically active compound is dependent on how many molecules there are in the cell, the temperature and the wavelength of light used. Therefore, the specific rotation [α] has been defined (eq. 4).

$$[\alpha] = \frac{\alpha}{l * c} \tag{4}$$

Where α is the observed optical rotation, c is the concentration or density of the substance in g/mL and l is the length of the cell in decimetres. To include wavelength and temperature it is common to give the specific rotation in the following manner (eq. 5).

$$[\alpha]_{\lambda}^{T} = +1.25 \tag{5}$$

Here the specific rotation has been measured to +1.25 at a temperature T and a wavelength λ.[3]

2. Results and discussion

2.1 Organic synthesis

This section covers the synthesis of **2** from starting material **1**, as well as the organic synthetic steps performed in the synthesis of **6** from starting material **3**.

2.1.1 α-Bromination of 1-(4-amino-3,5-dichlorophenyl)ethan-1-one (**1**) forming 4-amino-3,5-dichlorobenzoyl bromide (**2**)

The synthesis of 4-amino-3,5-dichlorobenzoyl bromide (**2**) was performed (Scheme 2.1.) in an attempt to reproduce the work of F. H. Blindheim performed in our research group.[37] Blindheim performed the synthesis of **2** by combining reaction conditions of González-Antuña *et al.*[54] and work-up procedures by Kerry Moore.[55]

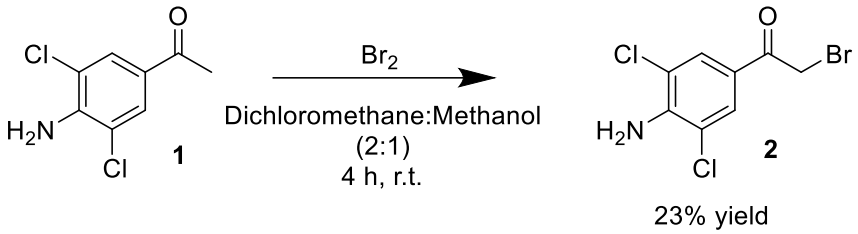

Scheme 2.1: Synthesis of 4-amino-3,5-dichlorobenzoyl bromide (**2**), by α-bromination of 1-(4-amino-3,5-dichlorophenyl)ethan-1-one (**1**) in dichloromethane and methanol (2:1) at room temperature.

Br_2 was used as the source of Br^+, and the solvent used was a 2:1 mixture of dichloromethane and methanol. Dissolvement of **1** gave a pale-yellow solution which changed colour to a bright red solution upon addition of the bromine solution. After 30 minutes of stirring, the colour changed back to pale yellow. Thin layer chromatography (TLC) showed remaining starting material as well as two other substances after the first addition. Four more portions of diluted Br_2 were added, giving in total an addition of 1 eq. of Br_2. The reaction was ended after four hours even though TLC showed remaining starting material, this was done because earlier works had shown that the formation of di-brominated by-product was a risk.[37] The TLC showed two products in the reaction mixture, assumed to be the wanted mono-brominated **2** and possibly a di-brominated by-product. In the work-up process a slurry was made with ethanol and a recrystallization was performed using ethyl acetate. The slurry was made with 4 mL ethanol per gram of starting material, stirring for 30 minutes at 50 ℃ followed by one hour at room temperature. The solid crude was then filtered off, leaving most of the remaining substrate in the ethanol. Recrystallization gave **2** as pale-yellow

crystals in 23% yield. The MS spectrum of **2** can be seen in attachment 1. The yield was low compared to the yield of 86% achieved by F. H. Blindheim.[37] The yield might have been higher had the reaction been continued until less or no starting material was observed by TLC. Further, the time between additions of the four portions of diluted Br_2 could have been extended to ensure that the added Br_2 had sufficient time to react with **1**.

2.1.2 Synthesis of 1-((1H-indol-4-yl)oxy)-3-chloropropan-2-ol (**5**) from 1H-Indol-4-ol (**3**)

Using 1H-Indol-4-ol (**3**) as starting material, epichlorohydrin as reagent and sodium hydroxide as base, the synthesis of 1-((1H-indol-4-yl)oxy)-3-chloropropan-2-ol **(5)** was attempted (Scheme 2.2).

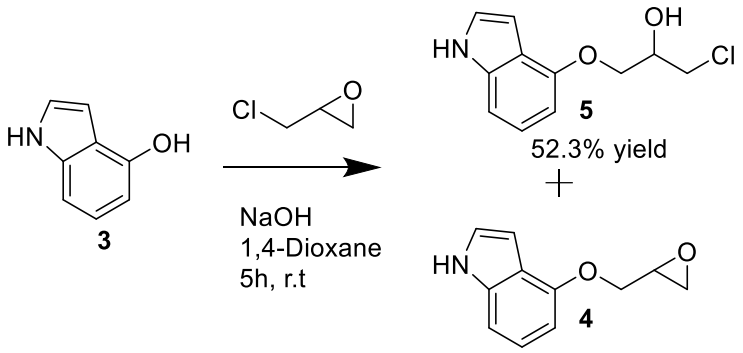

Scheme 2.2: Synthesis of 1-chloro-3-(1H-indol-4-yloxy)-propan-2-ol (**5**) and by-product 4-(oxiran-2-ylmethoxy)-1H-indole (**4**) from 1H-indol-4-ol (**3**).

Different reaction conditions were tested, shown in Table 2.1. All reactions gave the epoxide by-product 4-(oxiran-2-ylmethoxy)-1H-Indole (**4**). However, the ratio of **4** and **5** in the product mixture varied in the different reactions. All reactions were performed with a 1:1 ratio of NaOH:**3** and a 10:1 ratio of epichlorohydrin:**3**.

Table 2.1: Different reaction conditions with corresponding results for the synthesis of **5** from starting material **3**.

Reaction number	Solvent	NaOH state	Reaction time	Purity [%]	Ratio **4**:**5**[%]	Yield of **5** [%]
1	water	(aq.)	48h	nd*	nd*	nd*
2	water	(aq.)	2h	nd*	nd*	nd*
3	EtOAc/water	(s)	5h	nr*	nr*	nr*
4	water	(s)	2.5h	nr*	nr*	nr*
5	1,4-dioxane/water	(aq.)	6h	>99	75.2:24.8	7
6	1,4-dioxane/water	(aq.)	5h	86.3	27.4:58.9	52
7	1,4-dioxane/water	(aq.)	4.5h	>99	100:0	48
8	1,4-dioxane/water	(aq.)	5.5h	>99	97.2:2.7	44

**nd) Not determined*

**nr) No reaction*

In reaction 1 and 2, a small amount (<0.2 mmol) of the black starting material **3** was dissolved in a solution of water and NaOH. **3** did not dissolve in pure water but it did dissolve when the base was added, giving a black solution. After addition of epichlorohydrin, the reactions were followed by TLC, different eluent systems with ethyl acetate and pentane were tested, and a 3:10 ethyl acetate:pentane mixture was used. However, the eluent system was not suitable for separating products and starting material sufficiently.

A black precipitate was made in reaction 1, which made further work with the reaction mixture difficult. Extraction was performed with ethyl acetate, which after evaporation resulted in a brown oil. GC-MS analysis showed that the product contained both **4** and **5**, and that there was no starting material **3** left. However, **4** and **5** were produced in a very small amount and attempts of purification were not made. Reaction 2 was stopped after two hours in an attempt to avoid the precipitation of the black compound from reaction 1. Still, a small amount of the precipitate was produced. Extraction was performed with ethyl acetate, which after evaporation resulted in a brown oil. Analysis showed that there was still starting material left in the product.

In reaction 3, the starting material was dissolved in ethyl acetate, and epichlorohydrin was added. NaOH was added in solid form but did not dissolve. TLC showed no change; therefore, water was added to dissolve NaOH. Still, after five hours TLC showed no change, which was later confirmed by GC-MS [attachment 2]. The same was the result for reaction 4, where NaOH was added as a solid and not in solution, resulting in slow dissolvement of the base and the reaction was stopped after 2.5 hours [attachment 3]. In reaction 1 through 4, a darkly coloured water-phase was left after extraction. The water-phase also contained a black precipitate which was not successfully re-dissolved.

Reaction 5 through 8 were based on the reaction conditions reported by Lima *et al.* (Scheme 2.3).[16] The starting material was dissolved in 1,4-dioxane, and both NaOH (aq.) and epichlorohydrin were added. In all reactions a black precipitate was produced in the water-phase, and the product was obtained as a brown oil. The precipitate was not successfully dissolved, and it was therefore not analysed. All reactions were followed by TLC using dichloromethane as eluent.

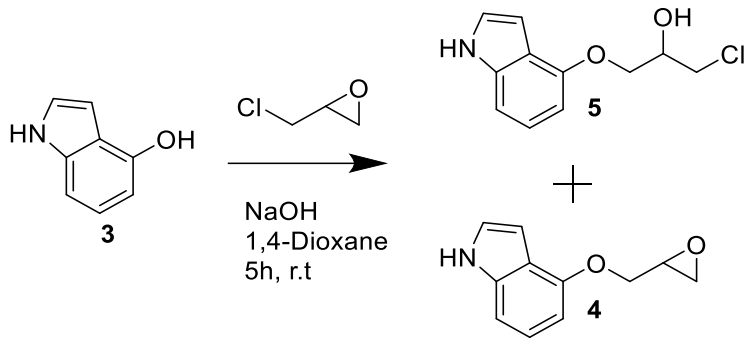

Scheme 2.3: Synthesis of 1-((1H-indol-4-yl)oxy)-3-chloropropan-2-ol (**5**) and by-product 4-(oxiran-2-ylmethoxy)-1H-indole (**4**) from 1H-indol-4-ol (**3**) as reported by Lima *et al.*[16]

Reaction 5 was ended after 6 hours. Extraction was performed with dichloromethane which was washed with ethyl acetate and water, during this process emulsions occurred, and copious amounts of solvent was used. In order to obtain separation between all phases in the funnel, the dichloromethane-phase was added first, then washed with water before ethyl acetate was added and the funnel was shaken slowly. Using this procedure gave three separate phases and a high degree of purity in the dichloromethane-phase, with little loss of product to the ethyl acetate-phase. GC-MS analysis showed pure products **4** and **5** in the dichloromethane-phase, and left-over epichlorohydrin as well as other impurities in the ethyl acetate-phase [attachment 4]. Even though the products were pure, the yield of the reaction

was very low at 7%. It was suspected that some product-loss might have occurred during the extraction, and that water-soluble by-products might have been produced.

The same reaction conditions were used in reaction 6 in an attempt to increase the yield. The reaction was ended after 5 hours, extraction was performed using dichloromethane which was washed with ethyl acetate and water. Emulsions occurred, and large amounts of solvents were used during the extraction process. The yield increased to 52.3% in 86,3% purity. Interestingly, the product showed a larger amount of **5** than earlier attempts. A new by-product was also observed, and GC-MS confirmed it to be 1,3-dichloro-2-propanol [attachment 5]. Reactions 7 and 8 were performed using the same conditions, and the same washing procedure after extraction. In these reactions, the products were obtained in high purity and medium yields. Interestingly both reactions showed low yields of product **5**. Reaction 7 yielded 100% of product **4**, and reaction 8 only gave 2.7% of product **5**, and 97.2% of product **4** [attachments 6 and 7].

In all reactions a black precipitate was formed. This precipitate was never successfully dissolved, making analysis difficult. Earlier work in the group has confirmed the formation of a dimer by-product formed by the reaction between the wanted halohydrin product and the deprotonated starting material.[47] It was hypothesised that the black precipitate observed could be a dimer, formed as suggested in Scheme 2.4.

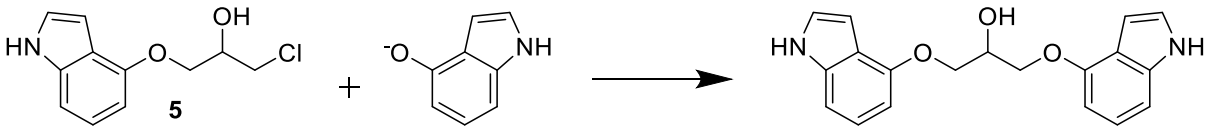

Scheme 2.4: Proposed reaction for the possible formation of a dimer by-product.

However, solid MS analysis of the black precipitate [attachment 8] showed no tall peaks at the expected mass of 322 g/mol, and the large variety of masses found in the MS analysis indicated that the precipitate contained several different compounds.

The percentages of products **4** and **5** varied greatly in all reactions. Only reaction 7 and 8 showed similar results, and both these reactions gave **4** as the main product. Seeing as all reactions were performed with the same ratios of starting material to reagents, more similar results would have been expected. Reaction times varied little, suggesting that other factors affected the results. The exact temperature and rotations per minute (rpm) were not registered

for the reactions and could have affected the result. Still, all reactions were performed in the same laboratory and temperature deviations have not been registered. An explanation for the large percentage of **4** produced in reaction 7 and 8, is the possibility of an internal reaction on product **5** depicted in Scheme 2.5. This reaction is possible because of the basic environment, where the alcohol group on **5** would be de-protonated.

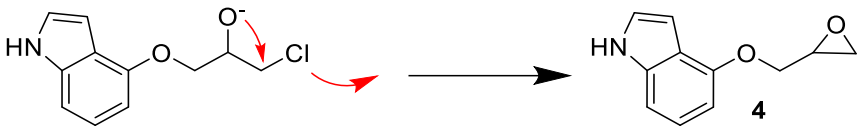

Scheme 2.5: Suggested mechanism for the formation of **4** from deprotonated product **5**.

A longer reaction time would allow for more of product **5** to convert to **4**, and therefore short reaction times were ensured by following the reactions by TLC.

2.1.3 Opening of epoxide on 4-(oxiran-2-ylmethoxy)-1H-indole (**4**) forming 1-((1H-indol-4-yl)oxy)-3-chloropropan-2-ol (**5**)

In earlier work in our research group, both LiCl and Li_2CuCl_4 had been used in the opening of epoxide functions on similar building blocks for β-blockers.[35, 37, 48] F. H. Blindheim used LiCl in acetic acid and reported a better yield in opening epoxide functions on precursors for β-blocker atenolol than previous work in our research group.[37, 48] Therefore, LiCl in acetic acid was chosen as reagents in this synthesis (Scheme 2.6).

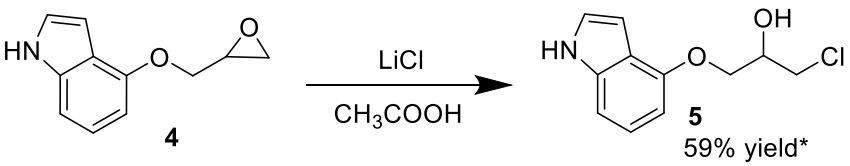

*calculated over two synthesis steps

Scheme 2.6: Opening of epoxide on 4-(oxiran-2-ylmethoxy)-1H-indole (**4**) forming 1-((1H-indol-4-yl)oxy)-3-chloropropan-2-ol (**5**), using LiCl in acetic acid.

In this reaction, different ratios of starting material to reagents were tested. Reaction conditions and results are presented in Table 2.2.

Table 2.2: Different reaction conditions with results for the synthesis of **5** from **4**.

Reaction number	Solvent	Equivalents of LiCl	Equivalents of AcOH	Reaction conditions	Purity [%]	Ratio **4**:**5**[%]	Yield [%]
1	CH_2Cl_2	1	5	r.t. 24h	nr*	nr*	nr*
2	THF	1	5	r.t. 3h	70.9	29.0:70.9	nd*
3	THF	1	10	r.t. 7h	75.4	24.5:75.4	nd*
4	THF	2	10	r.t. 72h	88.7	7.8:88.7	59[a]
5	THF	2	10	r.t. 143h	40.9	25.3:40.9	18[a]
6	THF	2	10	30℃, 6h	93.1	2.0:93.1	20[b]
S1	THF	1	10	r.t 36h	89	4.7:89	nd*

**a) Calculated over two steps*

**b) Calculated over three steps*

**nd) Not determined*

**nr) No reaction*

In all reactions, dichloromethane was used as eluent in the TLC analyses. All reactions were quenched by neutralizing the pH by use of $CaCO_3$. Extraction was performed with dichloromethane. In all reactions, except reaction 1, the colour of the solution changed from light brown to a red-brown colour.

In reaction 1, dichloromethane was used as solvent because it dissolved both **4** and **5** well. However, dichloromethane did not dissolve the lithium salt and no reaction was observed by TLC. In reaction 2, THF was used as solvent as had been done in earlier work in the research group. One equivalent of lithium salt was used, and five equivalents of acetic acid. After three hours the reaction was ended, and some conversion of **4** to **5** was found. Still, full conversion was not achieved [attachment 9]. Therefore, the amount of acetic acid was increased to ten equivalents in reaction 3. Little change was observed, and after 7 hours the reaction was ended. The percentage of **5** was higher than the previous reactions, but this could be due to the longer reaction time [attachment 10]. Still, full conversion was not observed.

In reaction 4, the amount of LiCl was doubled to two equivalents and acetic acid was held at ten equivalents. Reaction time was increased greatly, as TLC showed that full conversion was not achieved after 24h or 36h. The final reaction time was 72 hours and the amount of **5** was reported at 88.7% purity in 59% yield (calculated over two steps) [attachment 11]. Seeing as full conversion was still not achieved, the products from reaction 2 through 4 where used as starting materials in another attempt, reaction S1. Seeing as this starting material contained more **5** than **4**, only one equivalent of LiCl was used. The amount of acetic acid was held at 10 equivalents. At the same time, reaction 5 was started with the same conditions as reaction 4. Reaction 5 was stirred for 143 hours and still full conversion was not observed. The yield from reaction 5 was low, and the ratio of **4** to **5** had changed little [attachment 12]. In reaction S1, compound **4** was no longer observed by TLC after 36 hours and the reaction was ended. GC-MS analysis showed some of compound **4** still left in the mixture, as well as other impurities. Therefore, the product from S1 was purified by flash-chromatography using dichloromethane as eluent. Compound **5** was obtained in 89% purity, with 4.7% of **4** still left in the product [attachment 13]. After purification by flash-chromatography, **5** was obtained as a slightly yellow oil.

During the flash-chromatography, a red compound was observed in the column that did not eluate when dichloromethane was used as eluent. A change of eluent to methanol gave the compound as a red solid after evaporation. GC-MS analysis showed that the compound was not starting material, solvent or reagents [attachment 14]. Seeing as reaction 5 did not show full conversion, the product from this reaction was used in reaction 6. Here, the temperature was increased to 35℃ in an attempt to shorten the reaction time. After purification by flash-chromatography, **5** was obtained in 93.1% purity as a slightly yellow oil. Here too, the red by-product was observed in the column, and methanol was used to eluate it. MS analysis of the red compound gave no clear indication of structure, and probably it consists of a mixture of compounds [attachment 14].

2.1.4 Synthesis of racemic ester 1-((1H-indol-4-yl)oxy)-3-chloropropan-2-yl butyrate (**6**) from 1-((1H-indol-4-yl)oxy)-3-chloropropan-2-ol (**5**)

Small amounts of racemic ester **6** were produced in order to study separation of the enantiomers in chiral HPLC. **5** was used as starting material, butyric anhydride as reagent and pyridine was used as both base and solvent (Scheme 2.7).

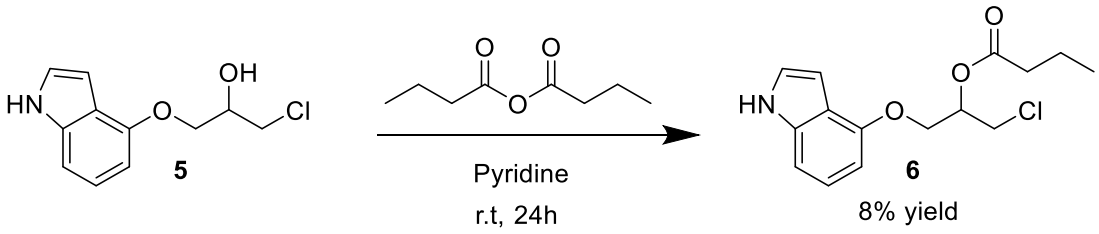

Scheme 2.7: Formation of 1-((1H-indol-4-yl)oxy)-3-chloropropan-2-yl butyrate (**6**) from 1-((1H-indol-4-yl)oxy)-3-chloropropan-2-ol (**5**) using butyric anhydride and pyridine as reagents.

The reaction was stirred at room temperature for 24 hours, after which the product was extracted using hexane and washed with brine. The reaction yielded 8% of **6**, which was very low. Chiral HPLC analysis showed that there was still 77.5% of starting material **5** left [attachment 15]. The low yield was probably due to the lack of 4-dimethylaminopyridine (DMAP) as co-reagent with pyridine, and because of the short reaction time. Austli achieved a yield of 86% in the synthesis of 1-(4-acetamidophenoxy)-3-chloropropan- 2-yl butyrate using butyric anhydride as reagent and pyridine with DMAP in a reaction lasting 48h.[47]

Several eluent systems were tested in order to separate the esters on a Chiralcel OD-H column, however, baseline separation of the esters was not achieved. A system with 2-propanol:hexane (20:80) was chosen as it allowed the identification of two peaks, although the peaks were not fully separated. The chromatogram can be seen in Figure 2.1, enantiomers of compound **6** are represented at retention times 13.8 minutes and 14.5 minutes (R_s = 1.2).

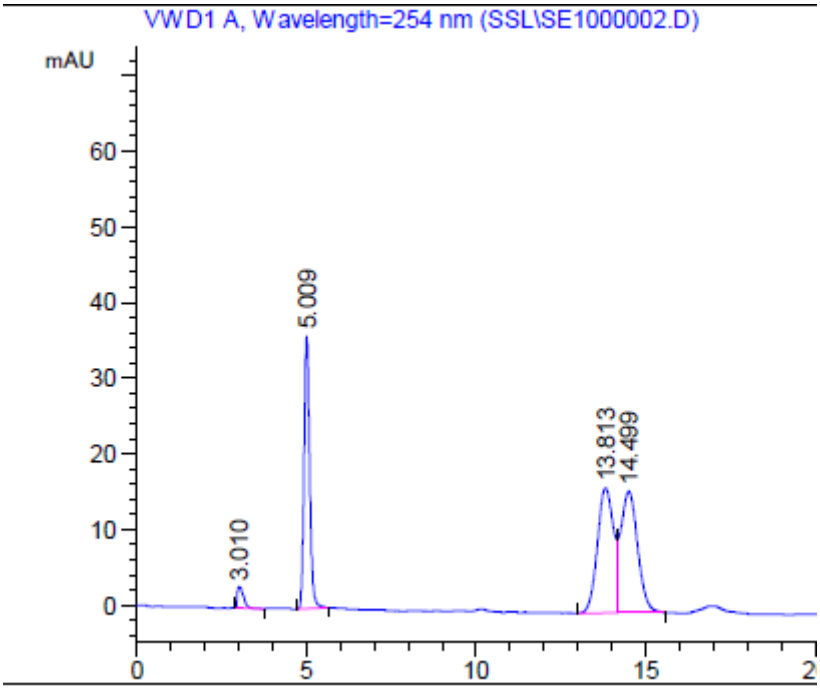

Figure 2.1: HPLC analysis of racemic ester **6** (t_R = 13,8 and 14,5 minutes) with Chiralcel OD-H column and hexane:2-propanol (80:20), 1 mL/min flow.

2.2 Kinetic resolutions in synthesis of an enantiopure building block for (*S*)-pindolol

2.2.1 Acylation of 1-((1H-indol-4-yl)oxy)-3-chloropropan-2-ol (**5**)

The kinetic resolution of **5** using CALB in dry dichloromethane with vinyl butyrate as reagent was performed in an incubator at 30 ℃ and 200 rpms (Scheme 2.8).

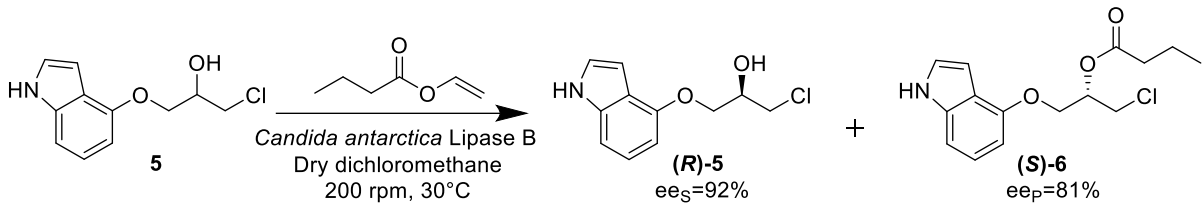

Scheme 2.8: Kinetic resolution of **5** forming (*S*)-**6** and (*R*)-**5**, using CALB and vinyl butyrate as acyl-donor in dry dichloromethane.

Three different parallels were tested with different amounts of **5** and CALB. In all parallels, 5 equivalents of vinyl butyrate were used. An overview of the amounts used, as well as the reaction times until 50% conversion, are shown in Table 2.3

Table 2.3: Amounts of **5** and immobilized CALB used in three different kinetic resolution parallels, as well as the reaction time until 50% conversion.

Reaction number	Amount of **5** [mg]	Amounts of CALB [mg]	Hours until 50% conversion
1	20.6	10.0	312
2	16.0	15.0	98
3	18.5	36.8	24

Chiral HPLC analyses were performed to follow the course of the reactions. Morante-Zarcero *et al.* reported that (*S*)-pindolol ((*S*)-**7**) were the most retained of the two enantiomers in their chiral HPLC analysis.[56] They used a column of 250 mm length and 4.6 mm in diameter, using Lux Cellulose-1/Sepapak-1 composed by cellulose tris-(3,5-dymethylphenylcarbamate) coated on a 5 mm silica-gel particle supplied by Phenomenex as the chiral stationary phase. In this thesis, a Chiralcel OD-H column of 250 mm length and 4.6 mm in diameter, with 5 µm particle size has been used. (*R*)-**5** shares the same spatial arrangement as (*S*)-**7**, and it was therefore expected that (*R*)-**5** would be the most retained of the two enantiomers. Further, CALB is often selective towards the (*S*)-configuration of the halohydrins that are precursors

for β-blockers.[47-48] Therefore, if chiral-HPLC analyses during a transesterification showed a decrease in peak-area for the least retained enantiomer of **5,** it would support this expectation. Chiral HPLC analyses of reaction 3 is used here as an example, and chromatograms from reaction time four hours and thirty hours can be seen in Figure 2.2 and Figure 2.3. At four hours reaction time, the chromatogram shows unknown impurities at t_R= 3.0 minutes, 9.5 minutes, 10.1 minutes and 16.7 minutes. Enantiomers of **5** are represented by peaks at t_R= 22.0 minutes and t_R= 48.9 minutes (R_s = 17.8). Enantiomers of **6** are represented by the asymmetric peak at t_R=14.5 minutes. At thirty hours reaction time, the chromatogram shows unknown impurities at t_R= 3.0 minutes, 4.6minutes and 7.2 minutes. Enantiomers of **5** are represented by peaks at t_R= 22.5 minutes and t_R= 50.7 minutes. As can be seen from comparing Figure 2.2 and Figure 2.3, the peak at t_R= 22.5 minutes has decreased greatly in size, while the most retained peak has decreased little. This supported the earlier hypothesis, and it was assumed that the most retained enantiomer of **5** was (*R*)-**5**. In Figure 2.3, two peaks that are not baseline separated can be seen at t_R= 14.0 minutes and t_R= 14.7 minutes. These peaks represent the enantiomers of **6**. Considering the observed decrease in the amount of (*S*)-**5**, it was presumed that the peak with t_R= 14.7 minutes represented (*S*)-**6** and that the peak with t_R= 14.0 minutes represented (*R*)-**6**.

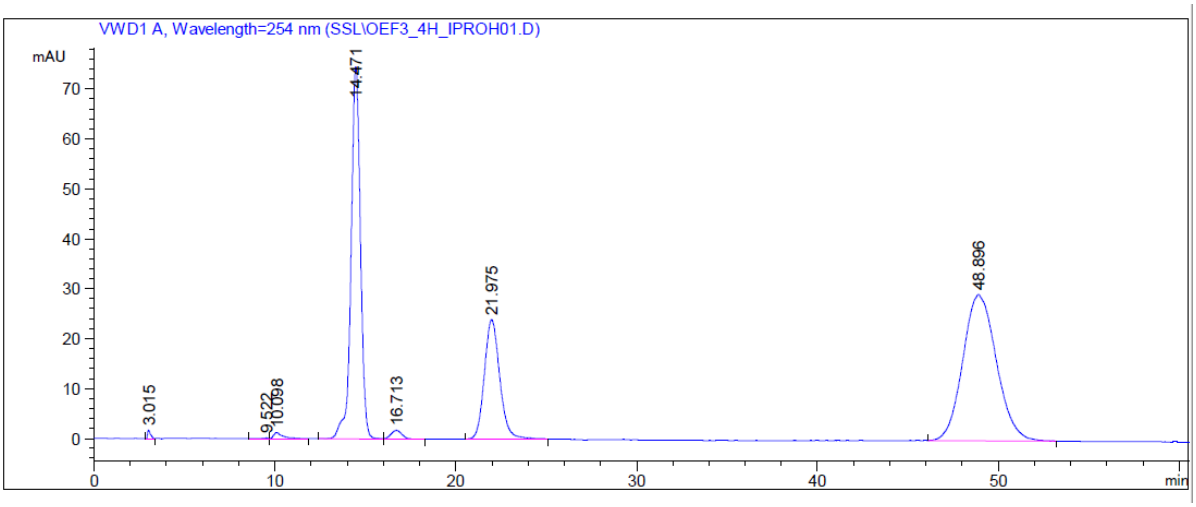

Figure 2.2: Chromatogram from chiral HPLC analysis of reaction 3 (see Table 2.3) after four hours reaction time. (*R*)-**5** has t_R=48.9 minutes and (*S*)-**5** has t_R=22.0 minutes. The racemic esters **6** are represented by the asymmetric peak at t_R=14.5 minutes (Chiralcel OD-H column and hexane:2-propanol (80:20), 1 mL/min flow.).

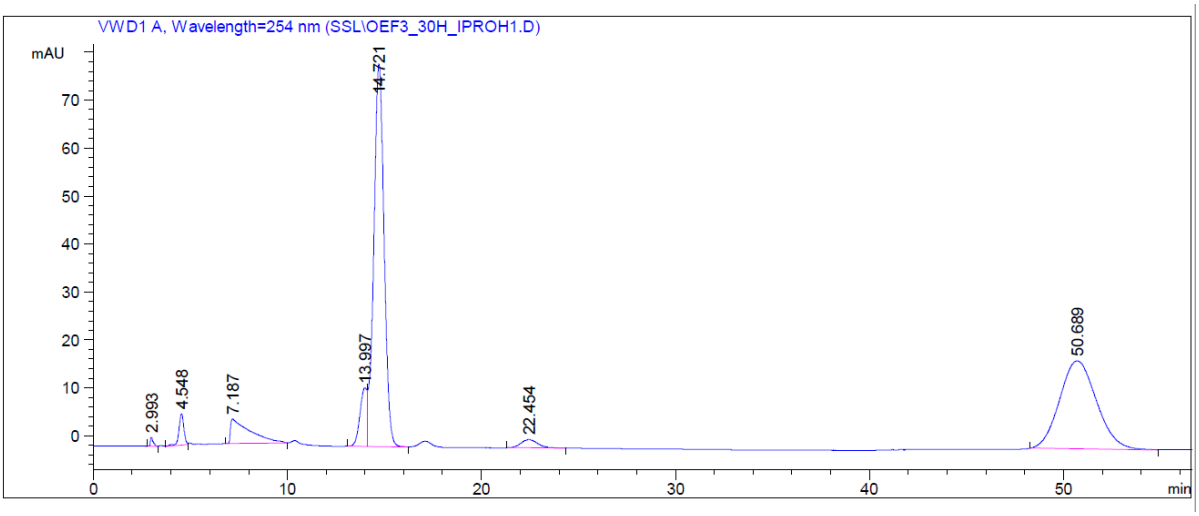

Figure 2.3: Chromatogram from chiral HPLC analysis of reaction 3 (see Table 2.3) after thirty hours reaction time. (*R*)-**5** has t_R=48.9minutes and (*S*)-**5** has t_R=22.0 minutes. (*S*)-**6** has t_R=14.7 minutes and (*R*)-**6** has t_R=14.0 minutes (Chiralcel OD-H column and hexane:2-propanol (80:20), 1 mL/min flow.).

In reactions 1-3, the amounts of CALB were 0.5, 1, and 2 mass equivalents of **5** respectively. The amounts of CALB were increased in reaction 2 and 3 to shorten the reaction time, and reaction 3 reached 50% conversion (c) after 24 hours. Chiral HPLC chromatograms were used to calculate ee_p, ee_s and c. The chromatograms and calculations for reaction 1 and 2 at ca. 50% conversion can be seen in attachments 16 and 17 respectively. For reaction 3, ee_p, ee_s and c were not only calculated at 50% conversion, but also at different conversion percentages. These values were used to calculate both an E-value of 66 for the reaction and graphs showing the change in ee_p and ee_s at different points of conversion (Figure 2.4). The squares in Figure 2.4 represent the datapoints calculated from chromatograms [attachment 18], the curves represent the datapoints calculated by an E&K calculator 2.1b0 PCC.

As can be seen from Figure 2.3, the enantiomers of **6** are not separated at the baseline, and manual integration was used to separate the two peaks. This adds uncertainty to the calculations performed for reaction 3. It was hoped that **6** could be separated from **5** by flash-chromatography and then hydrolysed back to the halohydrin in order for chiral HPLC analyses to show the correct areas for each enantiomer. Therefore, the hydrolysis of **6** was attempted using CALB as will be described in chapter 2.2.2. The results of this hydrolysis showed that CALB could not be used to hydrolyse both enantiomers. A synthetic hydrolysis of **6** should be performed in future work in order to gather the correct areas of the produced esters and thereby achieve correct calculations. Still, the results calculated for reaction 3 in

the kinetic resolution of **5** are interesting, and they give a strong indication of the enantioselectivity for CALB in this acylation.

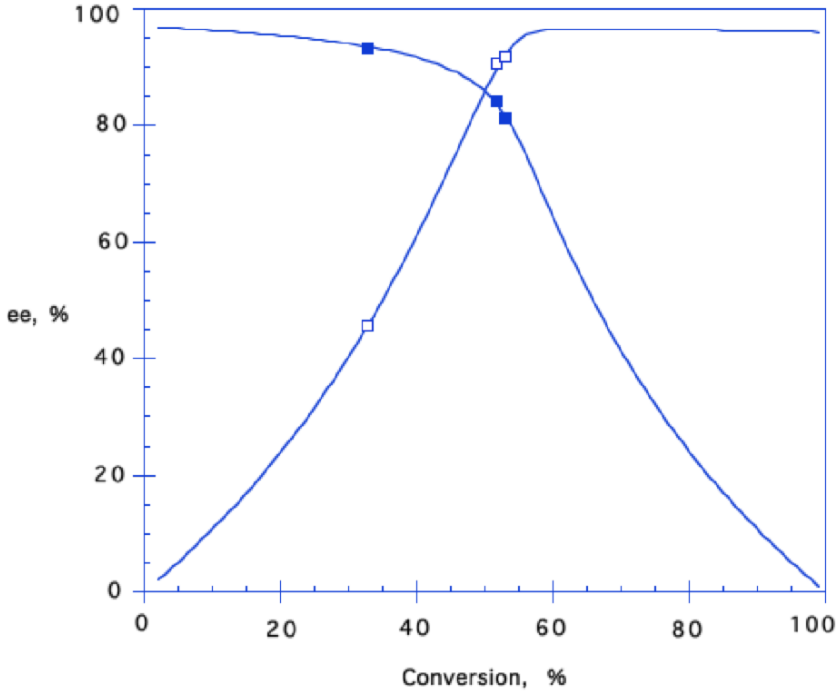

Figure 2.4: Graphical illustration of the change in ee_p (graph with filled squares) and ee_s (graph with unfilled squares) at different degrees of conversion for the kinetic resolution of **5** using CALB in acylation with E-value 66. The squares represent the datapoints calculated from chromatograms [attachment 15], the curves represent the datapoints calculated by an E&K calculator 2.1b0 PCC.

Lima *et al.* reported an E-value of 30 in the hydrolytic kinetic resolution of racemic esters **6** using Novozyme® 435[16], which is CALB immobilized on acrylic resin[57]. They used lipase from *Pseudomonas fluorescens* in acetylation of racemic **5**, reporting several E-values for different parallels performed. In the parallel where 50% conversion was reached, they reported an E-value of 11, an ee_s of 72% and ee_p of 69%. In this thesis an E-value of 66 was achieved for the acylation of **5** using CALB, and at 53% conversion ee_s and ee_p values were at 92% and 81% respectively.

Future work with these compounds should include crystallography in order to determine whether the hypothesis regarding elution order of enantiomers of both **5** and **6** is correct. This could also be used to confirm or confute the selectivity of CALB. Future work could also include measurements of optical rotations of enantiomers, which were not measured in this thesis.

2.2.2 Hydrolysis of 1-((1H-indol-4-yl)oxy)-3-chloropropan-2-yl butyrate (**6**)

Since the enantiomers of **6** were not separated on the Chiralcel OD-H column, the possibility of using CALB to hydrolyse the ester **6** to halohydrin **5** was investigated (Scheme 2.9). It was hoped that the products from the transesterifications could be separated by flash-chromatography before being hydrolysed back to the halohydrin **5**, which in turn could give the exact percentages of each enantiomer through chiral HPLC analysis.

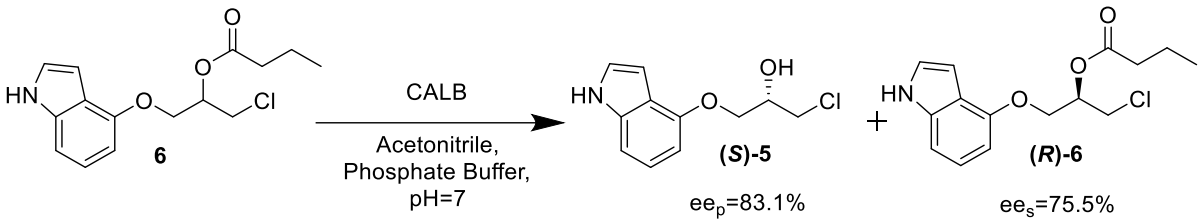

Scheme 2.9: Hydrolysis of **6** using CALB in phosphate buffer (pH=7) and acetonitrile as co-solvent.

The ester **6** was dissolved in acetonitrile, which was used as co-solvent together with a phosphate buffer (pH 7). CALB was added and the mixture was placed in an incubator at 30 C at 200 rpms. CALB had shown selectivity towards (*S*)-**5** in the transesterifications, hence a selectivity towards (*S*)-**6** was expected from the hydrolysis. Considering that hydrolyses are performed in buffer, there are generous amounts of water available for the enzyme and the water activity is high. Therefore, hydrolyses with enzymes are often much faster than the reactions performed in organic solvents. It was therefore hoped that, even though CALB had shown selectiveness toward the (*S*)-halohydrin, it would still hydrolyse both enantiomers of **6** given enough time. However, chiral HPLC showed that after 48 hours conversion was only at 47%, %ee_p and %ee_s were at 83.1% and 75.5% respectively [attachment 16].

2.3 Kinetic resolutions in hydrolysis of **9**, a possible precursor of vitamin K_2

2.3.1 Hydrolysis of 2-((2E,6E,10E,14E,18E,22E)-3,7,11,15,19,23,27-heptamethyloctacosa-2,6,10,14,18,22,26-heptaen-1-yl)-3-methylnaphthalene-1,4-diyl dipropionate (**9**)

Starting material **9** has two ester-groups which could be subject to hydrolysis by lipase catalysis. Depending on whether both or only one of the ester-groups would be hydrolysed, three possible products could be the outcome (Scheme 2.10). Because of the alcohol groups on the possible products, it was expected that potential products would eluate before the starting material in RF-HPLC analysis.

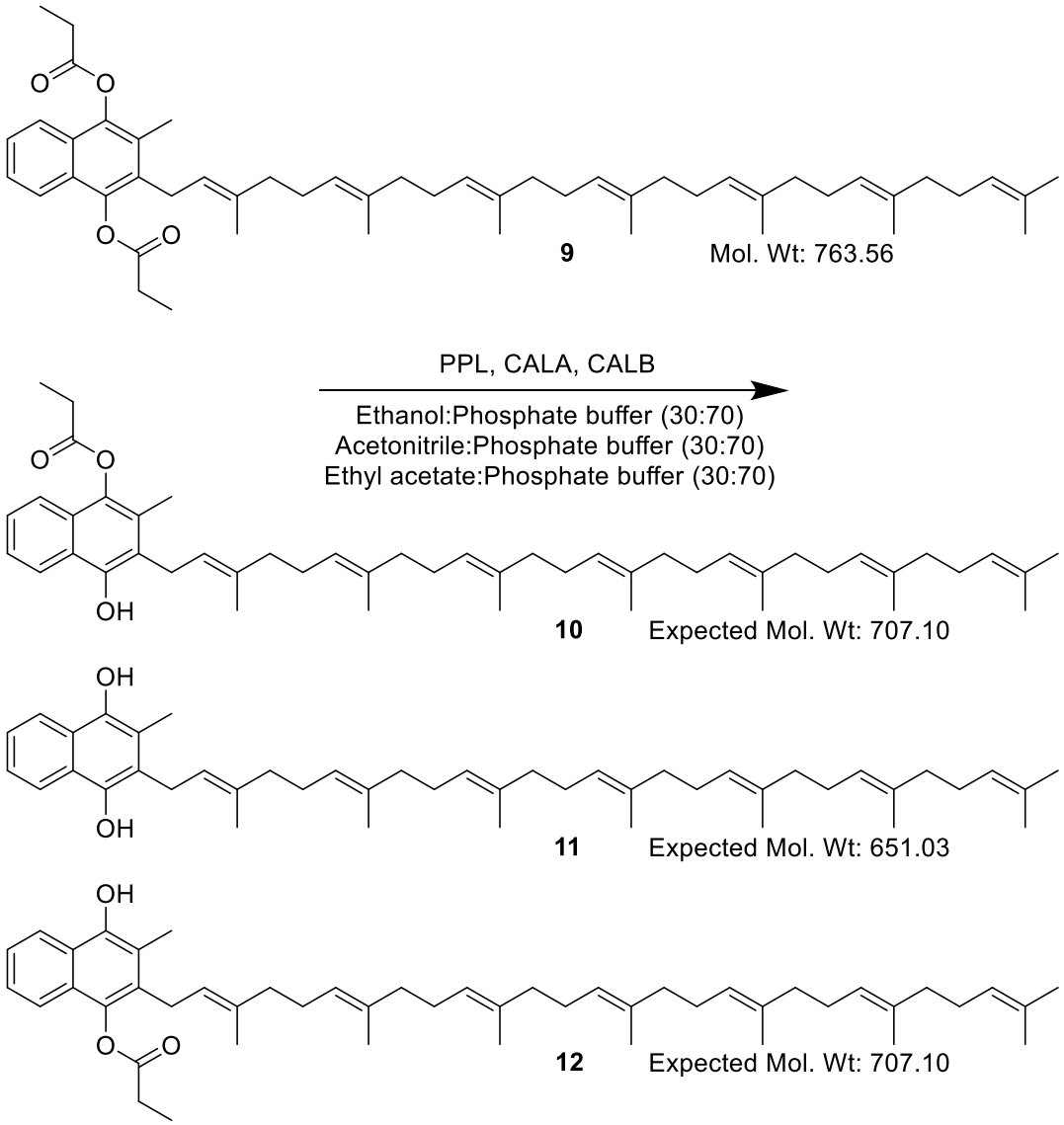

Scheme 2.10: Hydrolysis of **9** with the enzymes and solvent systems tested, showing possible products **10**, **11** and **12** with expected molecular weights.

Firstly, solubility tests were performed for starting material **9** to find possible co-solvents for the hydrolysis and to find suitable mobile phases for HPLC analysis. Compound **9** was found to be easily dissolved in ethyl acetate, and it also dissolved in acetonitrile and ethanol.

For reversed-phase HPLC (RF-HPLC) analysis, several gradients with acetonitrile and water were tried first. However, compound **9** did not elute. Using 100% acetonitrile in an isocratic analysis successfully eluted **9** after 78.6 minutes [attachment 20]. RF-HPLC analyses were performed on an Eclipse XDB - C18 column (Agilent Technologies, 4.6 x 150 mm ID, 5 μm particle size).

Three different co-solvents were tested; ethanol, acetonitrile and ethyl acetate, as well as three different lipases; CALA, CALB and PPL type II. An overview of the reactions can be seen in Table 2.4. Solvent systems were composed of 70% phosphate buffer and 30% co-solvent. Samples were collected at regular time intervals for HPLC analysis, and all reactions were monitored for 48 hours before they were ended.

Table 2.4: Overview of co-solvents and enzymes tested in the hydrolysis of **9** as seen in Scheme 2.10

Reaction number	Co-solvent	Enzyme	Comment on product formation
1	EtOH	PPL	npo*
2	EtOH	CALA	npo*
3	EtOH	CALB	npo*
4	MeCN	PPL	npo*
5	MeCN	CALA	npo*
6	MeCN	CALB	npo*
7	EtOAc	PPL	npo*
8	EtOAc	CALA	npo*
9	EtOAc	CALB	clear crystalline solid
10	EtOAc	CALB	clear crystalline solid
11	EtOAc	CALB	clear crystalline solid

**npo= no products observed*

In reaction 1-3, no products were observed by RF-HPLC analysis [attachment 21]. The same was the case for reaction 4-6 [attachment 22]. In reaction 7-9, no products were observed by RF-HPLC analyses [attachment 23], however a clear precipitate in crystalline form was

observed in reaction 9. Therefore, two more reactions, 10 and 11, were performed with the same reaction parameters as reaction 9. The crystals appeared in all three parallels.

In order to analyse the crystals, solubility tests were performed. The crystals did not dissolve in methanol, ethanol, 2-propanol, dichloromethane, ethyl acetate, acetonitrile, tetra hydro furan, 1,4-dioxane, dimethyl sulfoxide, acetone, pyridine, ethyl acetoacetate, pentane or hexane. The crystals precipitated in the buffer, therefore it was unexpected that the crystals dissolved in water. NMR analyses of the crystals using D_2O was attempted, however both ^{1}H and ^{13}C spectra showed no peaks apart from those of the solvent. The water solubility and the clear NMR spectra lead to the speculation that the crystals could be an inorganic salt. Another possibility is that the crystals did not dissolve properly in D_2O or re-precipitated in D_2O after being dissolved for NMR analyses.

The crystals were only observed in reactions with ethyl acetate as co-solvent and CALB as enzyme, indicating that the production of crystals was dependent on the reagents in the reaction. Solid MS analysis of the precipitate gave 663 g/mol as the highest mass [attachment 24]. Which did not fit with any of the expected products **10**, **11** or **12** (Scheme 2.10). The mass is also too high to be either K_2HPO_4 and KH_2PO_4, which was used to make the buffer. Compound **11** with two hydroxy-groups has an expected mass of 651.03 g/mol and could by saturation of six double bonds reach the found mass of the crystals. However, CALB has not been reported to saturate double bonds or to generate salts.

The MS analysis of the crystals also show possible chemical formulas that fit the spectrum. However, none of the suggested chemical formulas were found to fit with a hydrolytic process. Two of the suggested chemical formulas contained phosphorus. However, for phosphorous to be part of the structure, the number of carbons would have to be reduced by more than the six carbons in the ester-groups, which was judged to be unlikely.

To ensure the correct molecular structure of starting material **9**, MS analysis and NMR analysis were performed. MS confirmed the structure with a molecular weight of 763,56 g/mol [attachment 25]. NMR spectra were compared with spectra from SyntheticaA/S & Kappa Bioscience A/S, and the characterization can be seen in chapter 2.4.5.

The crystals have not been determined in this thesis. In future work the solubility of the crystals should be tested again, using larger amounts of solvents. If the crystals can be dissolved it would allow for further analysis. The use of different buffers should also be investigated.

2.4 Compound characterization

Compounds in this thesis have been characterized using NMR analyses. The characterization of compound **2** will be explained first in detail. The same procedure has been used in characterizing the following compounds as well, but it will not be described in the same detail. To determine the chemical shifts of common solvents and impurities, data reported by Fulmer *et al.* have been used.[58]

2.4.1 Determination of 1-(4-amino-3,5-dichlorophenyl)-2-bromoethan-1-one (**2**).

1-(4-amino-3,5-dichlorophenyl)-2-bromoethan-1-one (**2**) was determined by NMR using $CDCl_3$ as solvent. **2** with numbered positions can be seen in Figure 2.4.1.

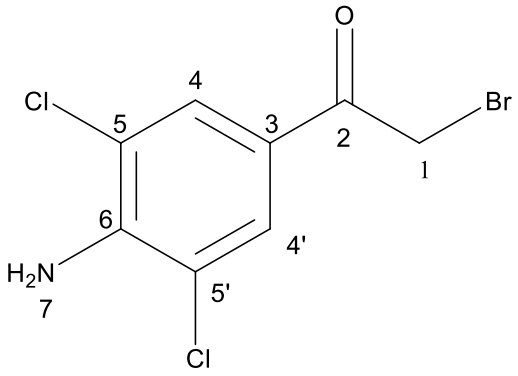

Figure 2.4.1: Structure of 1-(4-amino-3,5-dichlorophenyl)-2-bromoethan-1-one (**2**), with numbered positions correlating to NMR-shifts in Table 2.4.1.

^{1}H NMR of **2** (Figure 2.4.2) shows several peaks, where the NMR solvent $CDCl_3$ is represented by a peak at 7.26 ppm. A water peak can be seen at 1.56 ppm and a small acetone peak at 2.17 ppm. The peak at 2.49 ppm has an integral that is too small to be part of compound **2** and is an unknown impurity. The three remaining singlets represent three different spin systems that are too far from other systems to experience coupling, therefore no *J*-constants are observed. Further, no correlation is shown in the COSY spectrum (Figure 2.4.4) indicating that the protons are too far away to show correlation. On compound **2**, protons are situated on positions 1, 4, 4'and 7, where the protons at position 4 and 4' are expected to share the same shift. The singlet at 5.06 ppm is a broad peak, which is characteristic for amines, and corresponds to the two protons at position 7. Further, the two protons at positions 4 and 4' are aromatic protons represented by the shift at 7.86 ppm. The

last peak at 4.31 ppm corresponds to the two protons at position 1. The three peaks represent two protons each, which is shown by the integrals that are all close to equal in size.

The ^{13}C NMR of **2** (Figure 2.4.3) shows seven peaks, where $CDCl_3$ is represented by the peak at 77.16 ppm. The other six peaks represent the six different carbon positions on compound **2**. The HSQC spectrum (Figure 2.4.5) shows that the protons on position 1 with proton-shift 4.31 ppm are situated on the carbon with shift 29.9 ppm. It also shows that the protons on position 4 and 4' are situated on the carbons with shift 129.3 ppm. The carbon on position 2 is expected to have a high shift because of the carboxy-group, and it is represented by the carbon shift at 188.1 ppm. The carbon at position 6 has a neighbouring amino group and is represented by the second highest shift at 144.9 ppm. Two carbon shifts remain unassigned at this point, 123.9 ppm and 118.9 ppm. The HMBC spectrum (Figure 2.4.6) shows that only the peak at 123.9 ppm has correlation with protons at position 1. Hence, the peak at 123.9 ppm represents the carbon at position 3, and the peak at 118.9 ppm represents the carbon at position 5.

Table 2.4.1: NMR correlations for **2**, numbered positions corresponds to Figure 2.4.1. Spectra are shown in Figures 2.4.2-2.4.6.

Position	**^{1}H [ppm], (mult., int., ^{n}J[Hz])**	**^{13}C[ppm]**	**COSY**	**HMBC**
1	4.31 (s, 2H, -)	29.9	-	-
2	-	188.1	-	1,4,4'
3	-	123.9	-	1,4,4'
4/4'	7.86 (s, 2H, -)	129.3	-	1
5/5'	-	118.9	-	4,4'
6	-	144.9	-	4,4'
7	5.06 (s, 2H, -)	-	-	-

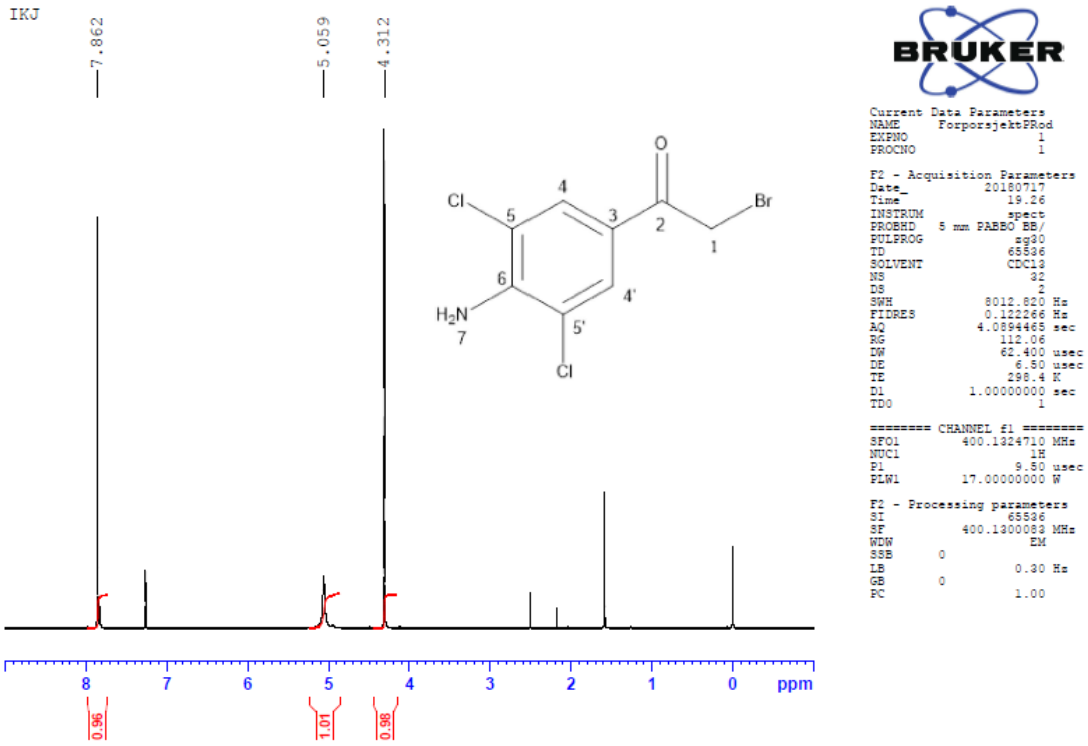

Figure 2.4.2: ^{1}H NMR spectrum for 1-(4-amino-3,5-dichlorophenyl)-2-bromoethan-1-one (**2**). See Table 2.4.1 for peak assignments.

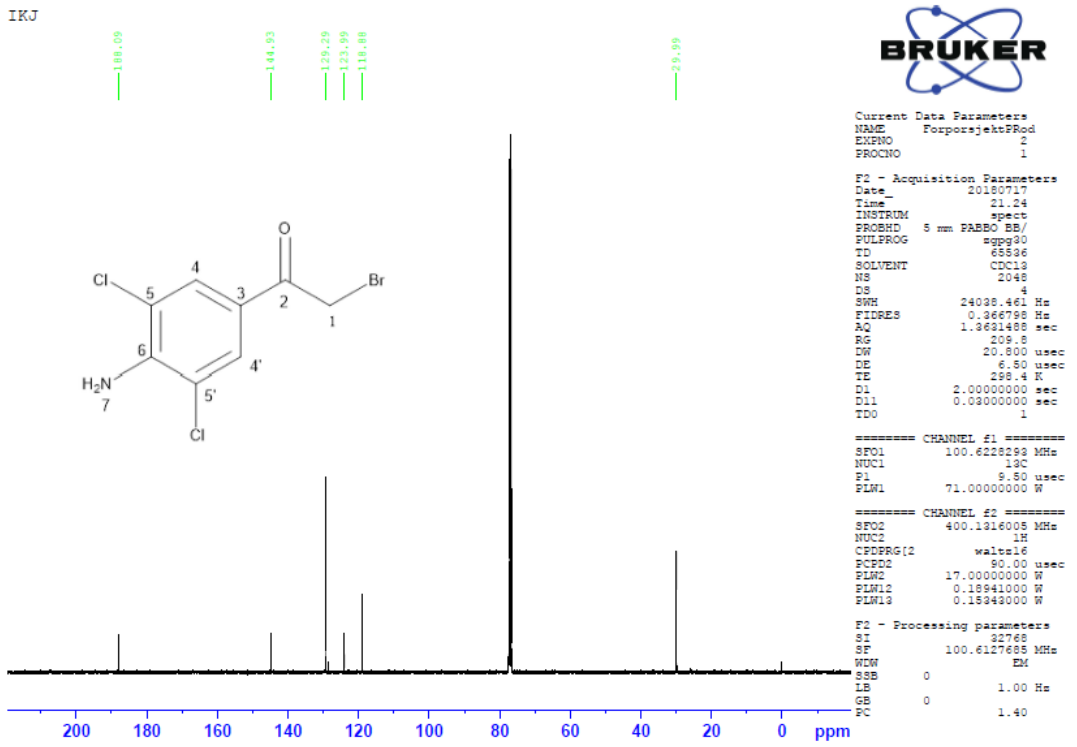

Figure 2.4.3: ^{13}C NMR spectrum for 1-(4-amino-3,5-dichlorophenyl)-2-bromoethan-1-one (**2**). See Table 2.4.1 for peak assignments.

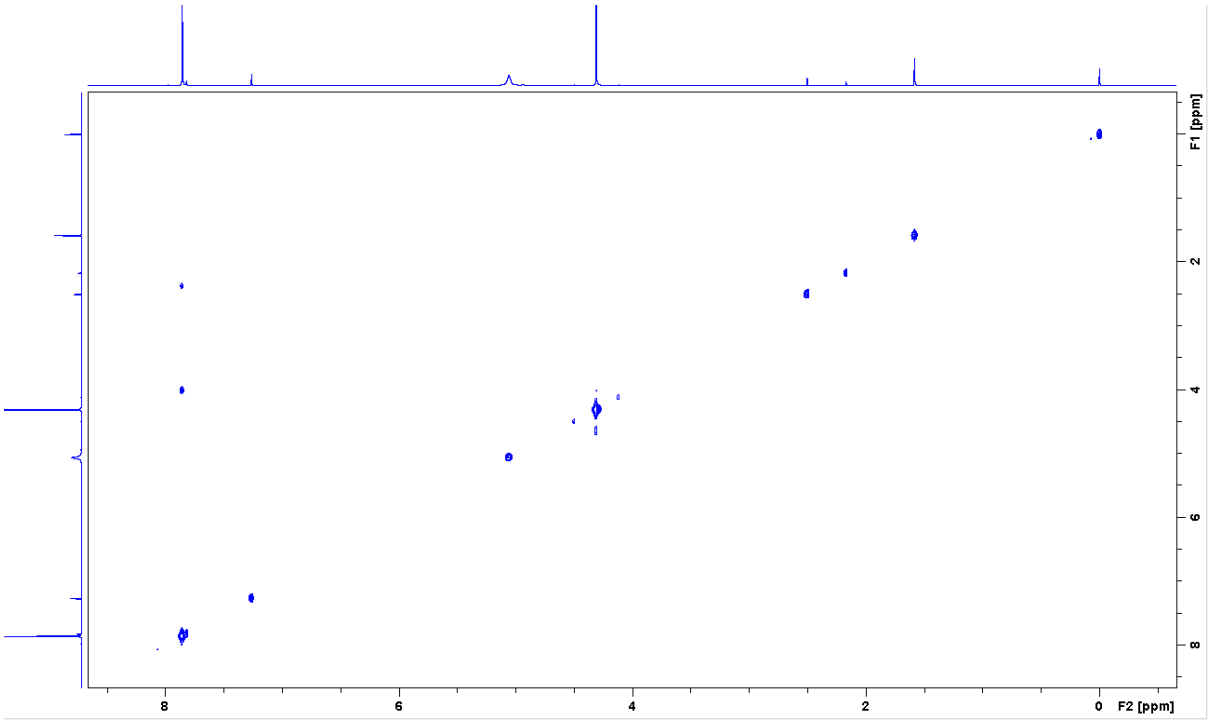

Figure 2.4.4: COSY spectrum for 1-(4-amino-3,5-dichlorophenyl)-2-bromoethan-1-one (**2**). See Table 2.4.1 for peak assignments.

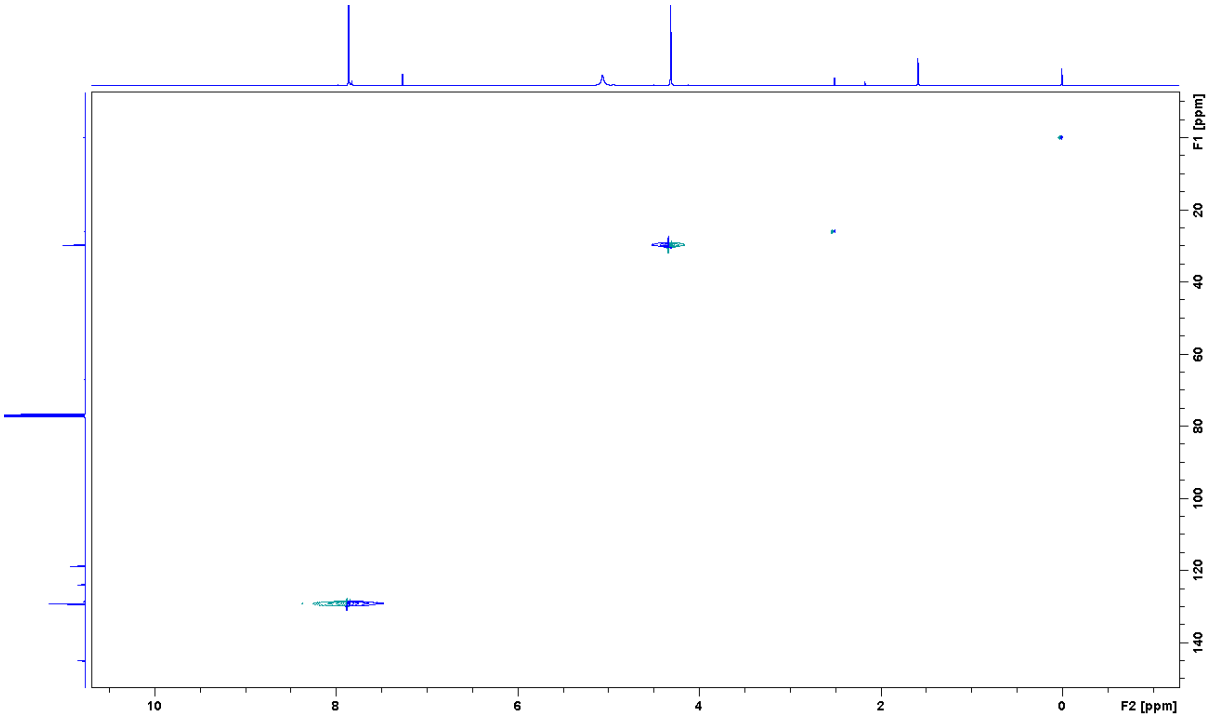

Figure 2.4.5: HSQC spectrum for 1-(4-amino-3,5-dichlorophenyl)-2-bromoethan-1-one (**2**). See Table 2.4.1 for peak assignments.

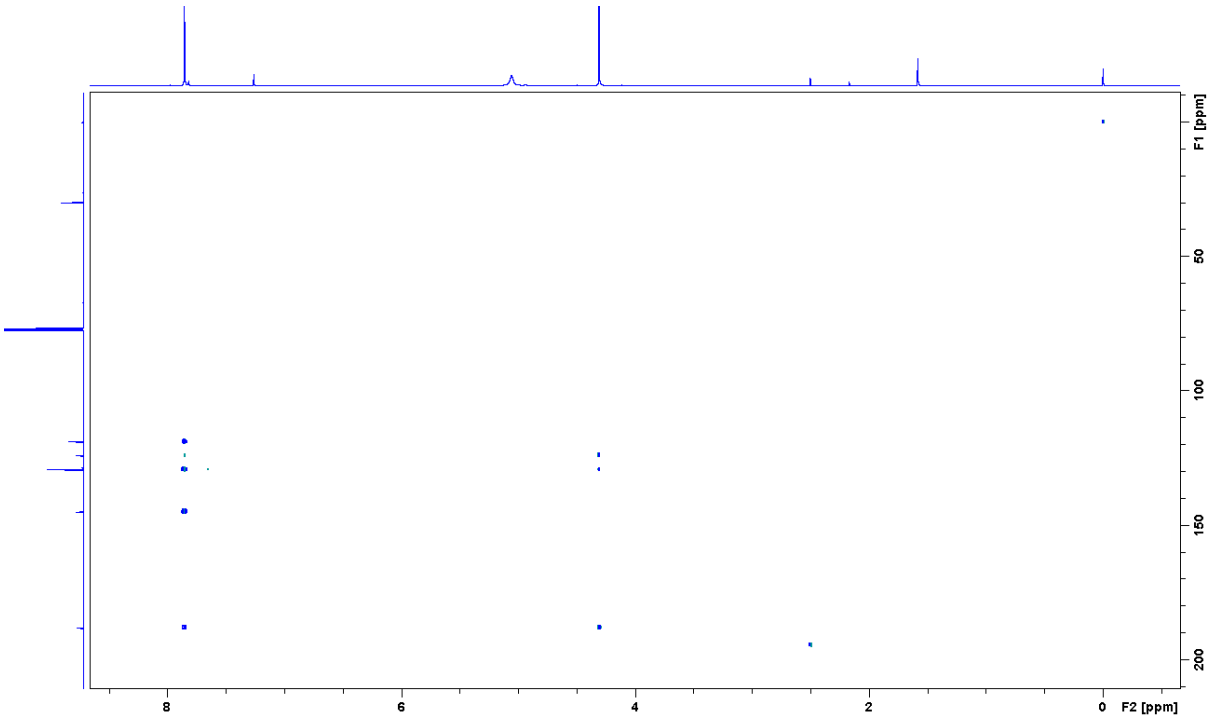

Figure 2.4.6: HMBC spectrum for 1-(4-amino-3,5-dichlorophenyl)-2-bromoethan-1-one (**2**). See Table 2.4.1 for peak assignments.

2.4.2 Determination of 4-(oxiran-2-ylmethoxy)-1H-indole (**4**)

4-(oxiran-2-ylmethoxy)-1H-indole (**4**) was determined by NMR using $CDCl_3$ as solvent. **4** with numbered positions can be seen in Figure 4.2.7.

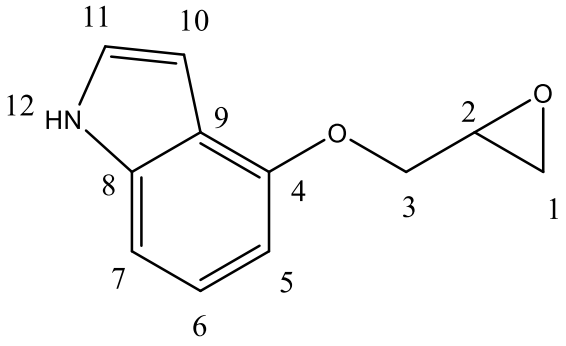

Figure 2.4.7: Structure of 4-(oxiran-2-ylmethoxy)-1H-indole (**4**)), with numbered positions correlating to NMR-shifts in Table 2.4.2.

^{1}H NMR of **4** (Figure 2.4.8) shows the solvent peak at 7.26 ppm, a water peak at 1.56 ppm, an acetone peak at 2.18 ppm and two unknown impurities at 5.34 ppm and 5.62 ppm. Assignment of peaks at the positions shown in Figure 2.4.7 can be seen in Table 2.4.2. The ^{13}C spectrum can be seen in Figure 2.4.9, where the solvent peak can be seen at 77.16 ppm.

The HSQC spectrum (Figure 2.4.11) was used to assign proton-shifts to carbon-shifts. The COSY spectrum (Figure 2.4.10) and the HMBC spectrum (Figure 2.4.12) were used to determine the neighbouring environments of the different positions. Zielinska-Pisklak *et al.* have studied the NMR characteristics of different β-blockers, including those of Pindolol. The assignments for the aromatic rings shown in Table 2.4.2 follow the pattern provided by Zielinska-Pisklak *et al*.[59]

Table 2.4.2: NMR correlations for **4**, numbered positions corresponds to Figure 2.4.8. Spectra are shown in Figures 2.4.8-2.4.12.

Position	**^{1}H [ppm], (mult., int., ^{n}J[Hz])**	**^{13}C[ppm]**	**COSY**	**HMBC**
1	2.83(q, 1H, -) 2.93 (t, 1H, -)	44.9	2	-
2	3.45 (m, 1H, -)	50.4	1,3	3
3	4.15 (q, 1H, -) 4.36 (dd, 1H, -)	68.8	2	-
4	-	152.3	-	-
5	6.53 (m, 1H, -)	100.1	6,7	-
6	7.11 (m, 3H, -)	122.7	5,10	-
7	7.11 (m, 3H, -)	105.1	5,10	5
8	-	137.5	-	6,7,11
9	-	118.7	-	5,6,7,11
10	6.68 (m, 1H, -)	100.9	11	-
11	7.11 (m, 3H, -)	122.7	5,10	-
12	8.17 (s, 1H, -)	-	10,11	-

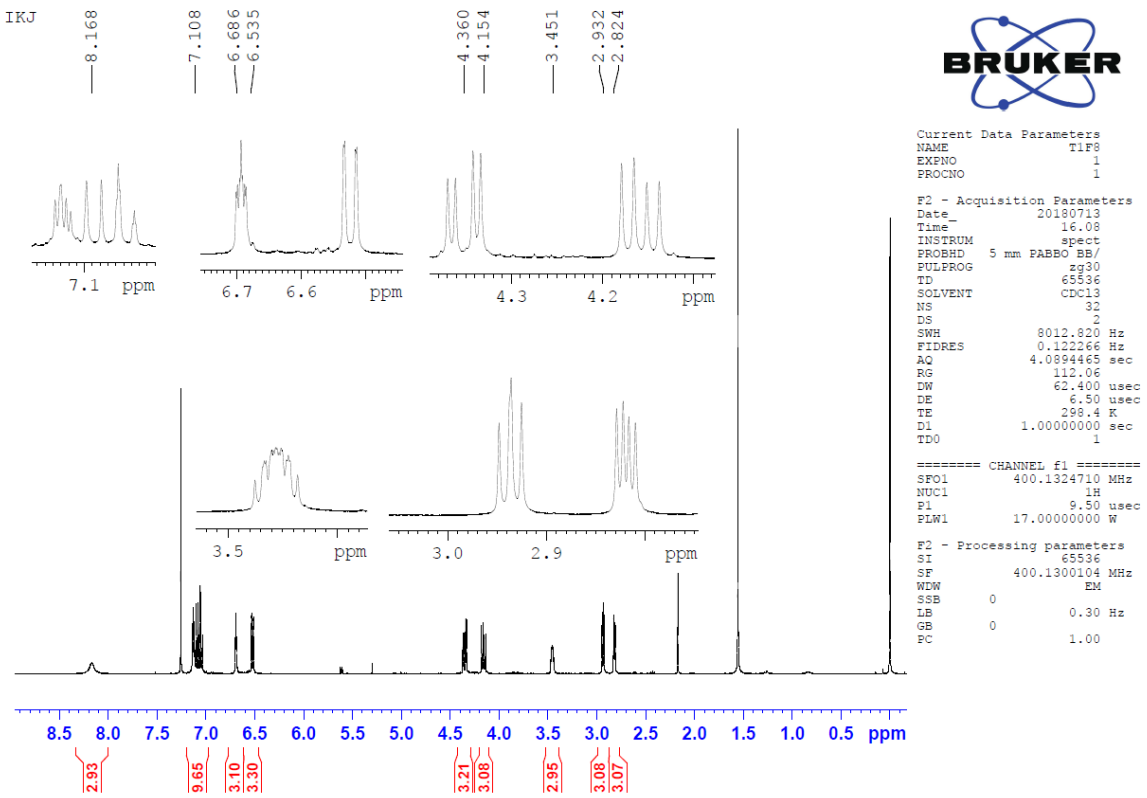

Figure 2.4.8: [1]H NMR spectrum of 4-(oxiran-2-ylmethoxy)-1H-indole (**4**). See Table 2.4.2 for peak assignments.

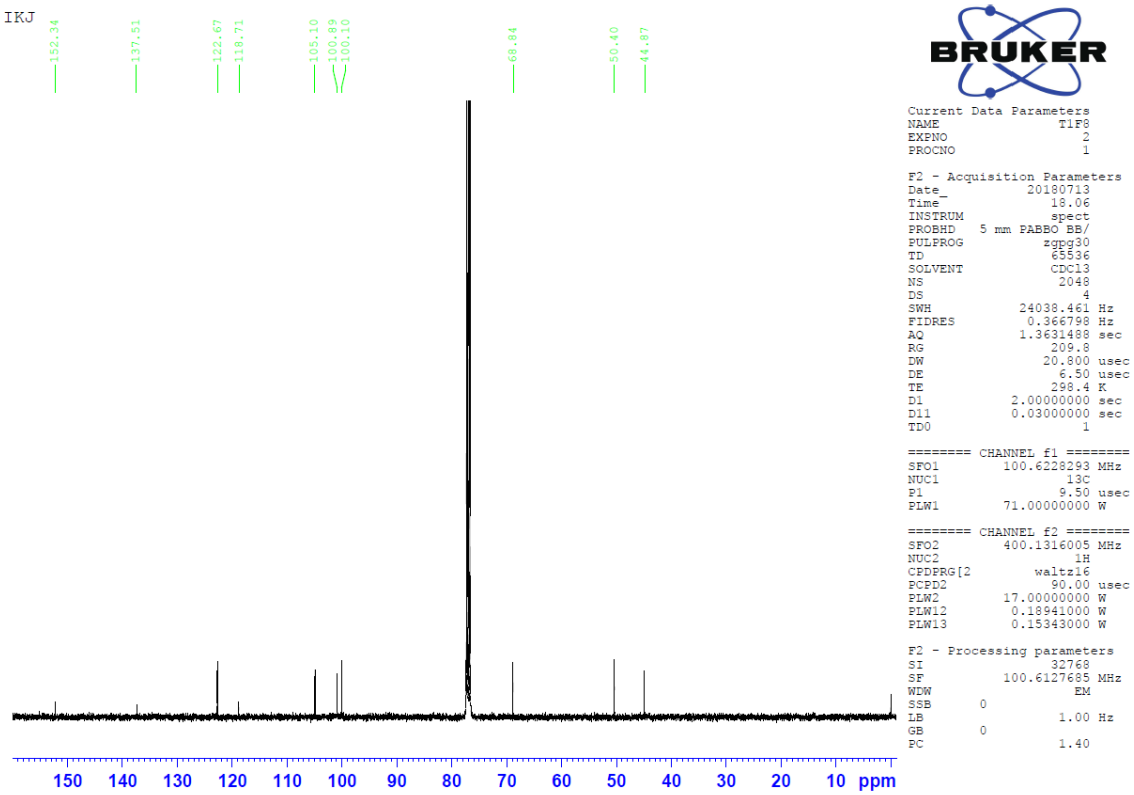

Figure 2.4.9: [13]C NMR spectrum of 4-(oxiran-2-ylmethoxy)-1H-indole (**4**). See Table 2.4.2 for peak assignments.

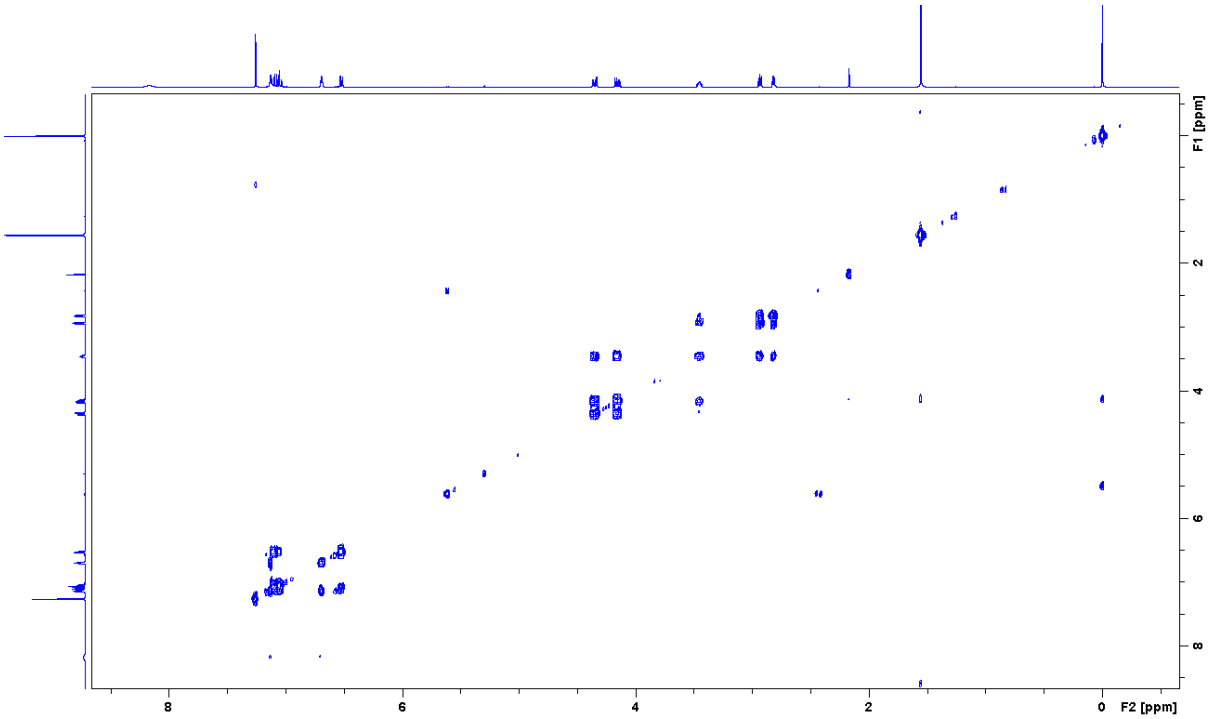

Figure 2.4.10: COSY spectrum of 4-(oxiran-2-ylmethoxy)-1H-indole (**4**). See Table 2.4.2 for peak assignments.

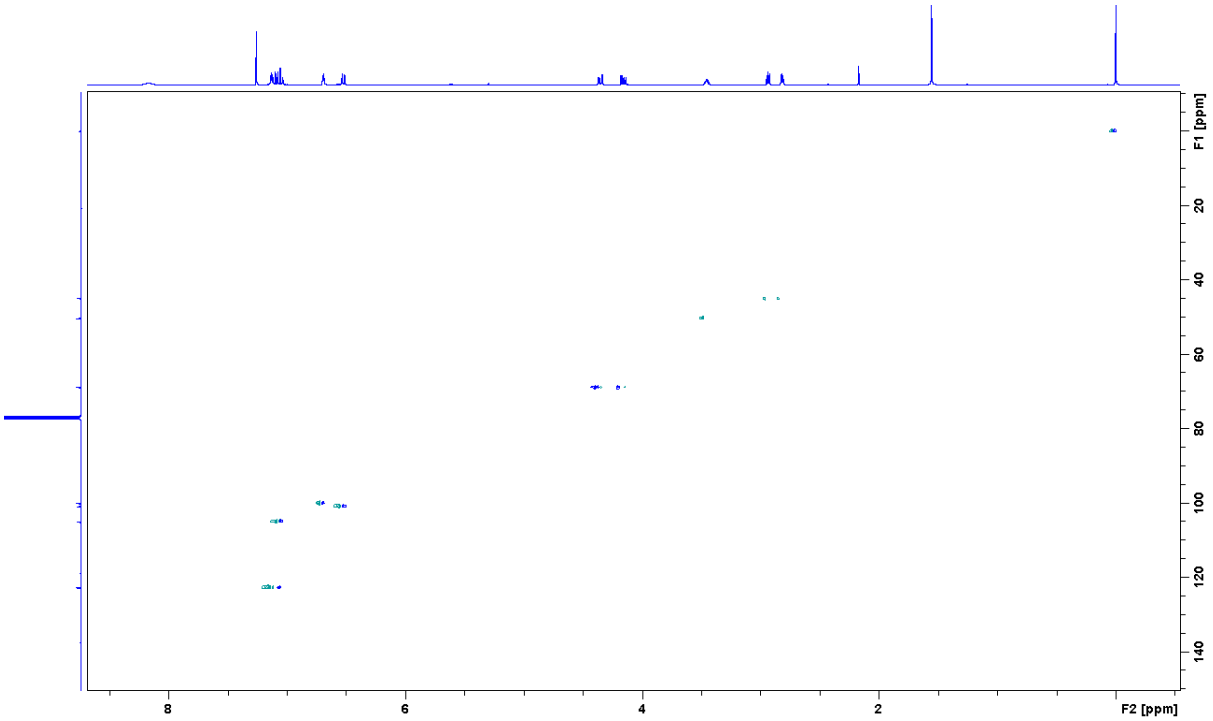

Figure 2.4.11: HSQC spectrum of 4-(oxiran-2-ylmethoxy)-1H-indole (**4**). See Table 2.4.2 for peak assignments.

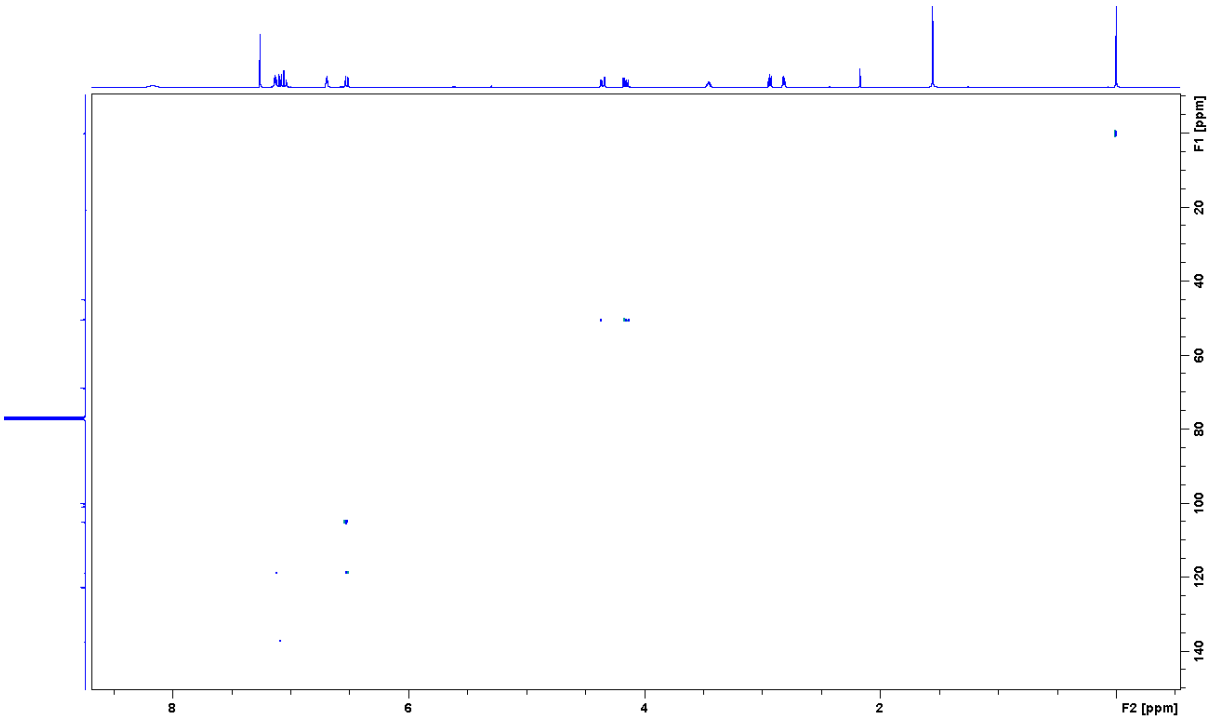

Figure 2.4.12: HMBC spectrum of 4-(oxiran-2-ylmethoxy)-1H-indole (**4**). See Table 2.4.2 for peak assignments.

2.4.3 Determination of 1-((1H-indol-4-yl)oxy)-3-chloropropan-2-ol (**5**)

The NMR analysis of **5** was performed using DMSO as a solvent. **5** with numbered positions can be seen in Figure 4.2.13.

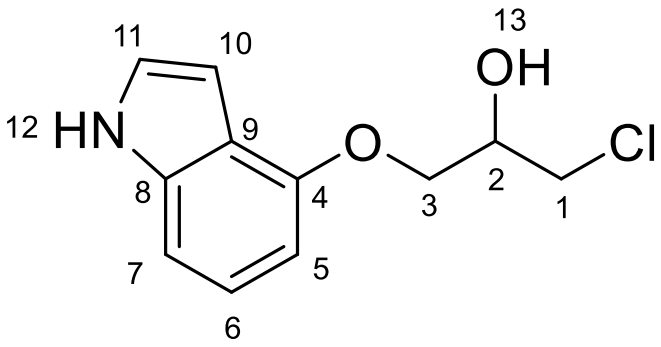

Figure 2.4.13: Structure of 1-((1H-indol-4-yl)oxy)-3-chloropropan-2-ol (**5**), with numbered positions correlating to NMR-shifts in Table 2.4.3.

The ^{1}H NMR of **5** (Figure 2.4.14) shows a solvent peak at 2.5 ppm, a water peak at 3.34 ppm and a small dichloromethane peak at 5.76 ppm. DMSO was used as a solvent in order to obtain the peak of the proton in position 13. This has led to shifts that are slightly different than those seen for compound **4,** which share much of the same structure. However, the shifts

follow the same patterns as the NMR analysis of **4** and those reported by Zielinska-Pisklak *et al*.[59] In the ^{13}C NMR spectrum (Figure 2.4.15), the solvent peak can be seen at 40.1 ppm. Just as with compound **4,** the HSQC spectrum (Figure 2.4.17) was used to assign proton-shifts to carbon-shifts. The COSY spectrum (Figure 2.4.16) and the HMBC spectrum (Figure 2.4.18) were used to determine the neighbouring environments of the different positions. The results of the assignments can be seen in Table 2.4.3, where the positions correspond to those seen in Figure 2.4.13.

Table 2.4.3: NMR correlations for **5**, numbered positions corresponds to Figure 2.4.13. Spectra are shown in Figures 2.4.14-2.4.18.

Position	**^{1}H [ppm], (mult., int., ^{n}J[Hz])**	**^{13}C[ppm]**	**COSY**	**HMBC**
1	3.75 (dd, 1H, $^{3}J_{HH}$ = 5.2 $^{2}J_{HH}$ = 11.3) 3.84 (dd, 1H, $^{3}J_{HH}$ = 4.3 $^{2}J_{HH}$ = 11.3)	47.5	2,3	2,3,13
2	4.09 (m, 3H, -)	69.2	1,4	1,3,13
3	4.09 (m, 3H, -)	69.3	1,4	1,2,13
4	-	152.4	-	2,3,5,6,7,10
5	6.49 (dd, 1H, $^{3}J_{HH}$ = 1.2 $^{2}J_{HH}$ = 7.1)	100.4	6,7,10,11,12	6,7
6	7.02 (m, 2H, -)	122.5	5,7,10	-
7	7.02 (m, 2H, -)	105.6	5,6,10	5,10
8	-	137.9	-	5,6,7,10,11
9	-	118.9	-	5,6,7,10,11
10	6.47 (t, 1H, $^{2}J_{HH}$ = 2.3)	98.7	5,6,7,11,12	11
11	7.22 (t, 1H, $^{2}J_{HH}$ = 2.6)	124.1	5,10,12	5,10
12	11.07 (s, 1H, -)	-	5,10,11	-
13	5.5 (s, 1H, -)	-	2,3	-

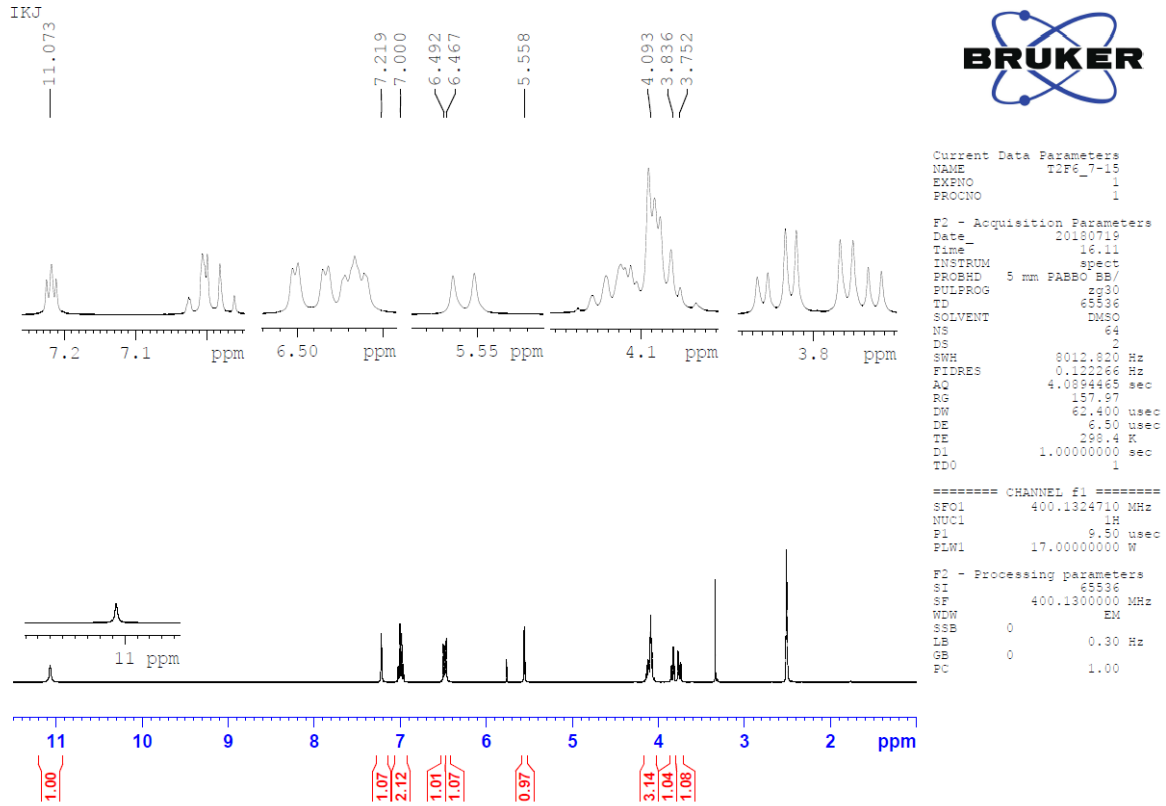

Figure 2.4.14: ^{1}H NMR spectrum of 1-((1H-indol-4-yl)oxy)-3-chloropropan-2-ol (**5**), see Table 2.4.3 for peak assignments.

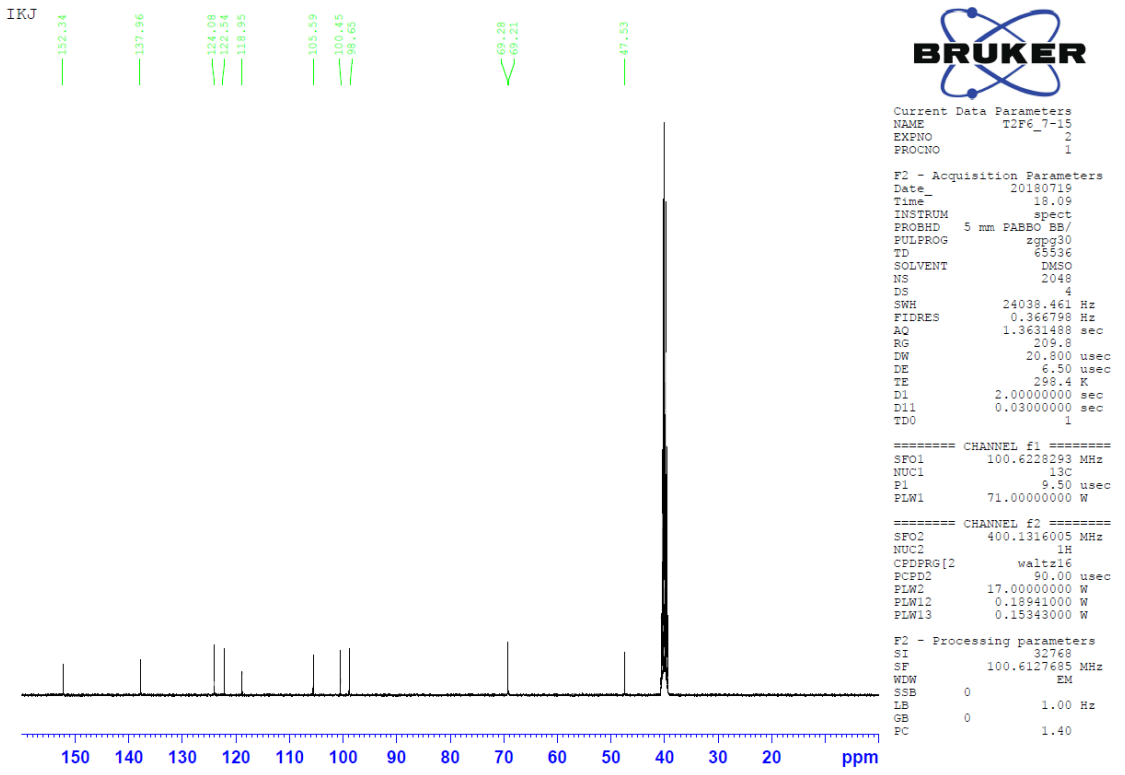

Figure 2.4.15: ^{13}C NMR spectrum of 1-((1H-indol-4-yl)oxy)-3-chloropropan-2-ol (**5**), see Table 2.4.3 for peak assignments.

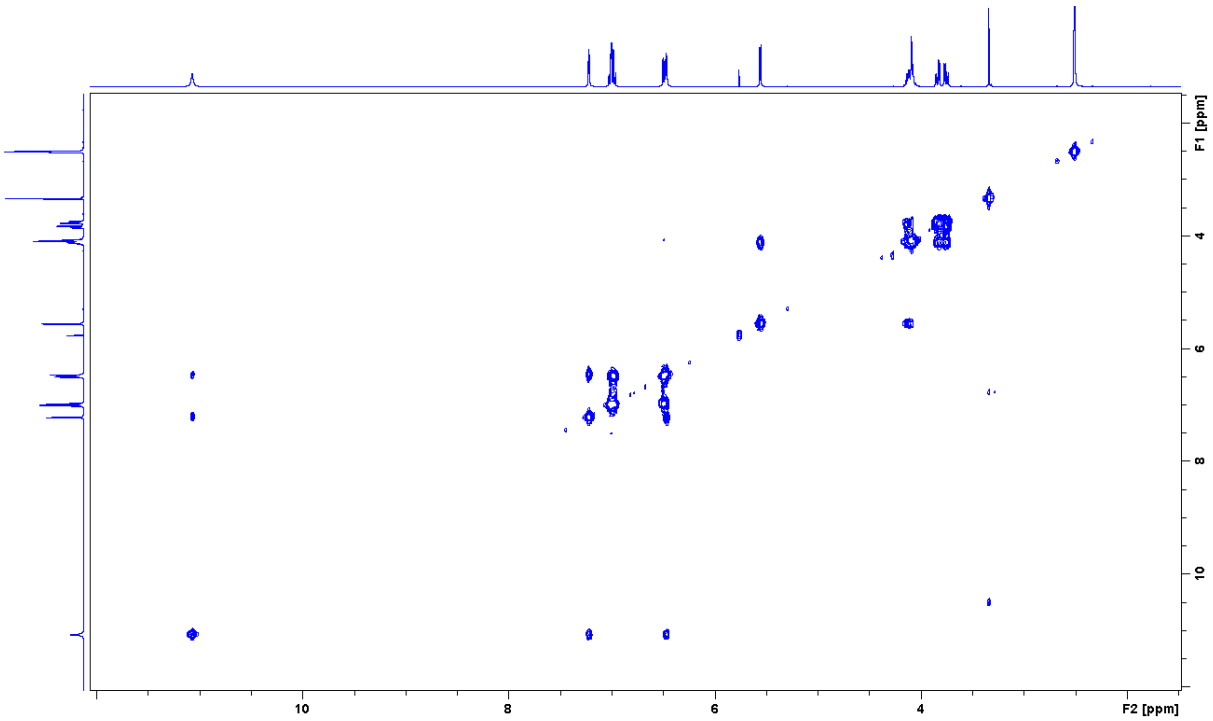

Figure 2.4.16: COSY spectrum of 1-((1H-indol-4-yl)oxy)-3-chloropropan-2-ol (**5**), see Table 2.4.3 for peak assignments.

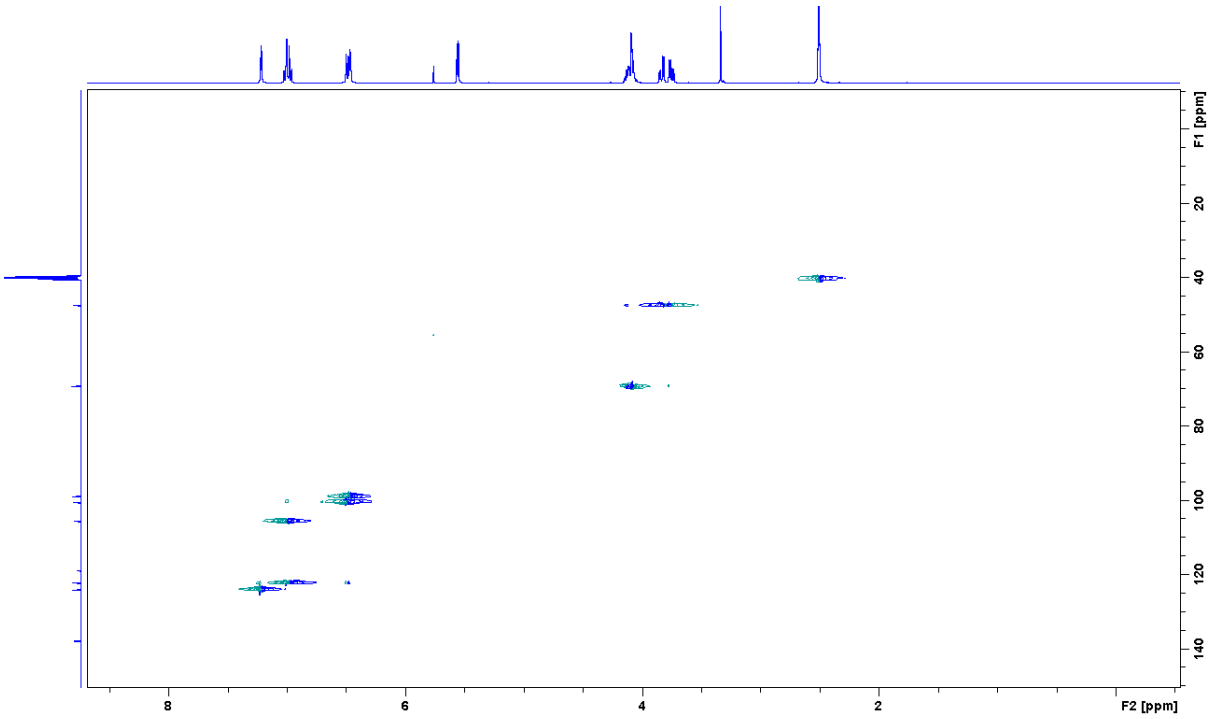

Figure 2.4.17: HSQC spectrum of 1-((1H-indol-4-yl)oxy)-3-chloropropan-2-ol (**5**), see Table 2.4.3 for peak assignments.

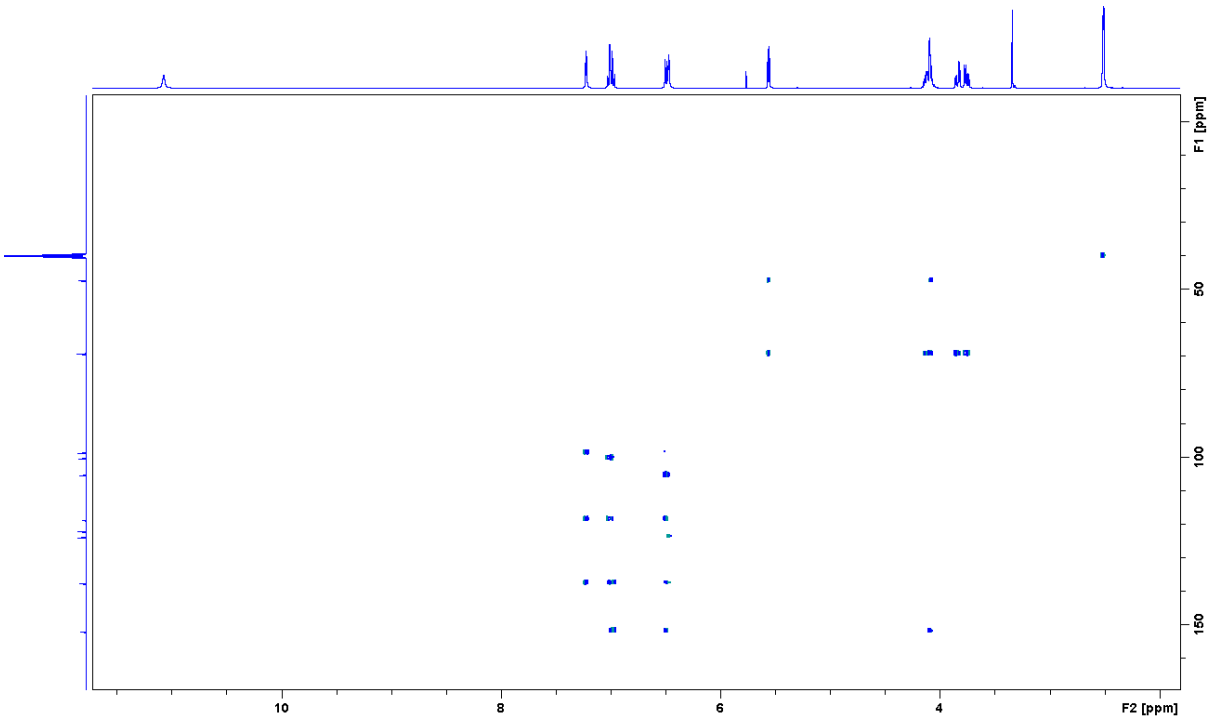

Figure 2.4.18: HMBC spectrum of 1-((1H-indol-4-yl)oxy)-3-chloropropan-2-ol (**5**), see Table 2.4.3 for peak assignments.

2.4.4 Determination of 1-((1H-indol-4-yl)oxy)-3-chloropropan-2-yl butyrate (**6**)

The NMR analysis of **6** was performed using $CDCl_3$ as a solvent. **6** with numbered positions can be seen in Figure 4.2.19.

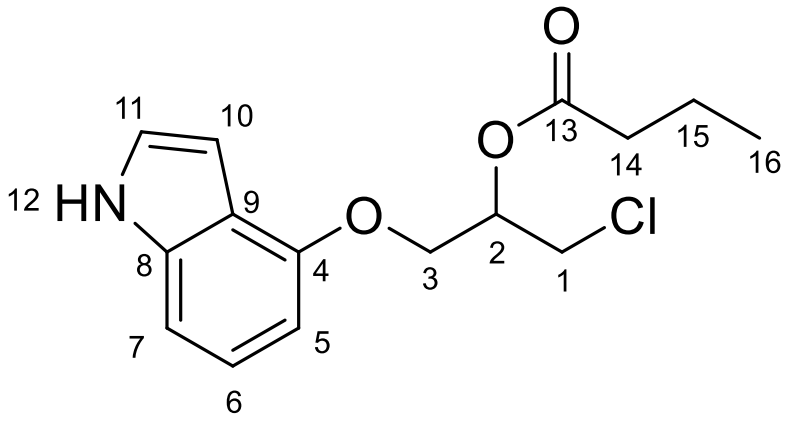

Figure 2.4.19: Structure of 1-((1H-indol-4-yl)oxy)-3-chloropropan-2-yl butyrate (**6**) with numbered positions correlating to NMR-shifts in Table 2.4.4.

^{1}H NMR of **6** (Figure 2.4.20) shows the solvent peak at 7.26 ppm, an acetone peak at 2.18 ppm and unknown impurities at 1.22ppm, 2.64ppm, 4.01ppm, 5.46ppm, 7.83ppm and 8.74ppm. Assignment of peaks to the positions shown in Figure 2.4.19 can be seen in Table

2.4.4. The ^{13}C spectrum can be seen in Figure 2.4.21, where the solvent peak can be seen at 77.16 ppm. Unfortunately, a carbon shift for position 13 were not detected by the ^{13}C NMR. The HSQC spectrum (Figure 2.4.23) was used to assign proton-shifts to carbon-shifts. The COSY spectrum (Figure 2.4.22) and the HMBC spectrum (Figure 2.4.24) were used to determine the neighbouring environments of the different positions. The shifts are slightly different than those seen for compounds **4** and **5**, which share much of the same structure. However, the shifts obtained for compound **6** follow the same patterns as those found for compounds **4** and **5**, and those reported by Zielinska-Pisklak *et al*.[59]

Table 2.4.4: NMR correlations for **6**, numbered positions corresponds to Figure 2.4.19. Spectra are shown in Figures 2.4.20-2.4.24.

Position	**^{1}H [ppm], (mult., int., ^{n}J[Hz])**	**^{13}C[ppm]**	**COSY**	**HMBC**
1	3.76-3.90 (m, 2H, …)	46.19	2,3	2,3
2	4.19-4.37 (m, 3H, …)	68.64	1	1
3	4.19-4.37 (m, 3H, …)	70.05	1	1,2
4	-	151.86	-	5,6,7,11
5	6.56 (dd, 1H, $^{2}J_{HH}$ = 0.86 $^{1}J_{HH}$ = 7.21)	101.01	6,7,11	6,7,11
6	7.03-7.16 (m, 3H, …)	122.77	5,10	-
7	7.03-7.16 (m, 3H, …)	105.20	5,10	5
8	-	137.38	-	6,7,11
9	-	118.68	-	6,7,11
10	6.64 (m, 1H, …)	99.67	6,7,11	11
11	7.03-7.16 (m, 3H, …)	122.93	-	-
12	8.22 (s, 1H, …)	-	6,7,10,11	-
13	-	no*	-	-
14	2.37 (td, 2H, $^{3}J_{HH}$ = 1.34 $^{2}J_{HH}$ = 7.33 $^{1}J_{HH}$ = 11.7)	36.40	15	16
15	1.69 (sex, 2H, $^{1}J_{HH}$ = 7.34)	18.44	14,16	16
16	0.97 (t, 3H, $^{1}J_{HH}$ = 7.64)	13.61	15	-

**no = Not obtained*

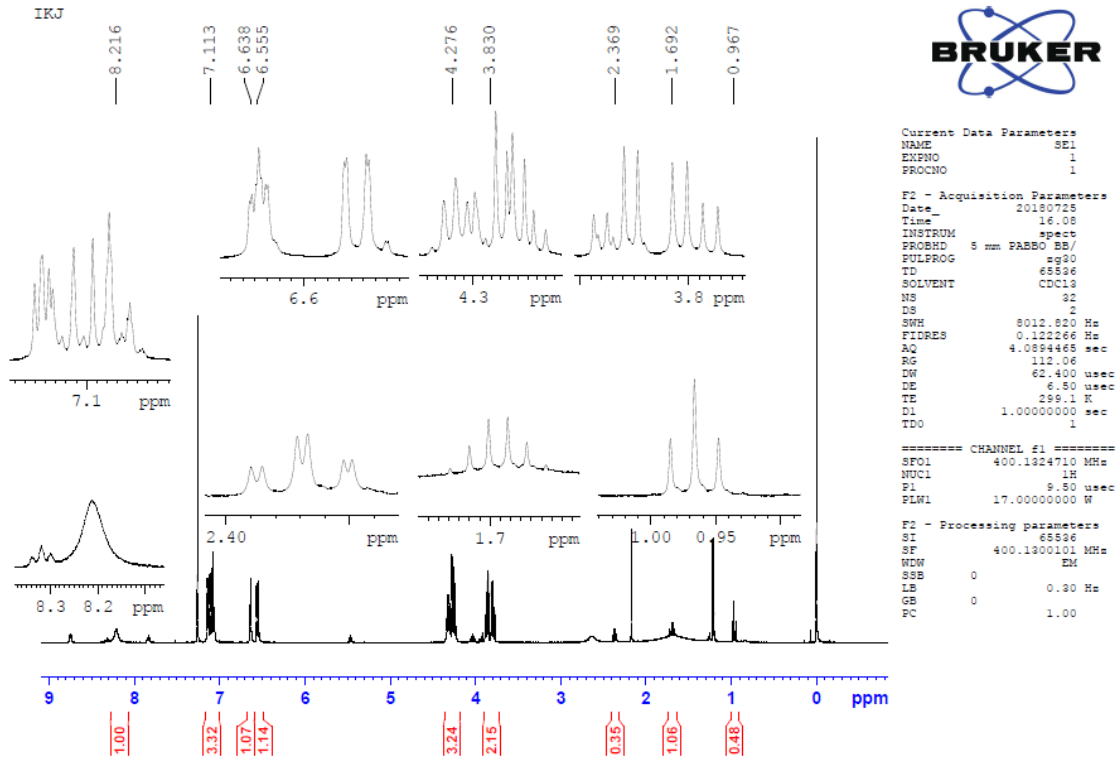

Figure 2.4.20: ^{1}H NMR spectrum of **6**, see Table 2.4.4 for peak assignments.

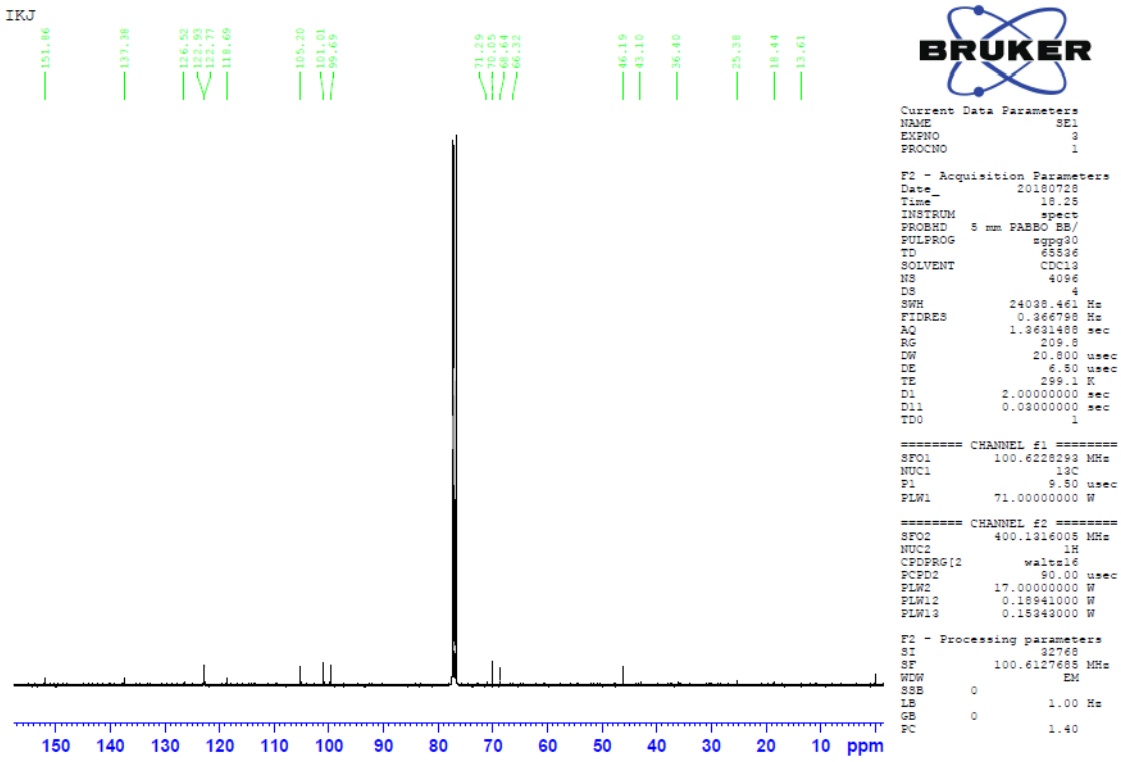

Figure 2.4.21: ^{13}C NMR spectrum of **6**, see Table 2.4.4 for peak assignments.

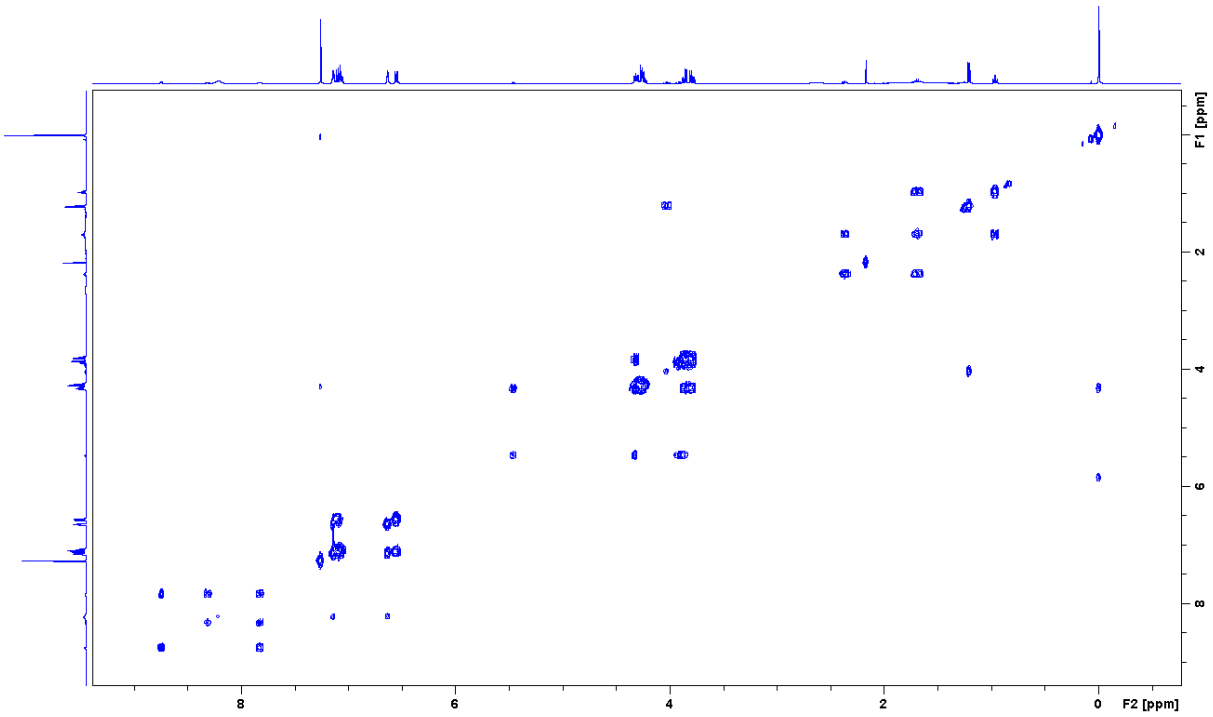

Figure 2.4.22: COSY spectrum of **6**, see Table 2.4.4 for peak assignments.

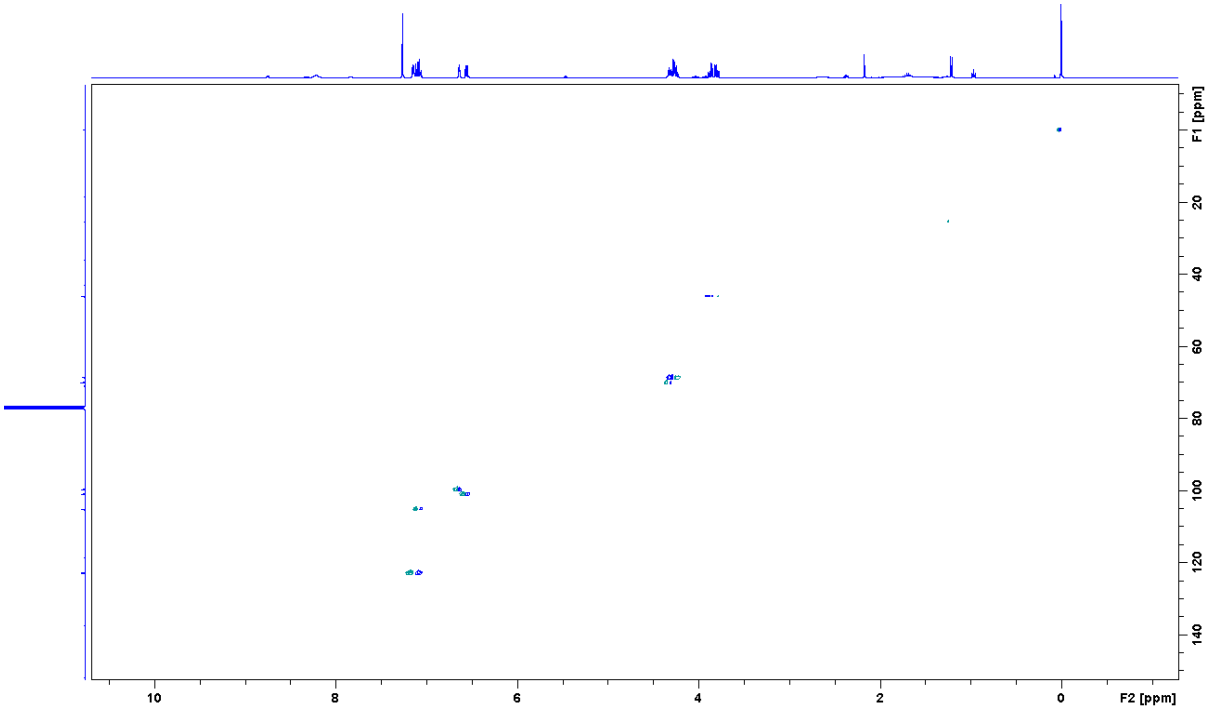

Figure 2.4.23: HSQC spectrum of **6**, see Table 2.4.4 for peak assignments.

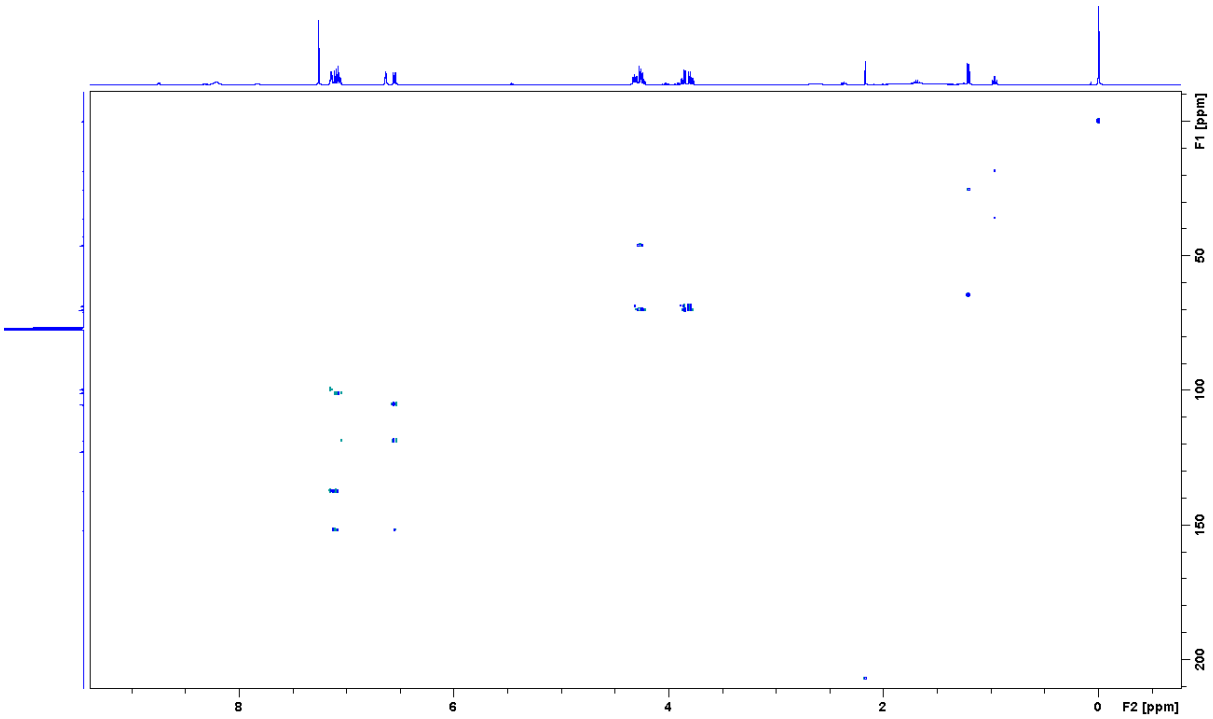

Figure 2.4.24: HMBC spectrum of **6**, see Table 2.4.4 for peak assignments.

2.4.5 Determination of 2-((2E,6E,10E,14E,18E,22E)-3,7,11,15,19,23,27-heptamethyloctacosa-2,6,10,14,18,22,26-heptaen-1-yl)-3-methylnaphthalene-1,4-diyldipropionate (**9**)

The NMR analysis of **9** was performed using $CDCl_3$ as a solvent. **9** with numbered positions can be seen in Figure 4.2.25.

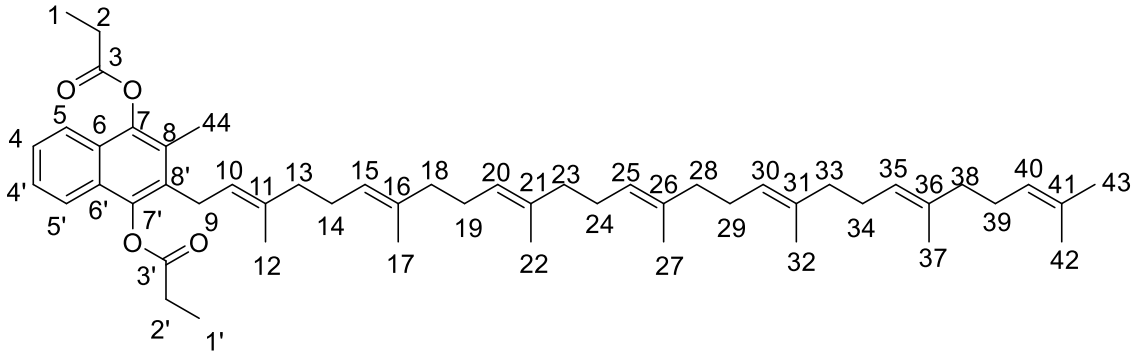

Figure 2.4.25: Structure of **9**, with numbered positions correlating to NMR-shifts in Table 2.4.5.

^{1}H NMR of **9** (Figure 2.4.26) shows the solvent peak at 7.26 ppm, an acetone peak at 2.18 ppm and an unknown impurity at 1.1 ppm. Assignment of peaks to the positions shown in Figure 2.4.19 can be seen in Table 2.4.4. The ^{13}C spectrum can be seen in Figure 2.4.27, where the solvent peak can be seen at 77.16 ppm. Unfortunately, a carbon shift for positions

3 and 3’ were not detected by the ^{13}C NMR. This was also the case for the carbon with the keto-group on substance **6**, as seen in chapter 2.4.4. Still, correlation with protons is seen for the expected ^{13}C shift for 3 and 3’ in the HMBC spectrum (Figure 2.4.30). The HSQC spectrum (Figure 2.4.29) was used to assign proton shifts to carbon shifts. The COSY spectrum (Figure 2.4.28) and the HMBC spectrum (Figure 2.4.30) were used to determine the neighbouring environments of the different positions. **9** is a relatively large structure, with several atoms in similar environments, and therefore several shifts are similar and have been difficult to assign.

Table 2.4.5: NMR correlations for **9**, numbered positions corresponds to Figure 2.4.25. Spectra are shown in Figures 2.4.26-2.4.30. Where assignment of one shift was not possible, “/” is used to separate the possible shifts.

Position	**^{1}H [ppm], (mult., int., ^{n}J[Hz])**	**^{13}C[ppm]**	**COSY**	**HMBC**
1/1’	1.38 (q, 6H, -)	9.40/9.43	2,2’	3,3’
2/2’	2.78 (quin, 4H, -)	27.53/27.56	1,1’	3,3’
3/3’	-	no*	-	1,1’,2,2’
4/4’	7.45 (m, 2H, -)	126.16/126.26/126.9	5,5’	44
5/5’	7.67 (m, 2H, -)	121.35/121.19/121.15	4,4’	-
6/6’	-	126.16/126.26/126.9	-	44
7/7’	-	142.53/142.24	-	44
8/8’	-	130.37/130.27	-	44
9	3.40 (s, 2H, -)	26.99	10,12,15,20, 25,30,35,40	-
10	5.09 (m, 7H, -)	121.35/121.19/121.15	9,13,14,18,19, 23,24,28,29, 33,34,38,39	-
11	-	136.25	-	
12	1.77 (s, 3H, -)	16.38/16.01	9,10,15,20, 25,30,35,40	5,5’,10,13,16, 18,21,23,26, 28,31,33,36 38,41

13/18/23/28/33/38	1.96-2.05 (m, 24H, -)	39.60/39.73/39.75	10,15,20, 25,30,35,40	14,15,16,19, 20,21,24,25, 26,29,30,31 34,35,36,39, 40,41
14/19/24/29/34/39	1.96-2.05 (m, 24H, -)	26.60-27.00	10,15,20, 25,30,35,40	14,15,16,19, 20,21,24,25, 26,29,30,31 34,35,36,39, 40,41
15/20/25/30/35/40	5.09 (m, 7H)	123.94-124.41	9,13,14,18,19, 23,24,28,29, 33,34,38,39	-
16/21/26/31/36/41	-	134.90-135.21	-	13,14,17,18, 19,22,23,24, 27,28,29,32, 33,34,37,38, 39
17/22/27/32/37	1.57-1.59 (m, 15H, -)	16.38/16.01	10,13,14,15, 18,19,20,23, 24,25,28,29 30,33,34,35, 38,39,40	-
42/43	1.68 (s, 6H, -)	17.68/25.69	10,13,14,15, 18,19,20,23, 24,25,28,29 30,33,34,35, 38,39,40	17,22,27,32, 37,42,43
44	2.23 (s, 3H, -)	13.04	-	-

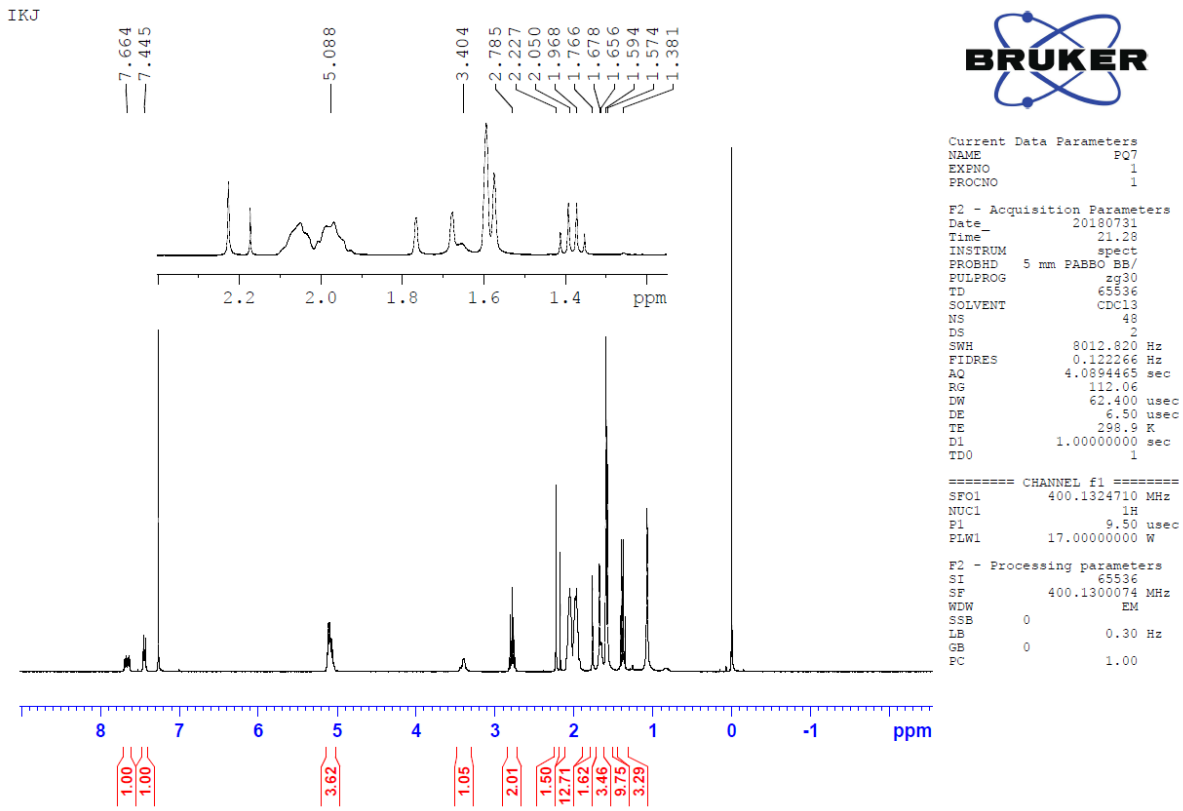

Figure 2.4.26: ^{1}H NMR spectrum of **9**, see Table 2.4.5 for peak assignments.

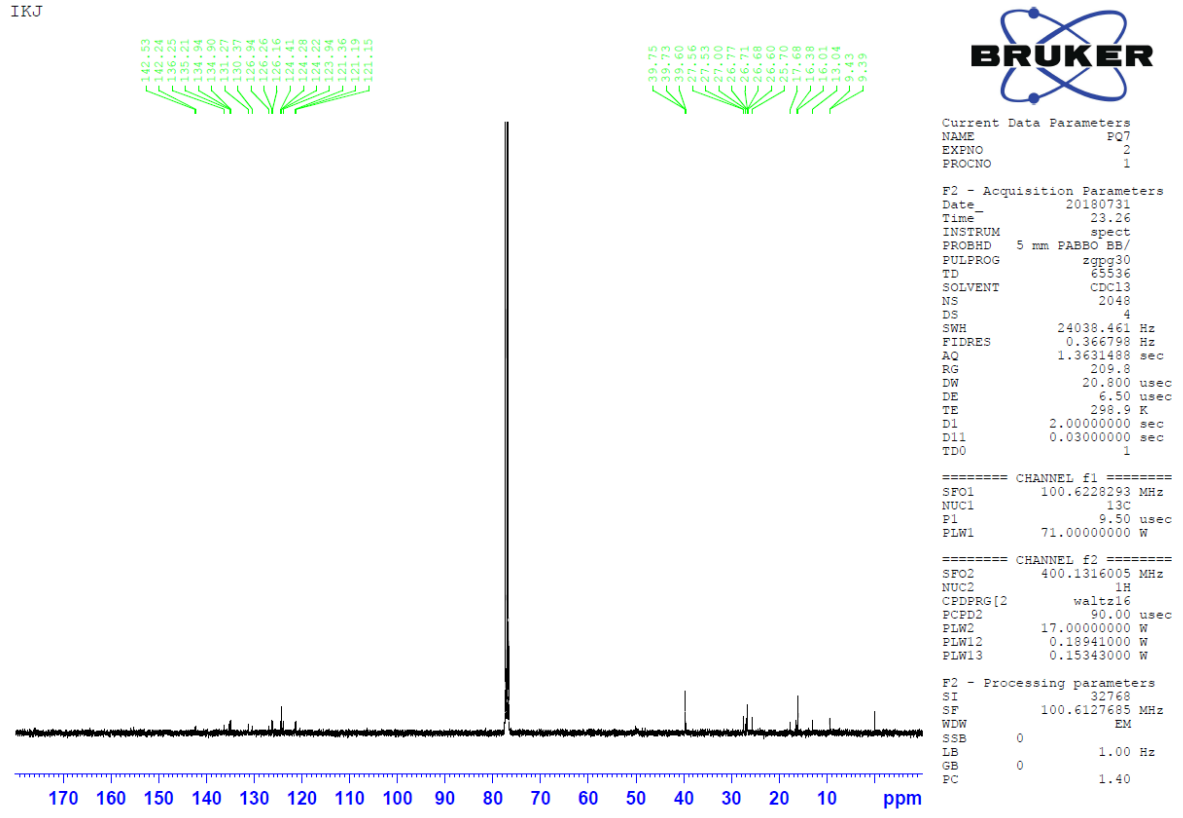

Figure 2.4.27: ^{13}C NMR spectrum of **9,** see Table 2.4.5 for peak assignments.

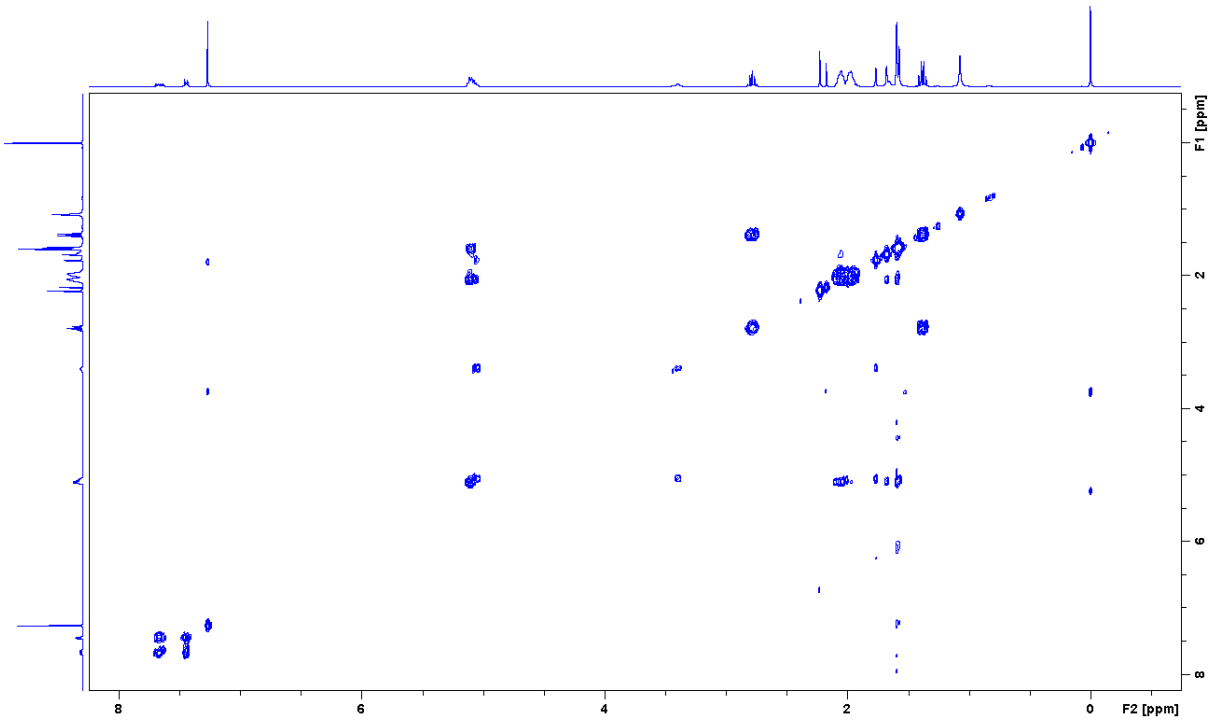

Figure 2.4.28: COSY spectrum of **9**, see Table 2.4.5 for peak assignments.

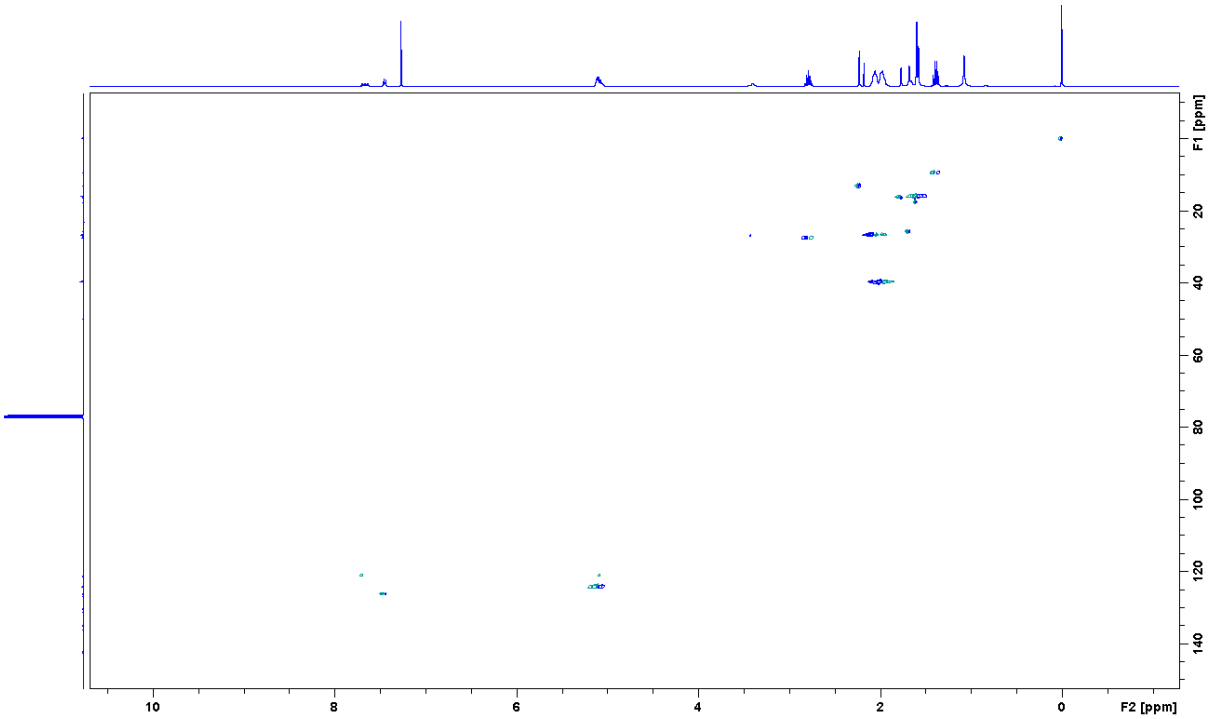

Figure 2.4.29: HSQC spectrum of **9**, see Table 2.4.5 for peak assignments.

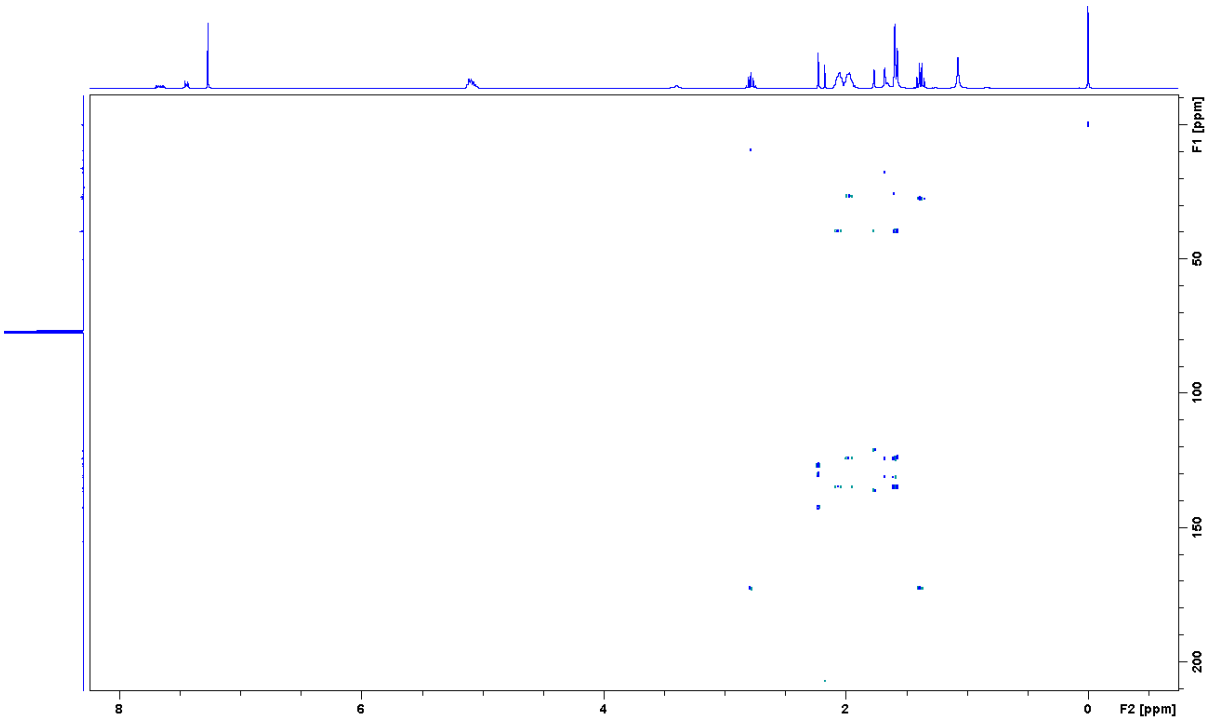

Figure 2.4.30: HMBC spectrum of **9**, see Table 2.4.5 for peak assignments.

The ^{1}H and ^{13}C NMR spectra of **9** from Synthetica A/S & Kappa Bioscience A/S (Figure 2.4.31 and 2.4.32) were compared with those seen in Figure 2.4.26 and 2.4.27. The spectra share the same peaks in the proton spectrum, and on the ^{13}C spectrum from Synthetica A/S & Kappa-Bioscience A/S the peak for position 3 and 3' can be seen.

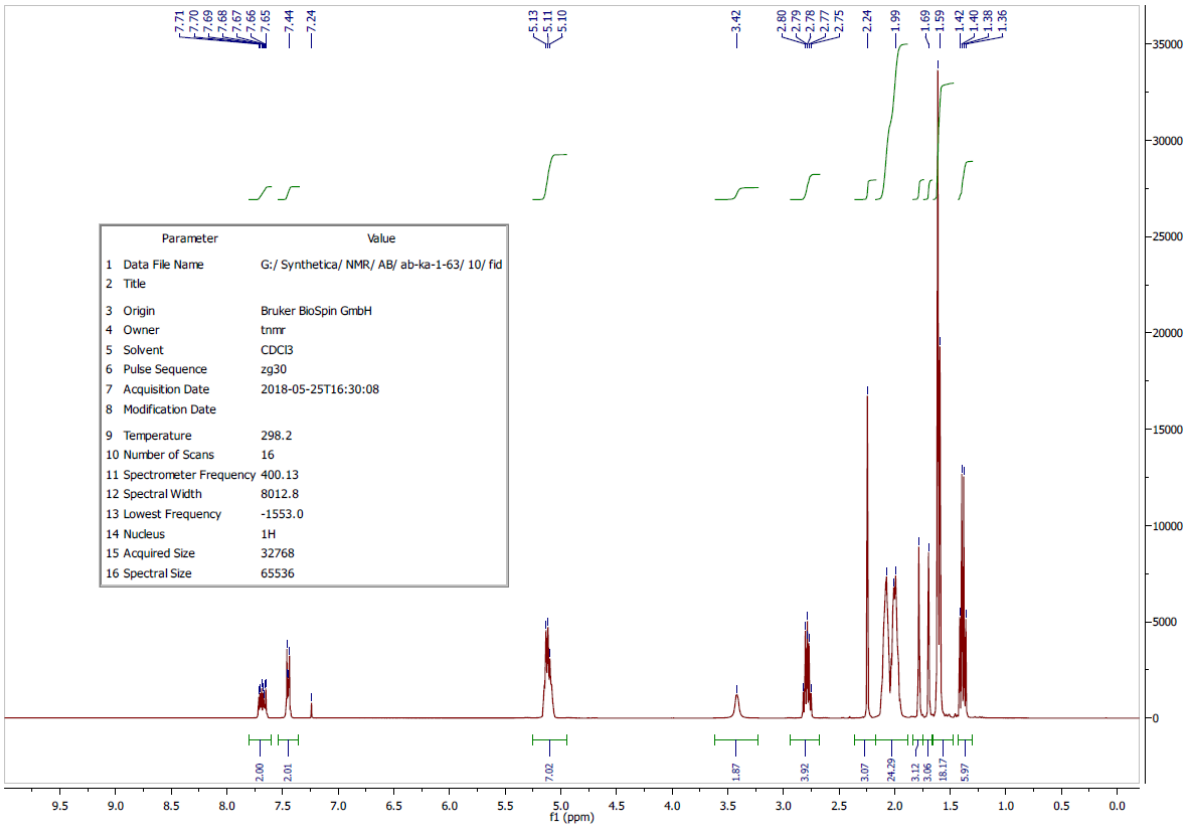

Figure 2.4.31: ^{1}H NMR spectrum of **9** from Synthetica A/S & Kappa Bioscience A/S.

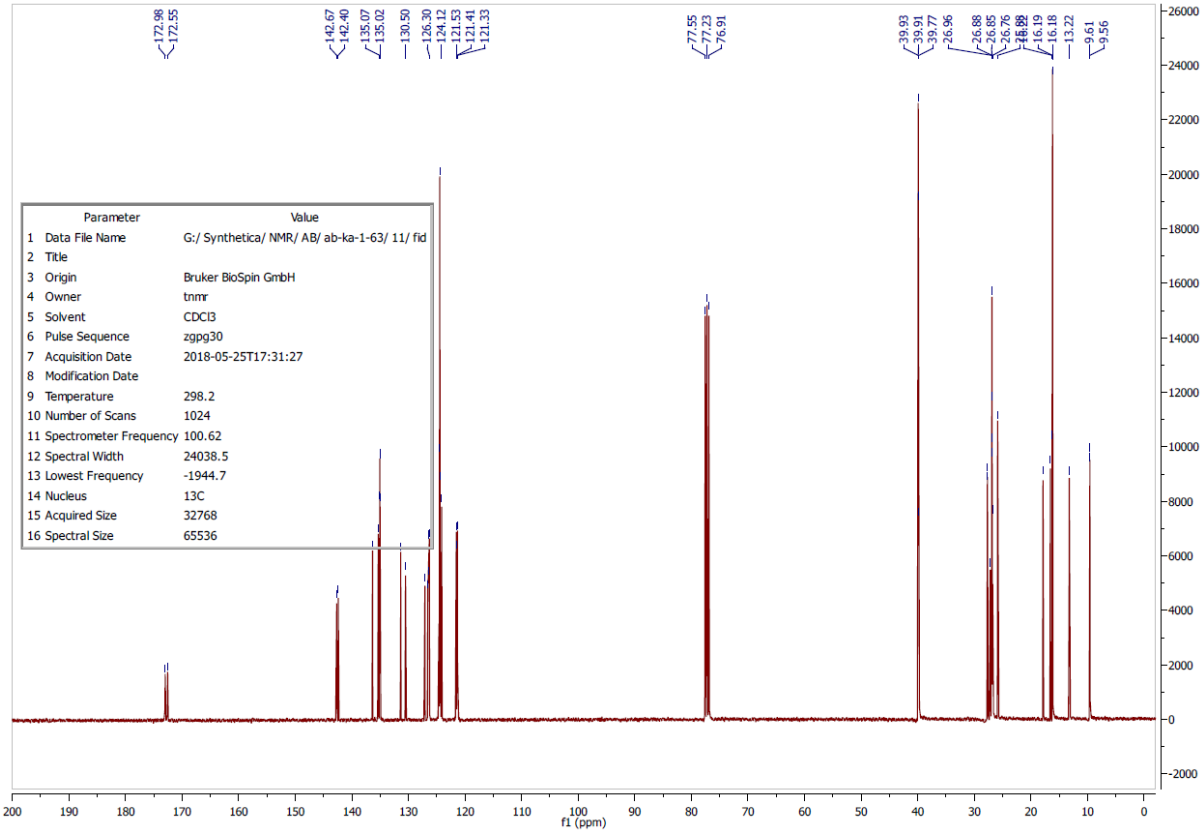

Figure 2.4.32: ^{13}C NMR spectrum of **9** from Synthetica A/S & Kappa Bioscience A/S.

3. Conclusion and further work

The aim of this master thesis was to find and evaluate synthetic pathways to an enantiopure precursor of β-blocker (*S*)-pindolol. As well as to evaluate the possibilities of using enzymes in the hydrolysis of **9**, and to synthetize **2**, a building block of β-blocker (*S*)-clenbuterol.

In the synthesis of an enantiopure precursor of β-blocker (*S*)-pindolol, several points of interest were found. In the first synthetic steps described in chapter 2.1.2 and 2.1.3 the yield of 85% reported my Lima *et al.*[16] was not reproduced. The highest yield reported in this thesis after the two first synthetic steps were 59%. Still, in this thesis a procedure for extraction and washing of the products in the first step is described. This procedure has in this project removed the need for purification by flash-chromatography after the first organic synthetic step. Further, by increasing the temperature in the second organic synthetic step, reaction time was shortened for the opening of the epoxide function on **4**.

In the kinetic resolution of **5** in an acylation using CALB, an E-value of 66 was achieved. At 53% conversion ee_s and ee_p values were at 92% and 81% respectively. However, these results are uncertain since the enantiomers of **6** were not successfully separated, making integration of the HPLC chromatograms incorrect. Still, the results show promise and in future work a synthetic hydrolysis of **6** should be performed in order to obtain the correct integrals of the produced esters and thereby correct calculations can be performed. Also, future work with these compounds should include crystallography in order to confirm or confute the elution order of enantiomers. This could also be used to confirm or confute the selectivity of CALB. Future work should also include measurement of optical rotation of enantiomers, which were not measured in this thesis.

In the hydrolysis of **9** using different co-solvents and enzymes no reactions showed the formation of the expected products **10**, **11** and **12**. Still, the formation of a clear crystalline precipitate was observed for the reactions where CALB was the enzyme used and EtOAc was used as co-solvent. Further work with this reaction should be performed in attempts to determine the structure of the formed crystals. Further solubility test of the crystals should also be performed, with larger amounts of solvents. If the crystals can be dissolved it would allow for further analysis. The use of different buffers should also be investigated.

4. Materials and methods

4.1 Chemicals, solvents and analysis

All experiments and analyses were performed at the Department of Chemistry, Faculty of Natural Sciences, Norwegian University of Science and Technology (NTNU), Trondheim, Norway.

4.1.1 Solvents and chemicals

Solvents and reagents

Starting material **9** was provided by Synthetica AS and Kappa Bioscience AS. All other solvents and chemicals used in this project was bought from Sigma-Aldrich, which is now Millipore Sigma.

Dry solvents

Dry solvents (dichloromethane) were acquired from a solvent purifier, MBraun MB-SPS-800, München, Germany. Dry solvents were stored in flasks containing molecular sieves (4Å).

Enzymes

Candida antarctica lipase A (CALA) (activity ≥500 U/g, lot# BCBR2259V) immobilized on immobead 150, recombinant from *Aspergillus oryzae*. Purchased from Sigma-Aldrich Norway, Oslo, Norway.

Candida antarctica Lipase B (CALB) (activity ≥10000 PLU/g, lot#20170315) immobilized at high hydrophobic macro porous resin, produced in fermentation with genetically modified *Pichia pastoris*. Gift from SyncoZymes Co, Ltd. (Shanghai, China).

Lipase, Type II, Crude; from Porcine pancreas (activity 50 units/mg protein, Lot#41H0954). Purchased from Sigma Aldrich (Oslo, Norway).

Molecular sieve

Molecular sieves (4Å) were activated by drying at 1000°C for 24 hours.

4.1.2 Chromatographic analyses

GC-MS

GC-MS analyses were run on an Agilent 7890A mass spectrometer coupled to an Agilent 5975 gas chromatograph equipped with an auto sampler (CTC PAL ALS). A split injector was used (280°C) with injection volumes of 1 µl and split ratio of 1:35. Supelco Equity®-1701 Capillary column (L × I.D. 30 m × 0.25 mm, df 0.25 µm) was used with a temperature program of 50°C for 1 min then 10°C/min to 280°C for 5 min. MS analyses were performed in scan mode from 50 to 550 m/z, temperature of the source was 230°C and Quadrupole 150°C.

HPLC

Chiral HPLC analyses were run on an Agilent HPLC 1100 system with a manual injector (Rheodyne 77245i/Agilent 20 µL loop), and a variable wavelength detector (VWD) set to 254 nm. The column used was a Chiralcel OD-H column (Diacel, Chiral Technologies Europe, 250 mm × 4.6 mm ID, 5 µm particle size). The method for the separation of chlorohydrin **5** was: 20% propan-2-ol/80% *n*-hexane; 1 mL/min, 10 µL injected.

Reversed-phase HPLC-analyses of **9** were performed on an Agilent Technologies Infinity 1260 uHPLC Binary LC system with auto sampler (4 µL injection), and a diode array detector (DAD) set to 254 nm. The column used was an Eclipse XDB - C18 column (Agilent Technologies, 4.6 x 150 mm ID, 5 µm particle size). The method for purity tests of samples from hydrolysis of **9** was an isocratic analysis using acetonitrile (100%) over 90 minutes, 1.0 mL/min flow.

TLC

The TLC analyses were performed on Merck silica 60 F254 plates and were detected by UV at $\lambda = 254$ nm.

Flash chromatography

Purification by flash chromatography was performed with silica gel (pore size 60 Å, 230-400 mesh particle size, 40-63 µm particle size) purchased from Sigma-Aldrich Norway, Oslo, Norway.

4.1.3 Spectroscopic analyses

NMR

All NMR analyses were performed on a Bruker 400 MHz Avance III HD, equipped with a 5-mm SmartProbe z-gradient probe and SampleCase.

MS

Exact masses were analysed with a Synapt G2-S Q-TOF mass spectrometer from Waters™. Ionization of samples was done with an ASAP probe (APCI), and calculation of exact masses and spectra processing was done with Waters™ Software (Masslynxs V4.1 SCN871).

4.1.4 Software

Figures

Figures 1.2.1, 1.2.2, 1.6.1, 1.8.1, and 1.8.2, were drawn using the open source scalable vector graphics editor Incskape 0.92 *draw freely*.

Chemical structures and predicted molecular weights

Compound structures were drawn using ChemDraw Professional 16.0 by Cambridgesoft. The same program was used to name compounds and estimate their molecular weight.

E-calculation

Calculation of E-Value was performed using E&K calculator 2.1b0 PCC.[60]

4.2 Organic synthesis

4.2.1. α-Bromination of 1-(4-amino-3,5-dichlorophenyl)ethan-1-one (**1**) forming 4-amino-3,5-dichlorobenzoyl bromide (**2**).

4-Amino-3,5-dichloroacetophenon (4.00 g, 19.6 mmol) was dissolved in CH_2Cl_2 and MeOH (70 mL, 2:1). Br_2 (0.6 mL) dissolved in CH_2Cl_2 (6 mL) was added dropwise, approximately 20 drops/min under constant vigorous stirring. After a colour change from dark brown-red to yellow another mixture of Br_2 (0.2 mL) in CH_2Cl_2 (2 mL) was added dropwise, approximately 20 drops/min. This was repeated four times. TLC was used to follow the formation of **2** (1:4 CH_2Cl_2:n-pentane, R_f = 0.62). The mixture was washed with brine before the organic-phase was dried over MgSO4, filtrated and evaporated. The resulting product was dissolved in a slurry using EtOH (16 mL) and stirred for 30 min at 50℃ and for 1 hour at room temperature. The slurry was filtrated off, and recrystallization were performed using EtOAc giving a yield of 23% of 4-amino-α-bromo-3,5-dichloroacetophenon (1.22 g, 4.5 mmol). Spectroscopic data for **2:** ^{1}H NMR (400 MHz, $CDCl_3$) δ_H: 7.86 (s, 2H, H4/H4'), 5.06 (s, 2H, H7), 4.31 (s, 2H, H1). ^{13}C NMR (400 MHz, $CDCl_3$) $\delta_{C:}$ 29.9 (C1), 188.1 (C2), 123.9 (C3) 129.3 (C4 and C4), 118.9 (C5 and C5'), 144.9 (C6). HRMS (TOF MS ASAP$^+$ *m/z*): 281.9091 [M+H] [attachment 1].

4.2.2 Synthesis of 1-((1H-indol-4-yl)oxy)-3-chloropropan-2-ol (**5**) from 1H-indol-4-ol (**3**).

The synthesis was performed as described by Lima *et al.*[16] 1H-Indol-4-ol (0.51 g, 3.80 mmol) was dissolved in 1,4-dioxane (3 mL) and NaOH (0.16 g, 3.93 mmol) was dissolved in water (5 mL) and added. (±)-Epichlorohydrin (2.98 mL, 38 mmol) was added. The mixture was stirred at room temperature for 5 hours until TLC showed no remaining starting material (CH_2Cl_2, R_f = 0.21). The product was extracted using CH_2Cl_2 (50 mL) and washed with EtOAc (30 mL*3) and water (30 mL*3). The CH_2Cl_2-phase was then dried using anhydrous $MgSO_4$ and evaporated, yielding 0,48 g of a mixture of 1-((1H-indol-4-yl)oxy)-3-chloropropan-2-ol (**5**) and 4-(oxiran-2-ylmethoxy)-1H-indole (**4**) in the form of a brown oil. Spectroscopic data for **4:** ^{1}H NMR (400 MHz, $CDCl_3$) δ_H: 8.17 (s, 1H, H12), 7.11 (m, 3H, H11/H6/H7), 6.68 (m, 1H, H10), 6.53 (m, 1H, H5), 4.36 (dd, 1H, H3), 4.15 (q, 1H, H3), 3.45 (m, 1H, H2), 2.93 (t, 1H, H1), 2.83 (q, 1H, H1). ^{13}C NMR (400 MHz, $CDCl_3$) $\delta_{C:}$ 122.7 (C11 and C6), 100.9 (C10), 118.9 (C9), 137.5 (C8), 105.1 (C7), 100.1 (C5), 152.3 (C4), 68.8 (C3), 50.4 (C3), 44.9 (C1). Spectroscopic data for **5:** ^{1}H NMR (400 MHz, DMSO) δ_H: 11.07 (s, 1H,

H12), 7.22 (t, 1H, H11), 7.02 (m, 2H, H6/H7), 6.49 (dd, 1H, H5), 6.47 (t, 1H, H10), 5.5 (s, 1H, H13), 4.09 (m, 3H, H3/H2), 3.84 (dd, 1H, H1), 3.75 (dd, 1H, H1). ^{13}C NMR (400 MHz, DMSO) $\delta_{C:}$ 152.4 (C4), 137.9 (C8), 124.1 (C11), 122.5 (C6), 118.9 (C9), 105.6 (C7), 100.4 (C5), 98.7 (C10), 69.3 (C3), 69.2 (C2), 47.5 (C1). HRMS (TOF MS ASAP$^+$ *m/z*): 226.0632 [M+H] [attachment 4, Figure A8].

4.2.3 Opening of epoxide on 4-(oxiran-2-ylmethoxy)-1H-indole (**4**) forming 1-((1H-indol-4-yl)oxy)-3-chloropropan-2-ol (**5**)

4-(Oxiran-2-ylmethoxy)-1H-indole (**4**) (0.48 g, 2.56 mmol) was dissolved in THF (8 mL) and AcOH (1.46 mL, 25.6 mmol) was added. LiCl (0.22 g, 5.12 mmol) was added. The mixture was stirred at room temperature for 72 hours. $NaCO_3$ was added until pH = 7. The product was extracted using CH_2Cl_2 (50 mL) and washed with brine (30mL*3). The CH_2Cl_2-phase was then dried using anhydrous $MgSO_4$ and evaporated, yielding 0,5701 g of a mixture of 1-((1H-indol-4-yl)oxy)-3-chloropropan-2-ol (**5**) and 4-(oxiran-2-ylmethoxy)-1H-indole (**4**) in the form of a brown oil. After purification by flash chromatography using CH_2Cl_2 as eluent, the product was obtained as a slightly yellow oil. Spectroscopic data for **4:** ^{1}H NMR (400 MHz, $CDCl_3$) δ_H: 8.17 (s, 1H, N**H**), 7.11 (m, 3H, H11/H6/H7), 6.68 (m, 1H, H10), 6.53 (m, 1H, H5), 4.36 (dd, 1H, H3), 4.15 (q, 1H, H3), 3.45 (m, 1H, H2), 2.93 (t, 1H, H1), 2.83 (q, 1H, H1). ^{13}C NMR (400 MHz, $CDCl_3$) $\delta_{C:}$ 122.7 (C11 and C6), 100.9 (C10), 118.9 (C9), 137.5 (C8), 105.1 (C7), 100.1 (C5), 152.3 (C4), 68.8 (C3), 50.4 (C3), 44.9 (C1). Spectroscopic data for **5:** ^{1}H NMR (400 MHz, DMSO) δ_H: 11.07 (s, 1H, H12), 7.22 (t, 1H, H11), 7.02 (m, 2H, H6 and H7), 6.47 (t, 1H, H10), 6.49 (dd, 1H, H5), 5.5 (s, 1H, H13), 4.09 (m, 3H, H3 and H2), 3.84 (dd, 1H, H1), 3.75 (dd, 1H, H1). ^{13}C NMR (400 MHz, DMSO) $\delta_{C:}$ 152.4 (C4), 137.9 (C8), 124.1 (C11), 122.5 (C6), 118.9 (C9), 105.6 (C7), 100.4 (C5), 98.7 (C10), 69.3 (C3), 69.2 (C2), 47.5 (C1). HRMS (TOF MS ASAP$^+$ *m/z*): 226.0632 [M+H] [attachment 4, Figure A8].

4.2.4 Synthesis of racemic ester 1-((1H-indol-4-yl)oxy)-3-chloropropan-2-yl butyrate (**6**) from 1-((1H-indol-4-yl)oxy)-3-chloropropan-2-ol (**5**)

1-((1H-Indol-4-yl)oxy)-3-chloropropan-2-ol (**5**) (0.08 g, 0.37 mmol) and butyric anhydride (0.075 mL, 0.46 mmol) were added to pyridine (0.05 mL, 0.62 mmol). The mixture was stirred for 24h at room temperature. Extraction was performed with hexane and CH_2Cl_2, washing with brine. The organic-phase was dried over anhydrous $MgSO_4$ and evaporated,

yielding 0,08 g of a mixture of **5** (84.6%) and **6** (11.0%). Separation by flash-chromatography using CH_2Cl_2 as eluent yielded 1% of **6** (0.80 mg, 0.003 mmol). Spectroscopic data for **6**: ^{1}H NMR (400 MHz, $CDCl_3$) δ_H: 8.22 (s, 1H, H12), 7.03-7.16 (m, 3H, H11/H7/H6), 6.64 (m, 1H, H10), 6.56 (dd, 1H, H5), 4.19-4.37 (m, 3H, H3/H2), 3.75-3.90 (m, 2H, H1), 2.37 (td, 2H, H14), 1.69 (sex, 2H, H15), 0.97 (t, 3H, C16). ^{13}C NMR (400 MHz, $CDCl_3$) $\delta_{C:}$ 151.86 (C4), 137.38 (C8), 122.93 (C11), 122.77 (C6), 118.68 (C9), 105.20 (C7), 101.01 (C5), 99.67 (C10), 70.05 (C3), 68.64 (C2), 46.19 (C1), 36.40 (C14), 18.44 (C15), 13.61 (C16).

4.3. Kinetic resolutions

4.3.1 Transesterification of 1-((1H-indol-4-yl)oxy)-3-chloropropan-2-ol (**5**)

Three different resolutions were tested with different amounts of CALB.

1. **0.5 Equivalents of CALB**

1-Chloro-3-(1H-indol-4-yloxy)-propan-2-ol (**5**) (20.6 mg, 0.09 mmol) was dissolved in dry CH_2Cl_2 (3 mL) and three lumps of molecular sieve was added. Vinyl butanoate (60 µL, 0.46 mmol) and immobilized CALB (10.0 mg) were added, and the reaction tube was placed in an orbital shaker (30°C, 200 rpm). Samples (150 µL) were collected regularly for chiral HPLC-analysis (t_R (*S*)-**5** = 50.7 min, t_R (*R*)-**5** = 22.5 min, t_R (*S*)-**6** = 14.0 min, t_R (*R*)-**6** = 14.7 min) (hexane:2-propanol (80:20), 1 mL/min flow). After 312 hours the reaction was ended, after 50% conversion was observed by HPLC [attachment 16].

2. **1 Equivalent of CALB**

1-Chloro-3-(1H-indol-4-yloxy)-propan-2-ol (**5**) (16.0 mg, 0.07 mmol) was dissolved in dry CH_2Cl_2 (3 mL) and three lumps of molecular sieve was added. Vinyl butanoate (60 µL, 0.46 mmol) and immobilized CALB (15.0 mg) were added, and the reaction tube was placed in an orbital shaker (30°C, 200 rpm). Samples (150 µL) were collected regularly for chiral HPLC-analysis (t_R (*S*)-**5** = 50.7 min, t_R (*R*)-**5** = 22.5 min, t_R (*S*)-**6** = 14.0 min, t_R (*R*)-**6** = 14.7 min) (hexane:2-propanol (80:20), 1 mL/min flow). After 98 hours the reaction was ended, after 50% conversion was observed by HPLC [attachment 17].

3. **2 Equivalents of CALB**

1-Chloro-3-(1H-indol-4-yloxy)-propan-2-ol (**5**) (18.5 mg, 0.08 mmol) was dissolved in dry CH_2Cl_2 (3 mL) and three lumps of molecular sieve was added. Vinyl butanoate (75 µL, 0.59 mmol) and immobilized CALB (36.8 mg) were added, and the reaction tube was placed in an orbital shaker (30°C, 200 rpm). Samples (150 µL) were collected regularly for chiral HPLC-analysis (t_R (*S*)-**5** = 50.7 min, t_R (*R*)-**5** = 22.5 min, t_R (*S*)-**6** = 14.0 min, t_R (*R*)-**6** = 14.7 min) (hexane:2-propanol (80:20), 1 mL/min flow). 50% conversion was reached after 24 hours. E-value was calculated using HPLC analyses and E&K calculator 2.1b0 PCC to be E = 66 [attachment 18].

4.3.2 Hydrolysis of 1-((1H-indol-4-yl)oxy)-3-chloropropan-2-yl butyrate (**6**)

1-((1H-Indol-4-yl)oxy)-3-chloropropan-2-yl butyrate (**6**) (5.5 mg, 0.02 mmol) was dissolved in MeCN (0.9 mL). Phosphate buffer (2.1 mL, pH=7) was added with immobilized CALB (100 mg) and the reaction tube was placed in an orbital shaker (30°C, 200 rpm). Samples (150 µL) were collected regularly for chiral HPLC-analysis (t_R (*S*)-**5** = 50.7 min, t_R (*R*)-**5** = 22.5 min, t_R (*S*)-**6** = 14.0 min, t_R (*R*)-**6** = 14.7 min) (hexane:2-propanol (80:20), 1 mL/min flow). The reaction was ended after 48 hours, HPLC showing 48.5% of (*R*)-**6** left un-hydrolysed in the mixture [attachment 19].

4.3.3 Hydrolysis of 2-((2E,6E,10E,14E,18E,22E)-3,7,11,15,19,23,27-heptamethyloctacosa-2,6,10,14,18,22,26-heptaen-1-yl)-3-methylnaphthalene-1,4-diyl dipropionate (**9**)

Three different parallels were performed using different co-solvents in the phosphate buffer.

1. **Phosphate buffer and ethanol**

Three portions of 2-((2E,6E,10E,14E,18E,22E)-3,7,11,15,19,23,27-heptamethyloctacosa-2,6,10,14,18,22,26-heptaen-1-yl)-3-methylnaphthalene-1,4-diyl dipropionate (**9**) (20 mg, 0.03 mmol) were added to three test tubes. EtOH (0.9 mL) and phosphate buffer (2.1 mL, pH=7) were added. PPL Type II (20.9 mg) was added to tube 1, CALA (46.7 mg) was added to tube 2, CALB (44.1 mg) was added to tube 3. All tubes were placed in an orbital shaker (30°C, 200 rpm). Samples (150 µL) were collected regularly for reversed-phase HPLC-analysis (t_R **9** = 77.8 minutes) (MeCN 100%, 1 mL/min flow). The reaction was ended after 48 hours, HPLC showed no products in the mixture [attachment 21].

2. **Phosphate buffer and acetonitrile**

Three portions of 2-((2E,6E,10E,14E,18E,22E)-3,7,11,15,19,23,27-heptamethyloctacosa-2,6,10,14,18,22,26-heptaen-1-yl)-3-methylnaphthalene-1,4-diyl dipropionate (**9**) (80 mg, 0.10 mmol) were added to three test tubes. MeCN (0.9 mL) and phosphate buffer (2.1 mL, pH=7) were added. PPL Type II (70.0 mg) was added to tube 1, CALA (73.0 mg) was added to tube 2, CALB (100.0 mg) was added to tube 3. All tubes were placed in an orbital shaker (30°C, 200 rpm). Samples (150 µL) were collected regularly for reversed-phase HPLC-analysis (t_R **9** = 77.8 minutes) (MeCN 100%, 1 mL/min flow). The reaction was ended after 48 hours, HPLC showed no products in the mixture [attachment 22].

3. Phosphate buffer and ethyl acetate

Three portions of 2-((2E,6E,10E,14E,18E,22E)-3,7,11,15,19,23,27-heptamethyloctacosa-2,6,10,14,18,22,26-heptaen-1-yl)-3-methylnaphthalene-1,4-diyl dipropionate (**9**) (80 mg, 0.10 mmol) were added to three test tubes. EtOAc (0.9 mL) and phosphate buffer (2.1 mL, pH=7) were added. PPL Type II (68.0 mg) was added to tube 1, CALA (70.0 mg) was added to tube 2, CALB (100.0 mg) was added to tube 3. All tubes were placed in an orbital shaker (30°C, 200 rpm). Samples (150 μL) were collected regularly for reversed-phase HPLC-analysis (t_R **9** = 77.8 minutes) (MeCN 100%, 1 mL/min flow). The reaction was ended after 48 hours, HPLC showed no products in the mixture [attachment 23]. In reaction tube 3 a non-coloured crystalline precipitate was observed. MS analysis gave a mass of 663 g/mol [attachment 24].

References

1. FDA's policy statement for the development of new stereoisomeric drugs. *Chirality* **1992,** *4* (5), 338.
2. Anastas, P. T.; Warner, J. C., *Green Chemistry: Theory and Practice*. Oxford University Press: Oxford, **1998**.
3. Solomons, T. W. G.; Fryhle, C. B.; Snyder, S. A., *Organic Chemistry*. Wiley: Singapore, **2014**.
4. Lin, G.-Q.; You, Q.-D.; Cheng, J.-F., *Chiral Drugs: Chemistry and Biological Action*. Wiley: Hoboken, J.N, **2011**.
5. Teo, S.; Colburn, W.; Tracewell, W.; Kook, K.; Stirling, D.; Jaworsky, M.; Scheffler, M.; Thomas, S.; Laskin, O., Clinical Pharmacokinetics of Thalidomide. *Clin. Pharmacokin.* **2004,** *43* (5), 311-327.
6. Marriott, J. B.; Muller, G.; Dalgleish, A. G., Thalidomide as an emerging immunotherapeutic agent. *Immunol. Today* **1999,** *20* (12), 538-540.
7. Blaschke, G.; Kraft, H. P.; Fickentscher, K.; Kohler, F., Chromatographic separation of racemic thalidomide and teratogenic activity of its enantiomers (author's transl). *Arzneimittel-Forschung* **1979,** *29* (10), 1640-2.
8. Ariëns, E., Stereochemistry, a basis for sophisticated nonsense in pharmacokinetics and clinical pharmacology. *Eur. J. Clin. Pharmacol.* **1984,** *26* (6), 663-668.
9. White, F. P.; Ham, L. J.; Way, L. W.; Trevor, L. A., Pharmacology of Ketamine Isomers in Surgical Patients. *Anesthesiology* **1980,** *52* (3), 231-239.
10. Gibson, A. J.; Raphael, A. B., Understanding beta-blockers. *Nursing* **2014,** *44* (6), 55-59.
11. Anderson, J., Beta-Blockers. *Card. Electrophysiol. Rev.* **2000,** *4* (3), 301-308.
12. Biaggioni, I.; Robertson, D., *Primer on the Autonomic Nervous System*. United States: Academic Press: **2011**.
13. Fox, S. I., *Human Physiology*. McGraw-Hill: New York, **2011**.
14. Patrick, G. L., *An Introduction to Medicinal Chemistry*. Oxford University Press: Oxford, **2013**.
15. Koch-Weser, J.; Frishman, W. H., Pindolol: A New β-Adrenoceptor Antagonist with Partial Agonist Activity. *N. Engl. J. Med.* **1983,** *308* (16), 940-944.
16. Lima, G. V.; Da Silva, M. R.; de Sousa Fonseca, T.; de Lima, L. B.; de Oliveira, M. D. C. F.; de Lemos, T. L. G.; Zampieri, D.; Dos Santos, J. C. S.; Rios, N. S.; Gonçalves, L. R. B.; Molinari, F.; de Mattos, M. C., Chemoenzymatic synthesis of (S)-Pindolol using lipases. *Appl. Catal. A, General* **2017,** *546*, 7-14.
17. Liu, Y.; Zhou, X.; Zhu, D.; Chen, J.; Qin, B.; Zhang, Y.; Wang, X.; Yang, D.; Meng, H.; Luo, Q.; Xie, P., Is pindolol augmentation effective in depressed patients resistant to selective serotonin reuptake inhibitors? A systematic review and meta-analysis. *Hum. psychopharmacol.* **2015,** *30* (3), 132-42.
18. da S. Mello, G.; de P. Cardoso, A.; Oliveira, E.; Siqueira, A., Tryptophan. *An Int. Forum for Thermal Studies* **2015,** *122* (3), 1395-1401.
19. Fricke, J.; Blei, F.; Hoffmeister, D., Enzymatic Synthesis of Psilocybin. *Angewandte Chemie International Edition* **2017,** *56* (40), 12352-12355.
20. Pharma, L. V. Dilaterol. http://www.levetpharma.com/our-registrations/dilaterol-25-microgramml-syrup-for-horses/ (accessed 05 July 2018).
21. U.S.F.D.A Ventipulmin Syrup - Original Approval. https://animaldrugsatfda.fda.gov/adafda/views/#/foiDrugSummaries#foiApplicationInfo (accessed 05 July 2018).

22. Administration, D. E. Clenbuterol. https://www.deadiversion.usdoj.gov/drug_chem_info/clenbuterol.pdf (accessed 05 July 2018).
23. W. A. D. A. Prohibited List. https://www.wada-ama.org/sites/default/files/prohibited_list_2018_en.pdf (accessed 05 July 2018).
24. Thevis, M.; Thomas, A.; Beuck, S.; Butch, A.; Dvorak, J.; Schanzer, W., Does the analysis of the enantiomeric composition of clenbuterol in human urine enable the differentiation of illicit clenbuterol administration from food contamination in sports drug testing? *Rapid Commun. in Mass Spectrom.* **2013,** *27* (4), 507.
25. Culmsee, C.; Junker, V.; Thal, S.; Kremers, W.; Maier, S.; Schneider, H. J.; Plesnila, N.; Krieglstein, J., Enantio-selective effects of clenbuterol in cultured neurons and astrocytes, and in a mouse model of cerebral ischemia. *Eur. J. Pharmacol.* **2007,** *575* (1), 57-65.
26. Martin, P.; Puech, A.-J.; Brochet, D.; Soubrié, P.; Simon, P., Comparison of clenbuterol enantiomers using four psychopharmacological tests sensitive to β-agonists. *Eur. J. Pharmacol.* **1985,** *117* (1), 127-129.
27. Linus Pauling Institute, O. S. U. Vitamin K. https://lpi.oregonstate.edu/mic/vitamins/vitamin-K (accessed August 08).
28. Jagannath, V. A.; Thaker, V.; Chang, A. B.; Price, A. I., Vitamin K supplementation for cystic fibrosis. *Cochrane Database syst. rev.* **2017,** *8*, Cd008482.
29. Hamidi, M. S.; Cheung, A. M., Vitamin K and musculoskeletal health in postmenopausal women. *Mol. Nutr. Food Res.* **2014,** *58* (8), 1647-1657.
30. Hamidi, M. S.; Gajic-Veljanoski, O.; Cheung, A. M., Vitamin K and Bone Health. *J. Clin. Densitom.* **2013,** *16* (4), 409-413.
31. Skattebol, L. Aukrust, I. R.; Sandberg, M. Process for the preparation of Vitamin K2. European Patent Office, 06.01.2016. https://worldwide.espacenet.com/publicationDetails/originalDocument?CC=EP&NR=2346806B1&KC=B1&FT=D&ND=&date=20160106&DB=EPODOC&locale=en_EP (accessed 09 August 2018)
32. Kappa Academy, C., Vitamin K2 Market Commercial Development - From Samurai to Supermarket. (Paper no. 3), 16.
33. Kappa Bioscience Company. About Us. https://www.kappabio.com/company/ (accessed August 09).
34. Faber, K., *Biotransformations in Organic Chemistry: A Textbook*. Springer: Berlin, **2011**.
35. Bøckmann, P. Synthesis of enantiopure β-blocker (S)-metoprolol and derivatives by lipase catalysis. Master's thesis, Norwegian University of Science and Technology, **2016**.
36. Lund, I. T.; Bøckmann, P.; Jacobsen, E. E., Highly enantioselective CALB-catalyzed kinetic resolution of building blocks for b-blocker atenolol. *Tetrahedron* **2016,** *72*, 7288-7292.
37. Blindheim, F. H. Synthesis of Enantiopure Precursors for Clenbuterol Master's thesis, Norwegian University of Science and Technology, **2017**.
38. Jaeger, K.-E.; Reetz, M. T., Microbial lipases form versatile tools for biotechnology. *Trends Biotechnol.* **1998,** *16* (9), 396-403.
39. Ericsson, D. J.; Kasrayan, A.; Johansson, P.; Bergfors, T.; Sandström, A. G.; Bäckvall, J.-E.; Mowbray, S. L., X-ray Structure of Candida antarctica Lipase A Shows a Novel Lid Structure and a Likely Mode of Interfacial Activation. *J. Mol. Biol.* **2008,** *376* (1), 109-119.
40. Castro, A. M. d.; Carniel, A., A novel process for poly(ethylene terephthalate) depolymerization via enzyme-catalyzed glycolysis. *Biochem. Eng. J.* **2017,** *124*, 64-68.

41. Sun, S.; Hu, B., A novel method for the synthesis of glyceryl monocaffeate by the enzymatic transesterification and kinetic analysis. *Food Chem.* **2017,** *214*, 192-198.
42. Meyer, J.; Horst, A. E. W.; Steinhagen, M.; Holtmann, D.; Ansorge-Schumacher, M. B.; Kraume, M.; Drews, A., A continuous single organic phase process for the lipase catalyzed synthesis of peroxy acids increases productivity.(Report). *Eng. Life Sci.* **2017,** *17* (7), 759.
43. Segura, R. L.; Palomo, J. M.; Mateo, C.; Cortes, A.; Terreni, M.; Fernandez-Lafuente, R.; Guisan, J. M., Different properties of the lipases contained in porcine pancreatic lipase extracts as enantioselective biocatalysts. *Biotechnol. prog.* **2004,** *20* (3), 825-9.
44. Anthonsen, T., Jongejan, J. A., Solvent Effect in Lipase Catalyzed Racemate Resolution. *Methods Enzymol.* **1997,** *286*, 473-495.
45. Jacobsen, E. E., Anthonsen, T., Single Enantiomers from Racemates. Lipase catalysed Kinetic Resolution of Secondary Alcohols. In situ Stereoinversion. *Trends Org. Chem.* **2017,** *18*
46. Salama, T. A.; Novák, Z., N-Halosuccinimide/SiCl4 as general, mild and efficient systems for the α-monohalogenation of carbonyl compounds and for benzylic halogenation. *Tetrahedron Lett.* **2011,** *52* (31), 4026-4029.
47. Austli, G. B. Synthesis of Enantiopure β-Blocker (S)-Practolol by Lipase Catalysis. Master's Thesis, Norwegian University of Science and Technology, **2018**.
48. Lund, I. T. Mekanistiske studier i kjemo-enzymatisk syntese av enantiomert rene byggestener for betablokkeren Atenolol. Master's thesis, Norwegian University of Science and Technology, **2015**.
49. Anslyn, E. V.; Dougherty, D. A., *Modern Physical Organic Chemistry*. University Science Books: Sausalito, Cal, **2006**.
50. Poole, C. F., *The Essence of Chromatography*. Elsevier: Amsterdam, **2003**.
51. Lystvet, S. M.; Hoff, B. H.; Anthonsen, T.; Jacobsen, E. E., Chemoenzymatic synthesis of enantiopure 1-phenyl-2-haloethanols and their esters. *Biocatal. Biotransform.* **2010,** *28* (4), *272-278*.
52. Uray, G.; Stampfer, W.; Fabian, W. M. F., Comparison of Chirasil-DEX CB as gas chromatographic and ULMO as liquid chromatographic chiral stationary phase for enantioseparation of aryl- and heteroarylcarbinols. *J. Chromatogr. A* **2003,** *992* (1), 151-157.
53. Silverstein, R. M.; Webster, F. X.; Kiemle, D. J.; Bryce, D. L., *Spectrometric identification of organic compounds*. Wiley: Hoboken, N.J, **2015**.
54. Antuña, A.; Lavandera, I.; Rodríguez-González, P.; Rodríguez, J.; Garcia Alonso, J.; Gotor, V., A straightforward route to obtain 13C1-labeled clenbuterol. *Tetrahedron* **2011**, *67 (31)*, 5577-5581.
55. Moore, K. E. INVESTIGATION OF THE 4-AMINO-α,α-DIHYDROXY-3,5-DICHLOROACETOPHENONE IMPURITY IN THE SYNTHESIS OF CLENBUTEROL HYDROCHLORIDE. Masters Thesis, Virginia Commonwealth Univeristy, Richmond, Virginia, **2014**.
56. Morante-Zarcero, S.; Sierra, I., Simultaneous enantiomeric determination of propranolol, metoprolol, pindolol, and atenolol in natural waters by HPLC on new polysaccharide-based stationary phase using a highly selective molecularly imprinted polymer extraction. *Chirality* **2012,** *24* (10), 860-866.
57. Novozymes A/S, Immobilized lipases for biocatalysis. In *Biocatalysis Brochure from Immobilized Lipases*.
58. Fulmer, G. R.; Miller, A. J. M.; Sherden, N. H.; Gottlieb, H. E.; Nudelman, A.; Stoltz, B. M.; Bercaw, J. E.; Goldberg, K. I., NMR chemical shifts of trace impurities: Common laboratory solvents, organics, and gases in deuterated solvents relevant to the organometallic chemist. *Organometall.* **2010,** *29* (9), 2176-2179.

59. Zielinska-Pisklak, M.; Pisklak, D.; Wawer, I.; Zielinska-Pisklak, M., 1H and 13C NMR characteristics of Delta *b-blockers. *Magn. Reson. Chem.* **2011,** *49* (5), 284-290.
60. Anthonsen, H. W.; Hoff, B. H.; Anthonsen T. Calculation of Enantiomer Ratio and Equilibrium Constants in Biocatalytic Ping-Pong Bi-Bi Resolutions. *Tetrahedron: Assymetry* **1996,** *7* (9), 2633-2638.

Attachements

1. MS spectrum of 4-amino-3,5-dichlorobenzoyl bromide (**2**)

Figure A1 shows the MS spectrum of compound **2**, where the ion observed is [M+H].

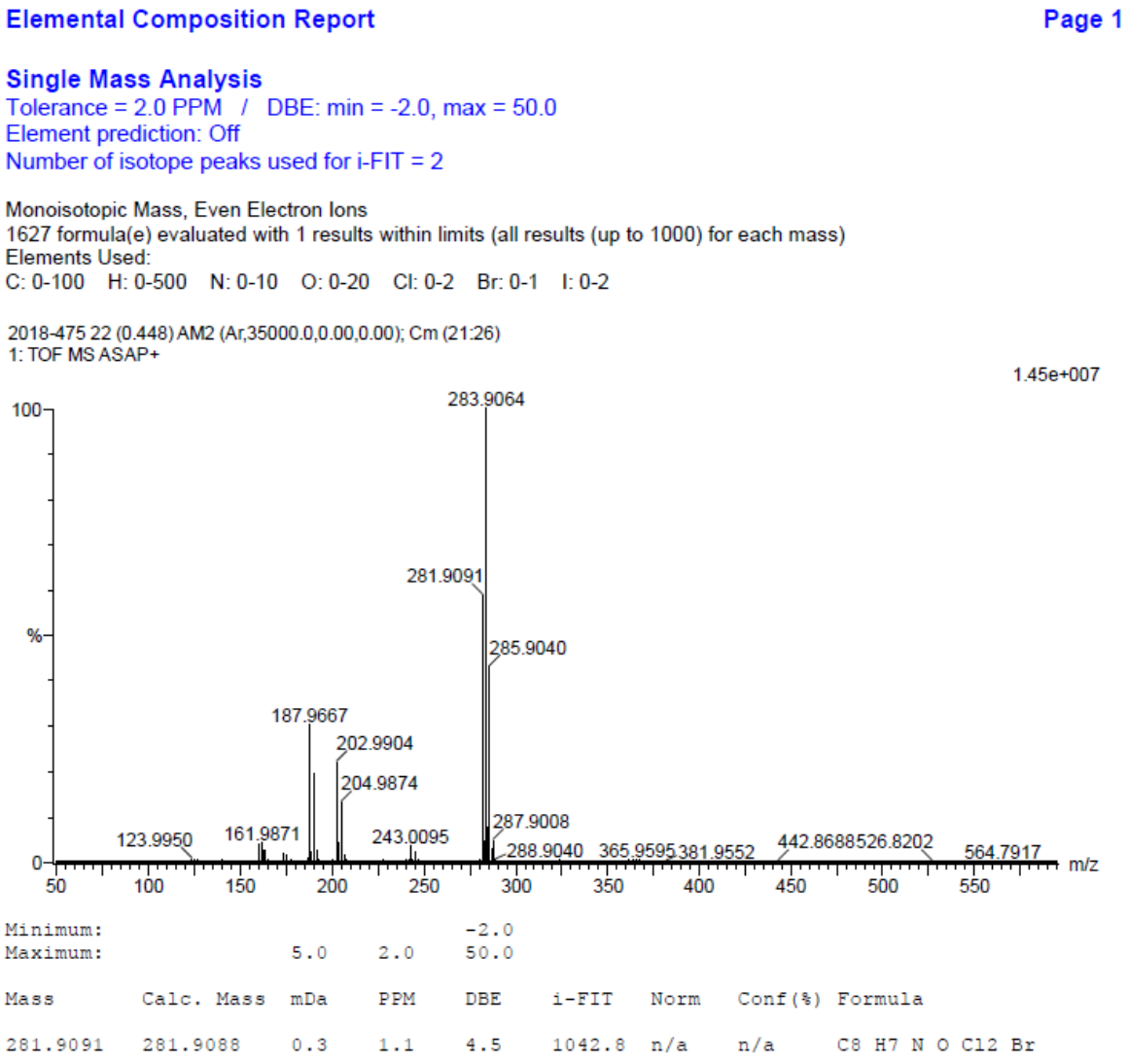

Figure A1: MS spectrum of 4-amino-3,5-dichlorobenzoyl bromide (**2**) [M+H].

2. GC-MS analysis of product from reaction 3 in the synthesis of 1-((1H-indol-4-yl)oxy)-3-chloropropan-2-ol (**5**) from 1H-indol-4-ol (**3**)

The GC spectrum of product from reaction 3 shows one peak at 18.8 minutes (Figure A2), the MS spectrum is shown in Figure A3 and shows molecular mass of 133 which corresponds to the starting material **3**.

peak #	R.T. min	first scan	max scan	last scan	PK TY	peak height	corr. area	corr. % max.	% of total
1	18.807	2739	2747	2770	BB	636986	13066971	100.00%	100.000%

Sum of corrected areas: 13066971

2017_JENS-SPME.M Thu Apr 05 07:58:12 2018

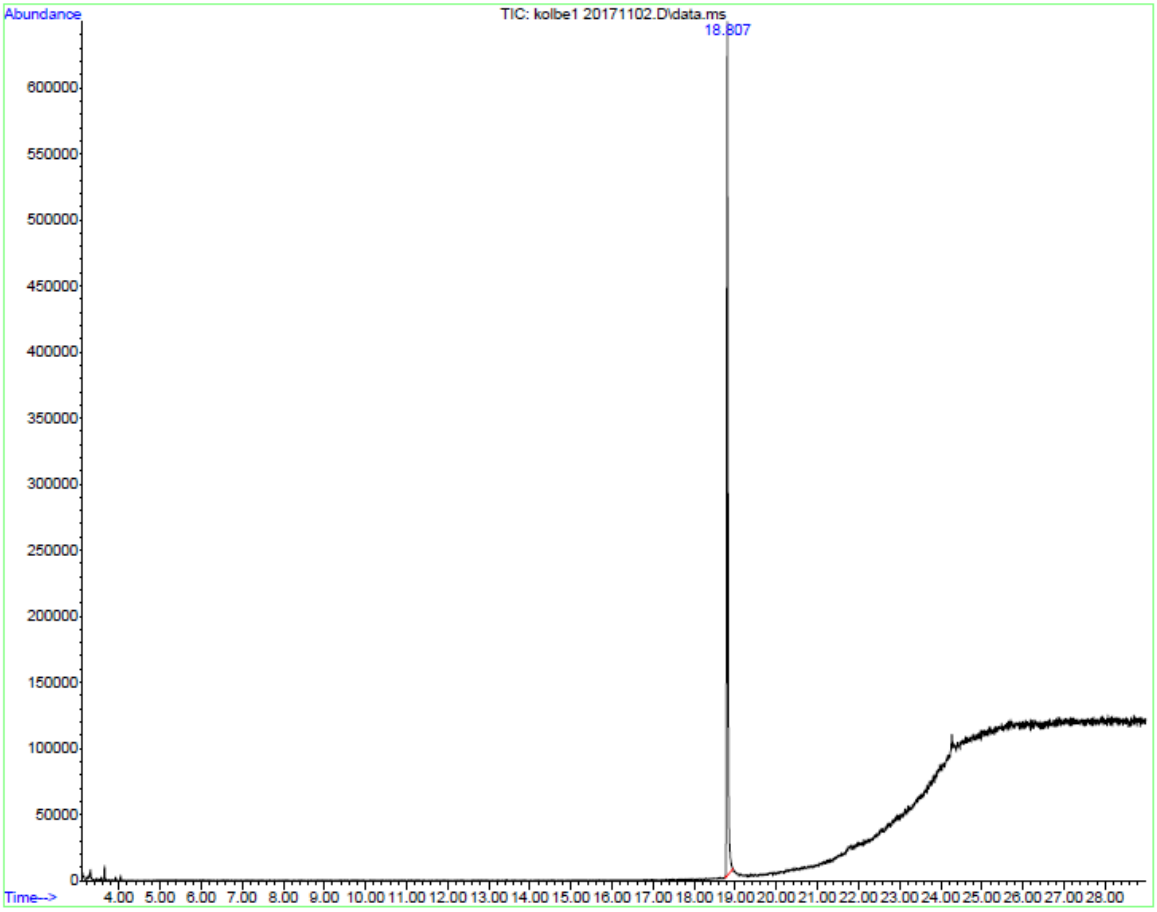

Figure A2: GC spectrum of product from reaction 3 in the synthesis of 1-((1H-indol-4-yl)oxy)-3-chloropropan-2-ol (**5**) from 1H-indol-4-ol (**3**).

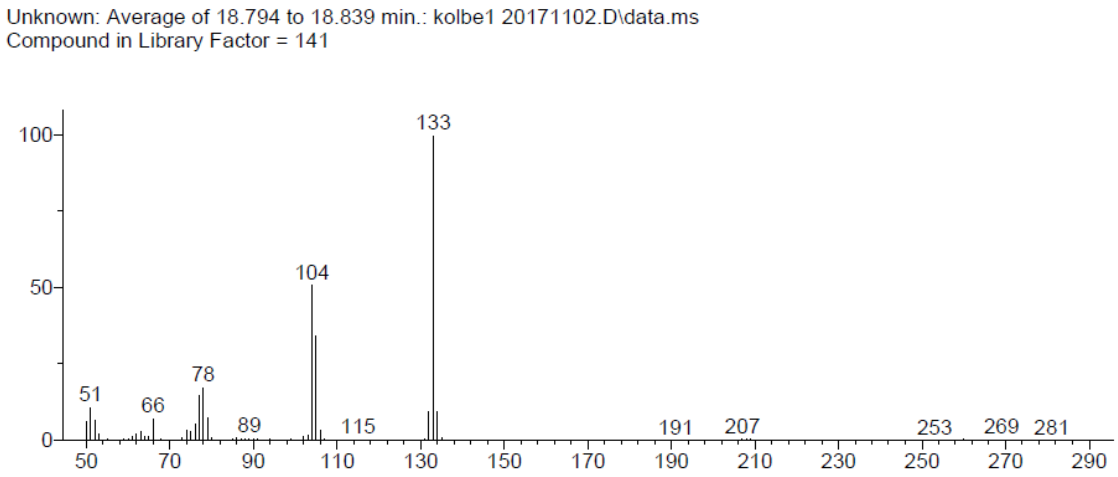

Figure A3: MS spectrum of substance retained at 18.8 minutes in shown in Figure A1, the mass is matching that of the starting material **3**.

3. GC-MS analysis of product from reaction 4 in the synthesis of 1-((1H-indol-4-yl)oxy)-3-chloropropan-2-ol from 1H-indol-4-ol (**3**)

The GC spectrum of product from reaction 4 shows one peak at 18.8 minutes (Figure A4). The MS spectrum for this substance was recorded in reaction 3 (Figure A3) and is therefore not repeated here.

peak #	R.T. min	first scan	max scan	last scan	PK TY	peak height	corr. area	corr. % max.	% of total
1	18.806	2738	2747	2770	BB	546514	11317182	100.00%	100.000%

Sum of corrected areas: 11317182

2017_JENS-SPME.M Thu Apr 05 08:02:56 2018

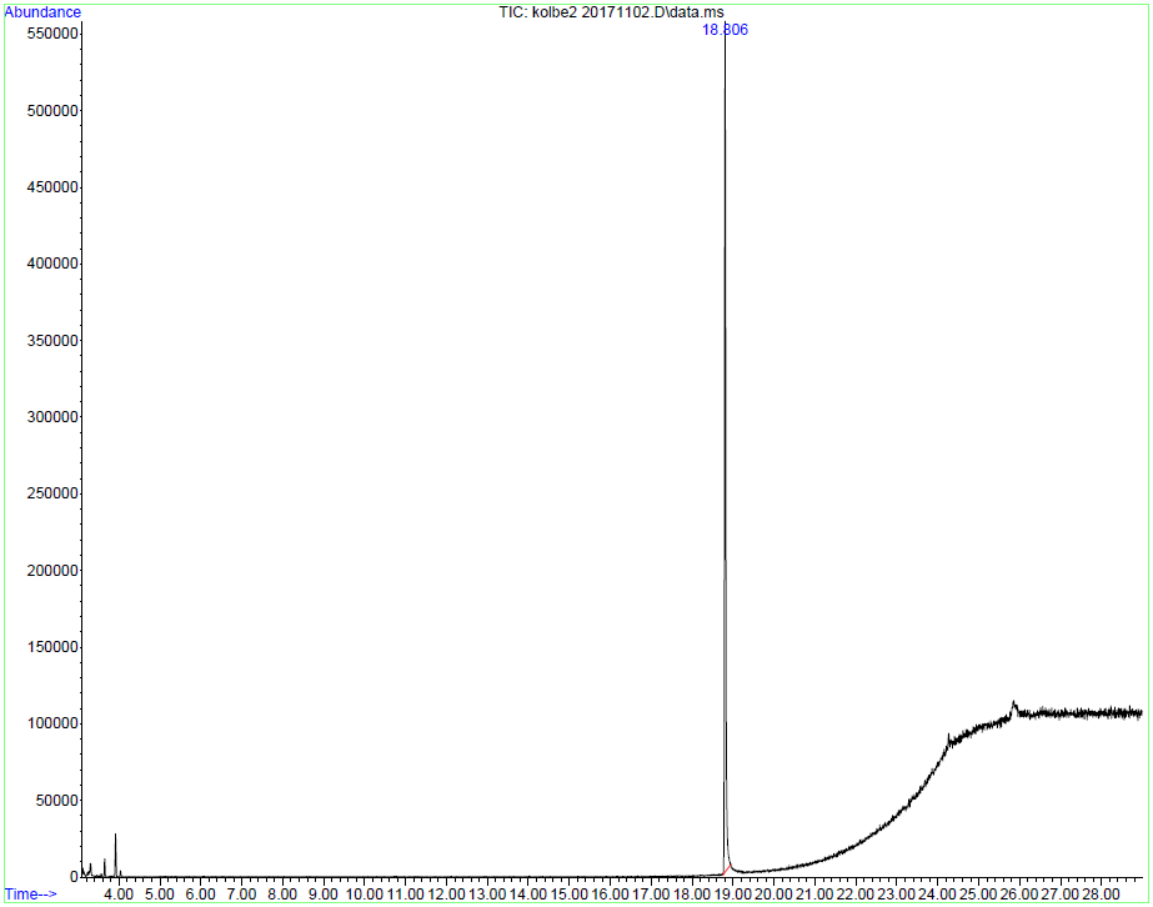

Figure A4: GC spectrum of product from reaction 4 in the synthesis of 1-((1H-indol-4-yl)oxy)-3-chloropropan-2-ol (**5**) from 1H-indol-4-ol (**3**).

4. GC-MS analysis of product from reaction 5 in the synthesis of 1-((1H-indol-4-yl)oxy)-3-chloropropan-2-ol (**5**) from 1H-indol-4-ol (**3**)

The GC spectra from both CH_2Cl_2- and EtOAC-phases from reaction 5 are shown in Figure A5 and A9. They show two substances in the CH_2Cl_2-phase at 21.8 and 23.7 minutes, MS spectra (Figure A6, A7 and A8) of these substances confirms them to be products **4** and **5** respectively. The EtOAc-phase is shown to contain some of the product **4** (21.8 minutes) and two other substances with retention times 3.4 min and 3.9 min. The MS spectra of these two peaks (Figure A10 and A11) confirms them to be the solvent 1,4-dioxane and the reagent epichlorohydrin respectively.

peak #	R.T. min	first scan	max scan	last scan	PK TY	peak height	corr. area	corr. % max.	% of total
1	21.781	3256	3267	3288	BB	2659505	46321520	100.00%	75.226%
2	23.711	3573	3604	3639	BB	631444	15254963	32.93%	24.774%

Sum of corrected areas: 61576483

2017_JENS-SPME.M Thu Apr 05 07:46:11 2018

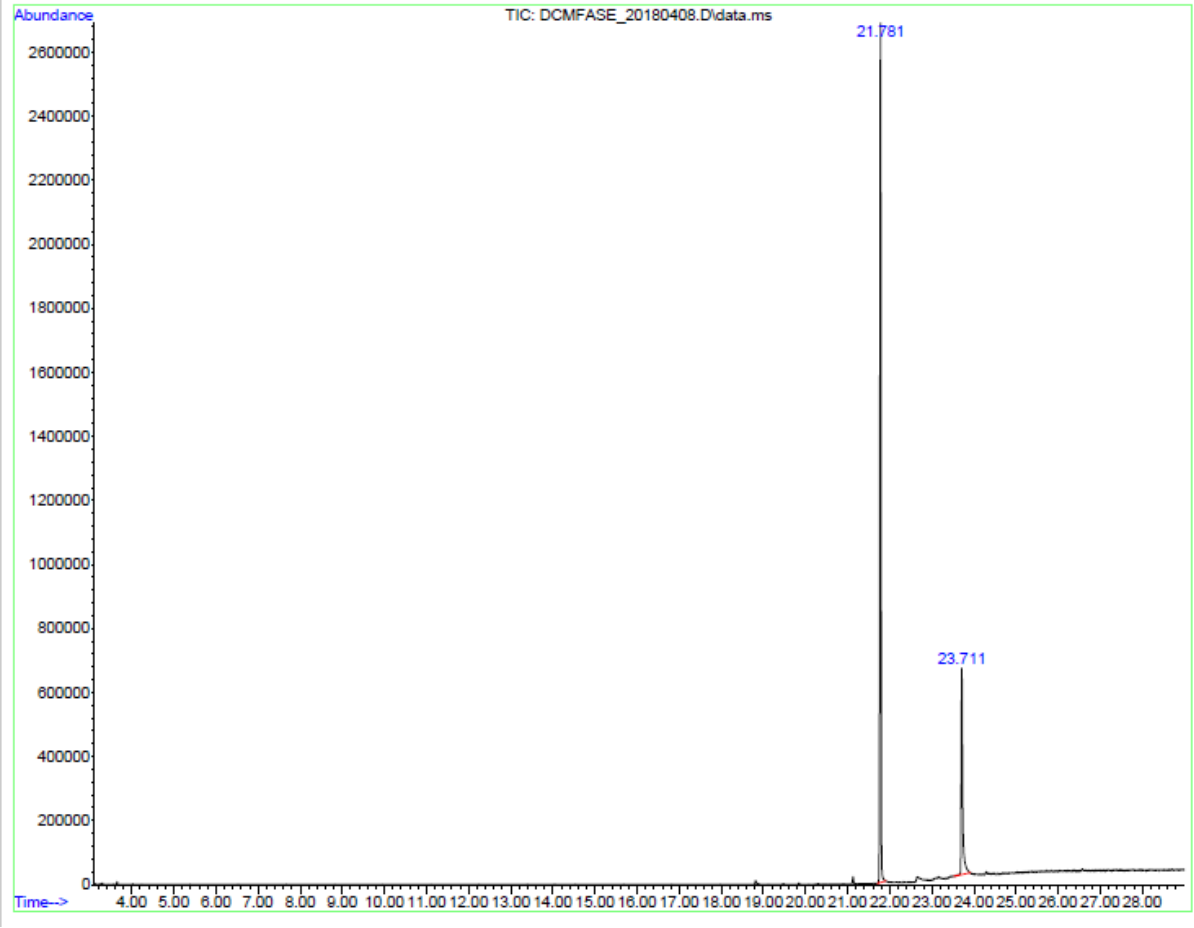

Figure A5: GC spectrum of product in the CH_2Cl_2-phase from reaction 5 in the synthesis of 1-((1H-indol-4-yl)oxy)-3-chloropropan-2-ol (**5**) from 1H-indol-4-ol (**3**).

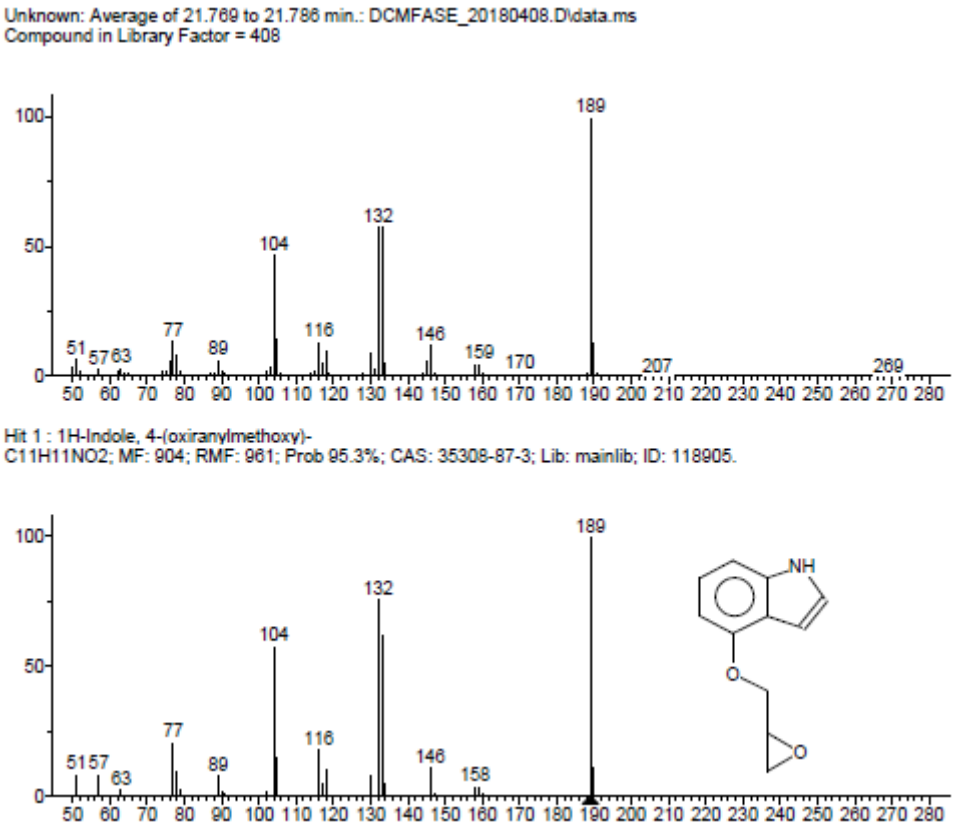

Figure A6: MS spectrum of substance retained at 21.8 minutes in shown in Figure A4, together with MS spectra of **4**.

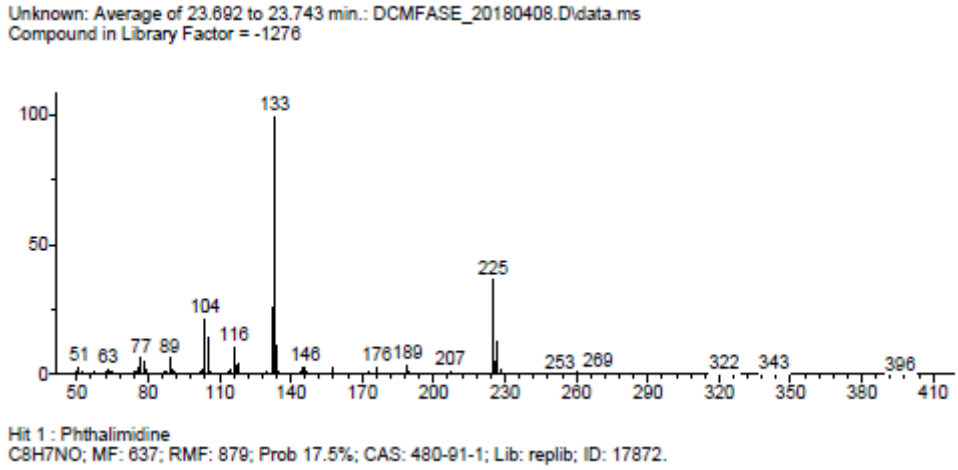

Figure A7: MS spectrum of substance retained at 23.7 minutes in shown in Figure A4.

Elemental Composition Report **Page 1**

Single Mass Analysis
Tolerance = 5.0 PPM / DBE: min = -2.0, max = 50.0
Element prediction: Off
Number of isotope peaks used for i-FIT = 2

Monoisotopic Mass, Even Electron Ions
462 formula(e) evaluated with 1 results within limits (all results (up to 1000) for each mass)
Elements Used:
C: 0-100 H: 0-500 N: 0-10 O: 0-20 Cl: 0-1
2018-465 104 (2.032) AM2 (Ar,35000.0,0.00,0.00); Cm (103:106)
1: TOF MS ASAP+

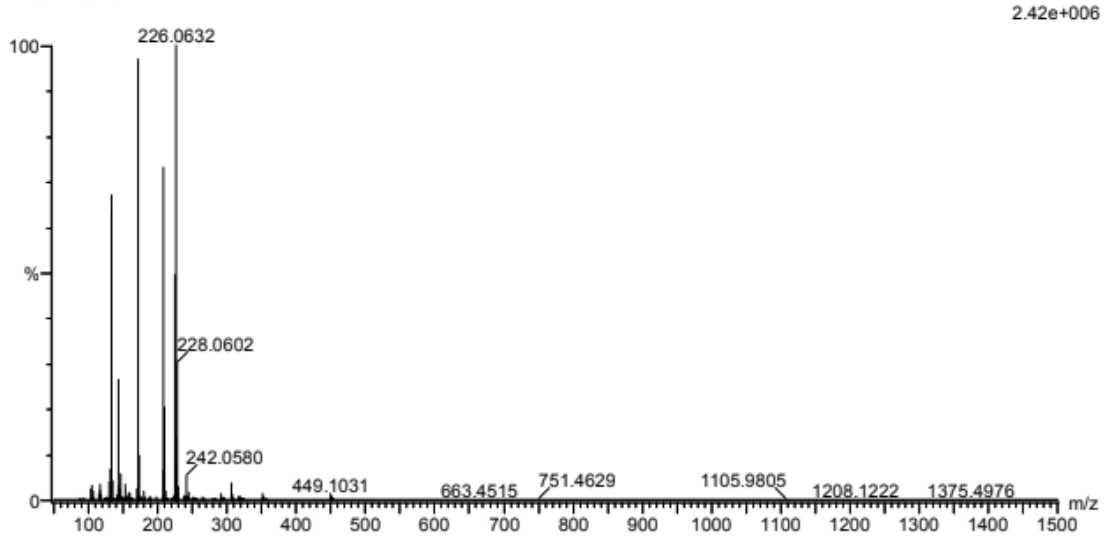

Minimum:				-2.0				
Maximum:		5.0	5.0	50.0				
Mass	Calc. Mass	mDa	PPM	DBE	i-FIT	Norm	Conf(%)	Formula
226.0632	226.0635	-0.3	-1.3	5.5	1073.1	n/a	n/a	C11 H13 N O2 Cl

Figure A8: MS spectrum of **5** with ion observed [M+H].

peak #	R.T. min	first scan	max scan	last scan	PK TY	peak height	corr. area	corr. % max.	% of total
1	3.405	43	56	71	BB	1723381	23926976	100.00%	73.932%
2	3.908	136	143	153	BB	312805	4371283	18.27%	13.507%
3	21.776	3258	3266	3277	BB	235333	4065039	16.99%	12.561%

Sum of corrected areas: 32363298

2017_JENS-SPME.M Thu Apr 05 07:49:00 2018

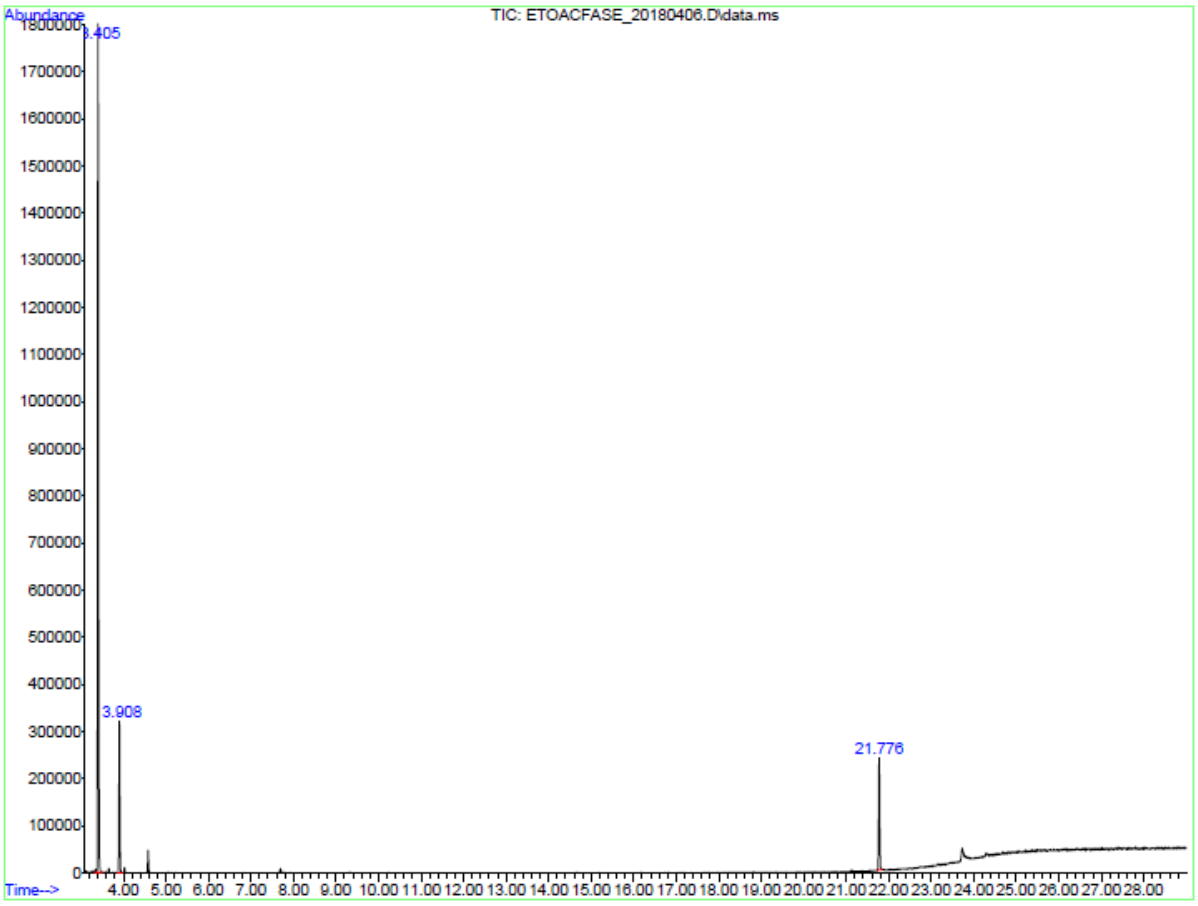

Figure A9: GC spectrum of the EtOAC-phase from reaction 5 in the synthesis of 1-((1H-indol-4-yl)oxy)-3-chloropropan-2-ol (**5**) from 1H-indol-4-ol (**3**).

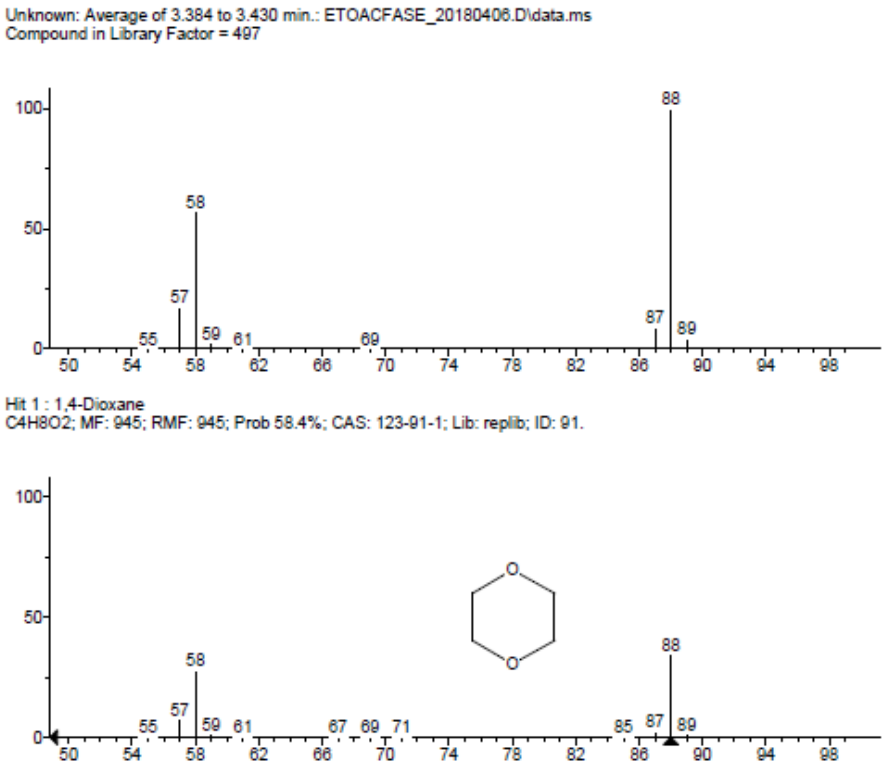

Figure A10: MS spectrum of substance retained at 3.4 minutes shown in Figure A8, together with MS spectra of the used solvent 1,4-dioxane.

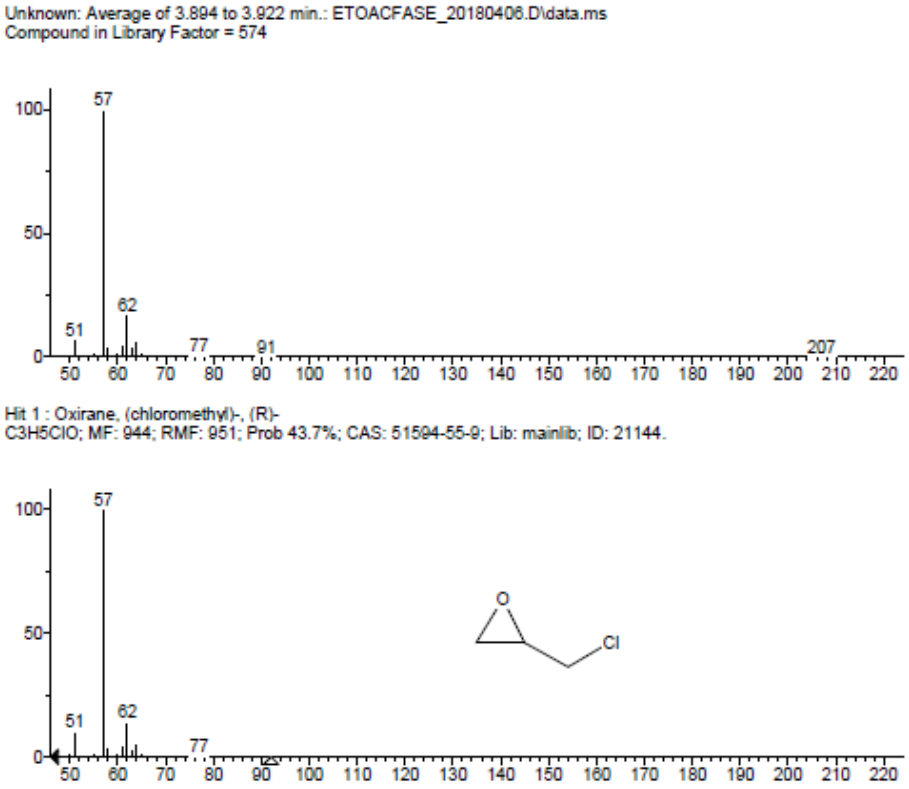

Figure A11: MS spectrum of substance retained at 3.9 minutes shown in Figure A8, together with MS spectra of the used reagent epichlorohydrin.

5. GC-MS analysis of product from reaction 6 in the synthesis of 1-((1H-indol-4-yl)oxy)-3-chloropropan-2-ol from 1H-indol-4-ol (**3**)

The product from reaction 6 is shown to contain four substances (Figure A12). Two are the products **4** and **5** at retention times 21.8 minutes and 23.7 minutes. One is the solvent 1,4-dioxane at retention time 3.4 minutes. The last substance is found at retention time 7.7 minutes, and it is shown by MS (Figure A13) to be the by-product 1,3-dichloro-2-propanol.

peak #	R.T. min	first scan	max scan	last scan	PK TY	peak height	corr. area	corr. % max.	% of total
1	3.404	50	55	69	BB	254765	3891898	11.06%	6.515%
2	7.689	795	804	819	BB	250927	4305194	12.23%	7.206%
3	21.772	3256	3266	3282	BB	962714	16354953	46.48%	27.377%
4	23.706	3572	3604	3653	BB	1513667	35188768	100.00%	58.902%

Sum of corrected areas: 59740813

GBA_20170925.M Wed Apr 18 00:46:16 2018

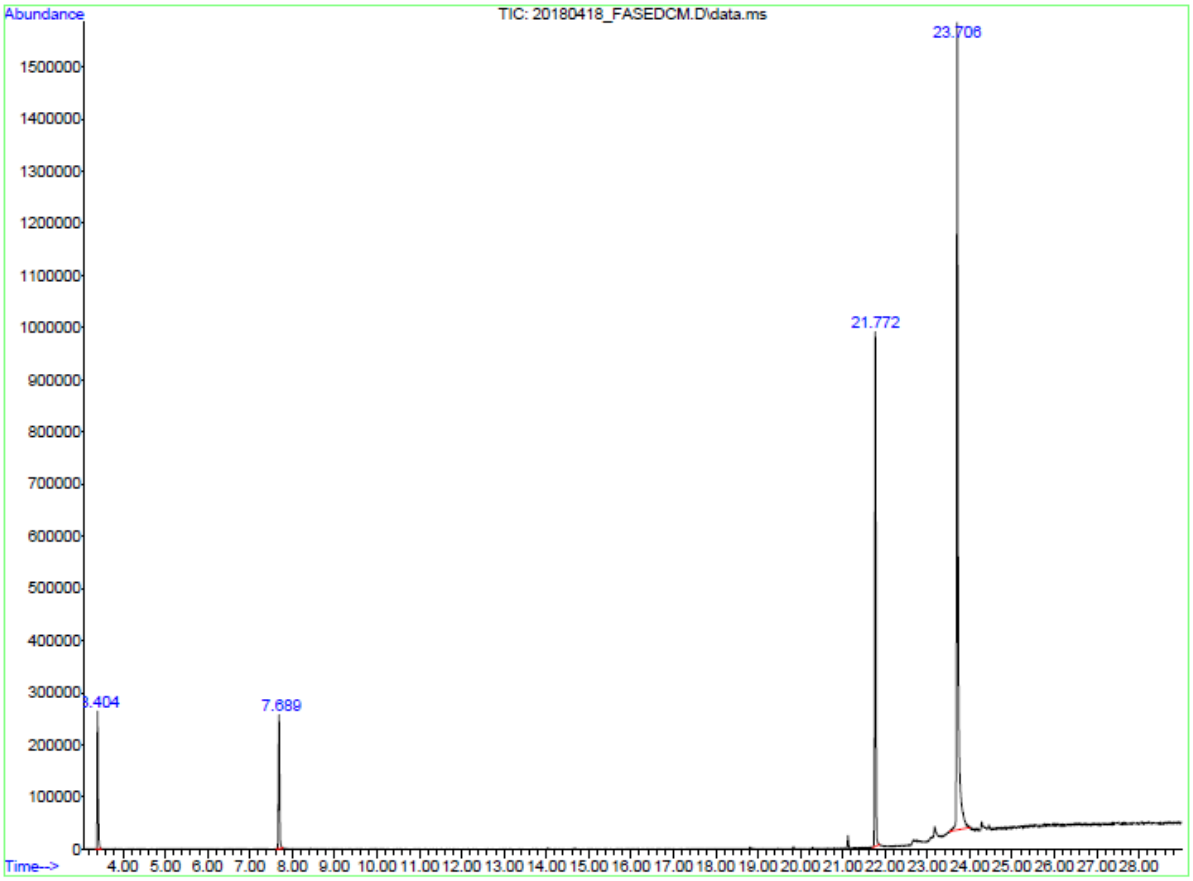

Figure A12: GC spectrum of product in the CH_2Cl_2-phase from reaction 6 in the synthesis of 1-((1H-indol-4-yl)oxy)-3-chloropropan-2-ol (**5**) from 1H-indol-4-ol (**3**).

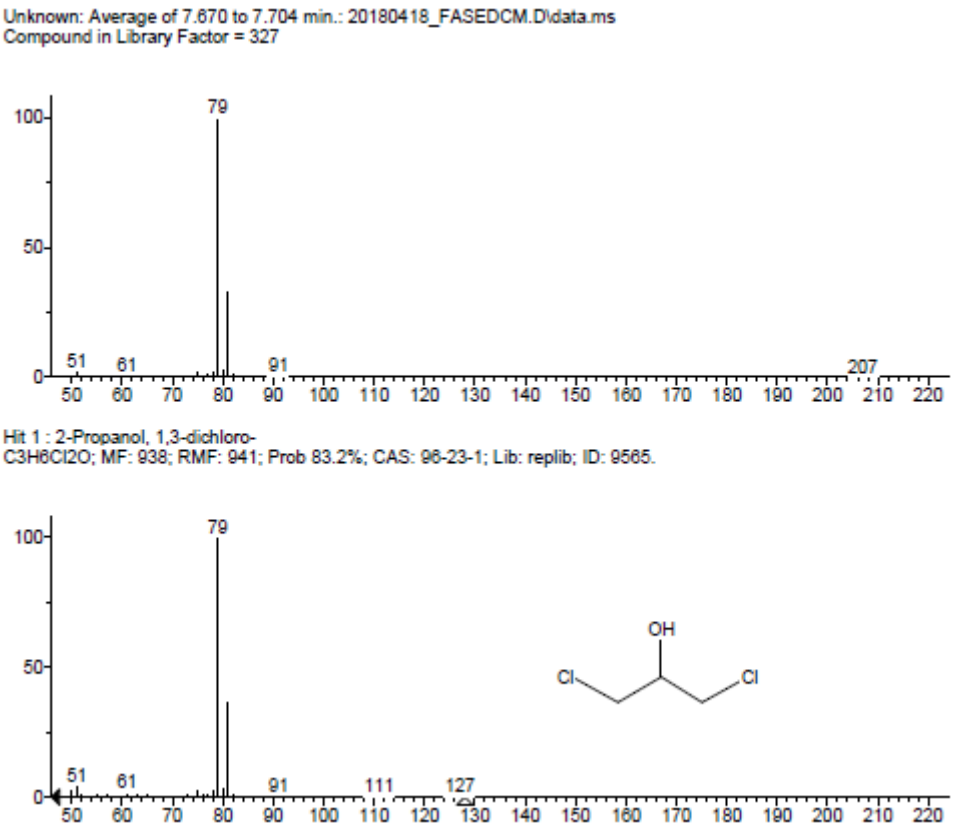

Figure A13: MS spectrum of substance retained at 7.7 minutes shown in Figure A11, together with MS spectra of the by-product 1,3-dichloro-2-propanol.

6. GC-MS analysis of product from reaction 7 in the synthesis of 1-((1H-indol-4-yl)oxy)-3-chloropropan-2-ol ol (**5**) from 1H-indol-4-ol (**3**)

GC spectrum of product from reaction 7 is shown in Figure A14 and shows one product at retention time 21.7. MS spectra of this compound shows it to be the product **4** (Figure A5).

peak #	R.T. min	first scan	max scan	last scan	PK TY	peak height	corr. area	corr. % max.	% of total
1	21.729	3243	3258	3271	BB	350253	6069467	100.00%	100.000%

Sum of corrected areas: 6069467

GBA_20170925.M Tue Jun 26 03:14:13 2018

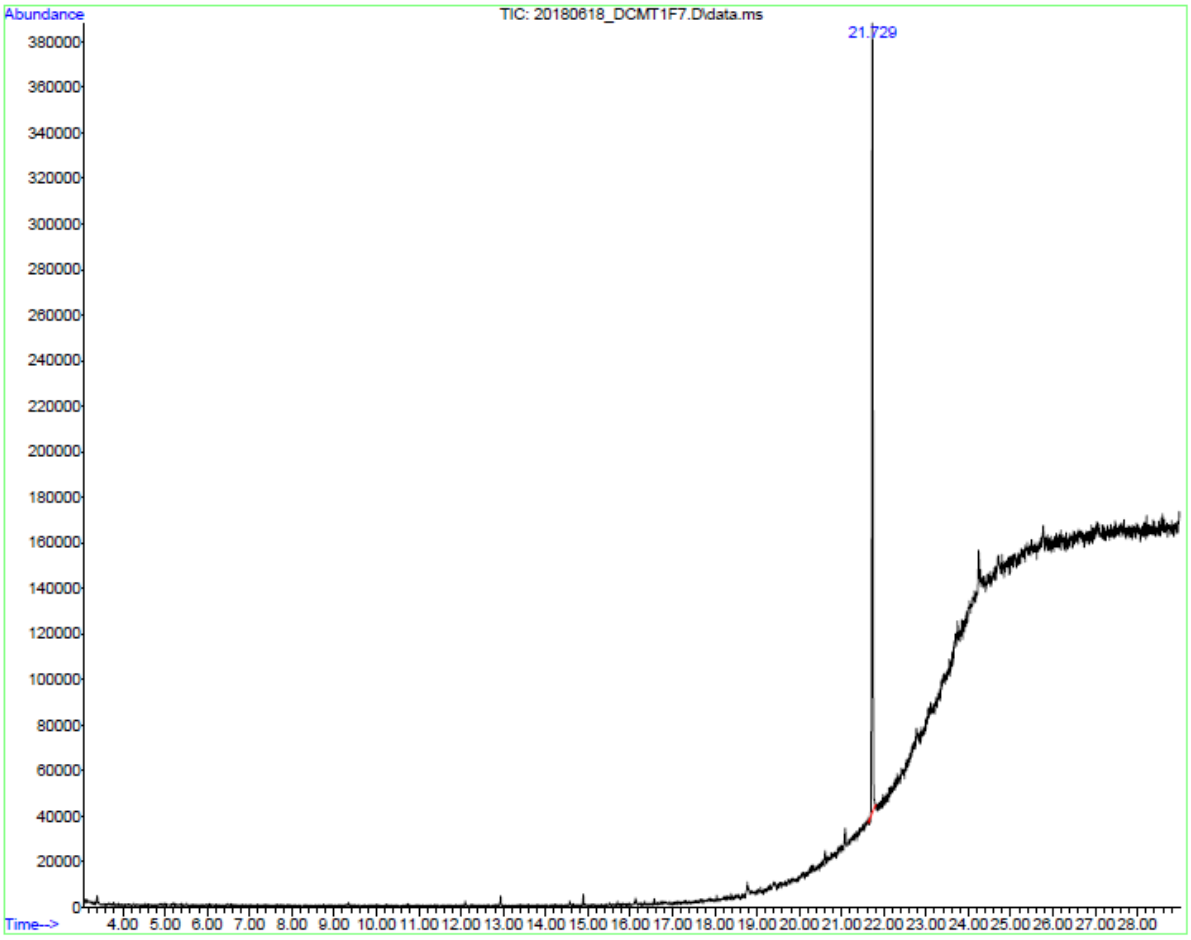

Figure A14: GC spectrum of product in the CH_2Cl_2-phase from reaction 7 in the synthesis of 1-((1H-indol-4-yl)oxy)-3-chloropropan-2-ol (**5**) from 1H-indol-4-ol (**3**).

7. GC-MS analysis of product from reaction 8 in the synthesis of 1-((1H-indol-4-yl)oxy)-3-chloropropan-2-ol (**5**) from 1H-indol-4-ol (**3**)

GC spectrum of product from reaction 8 is shown in Figure A15 and shows two products at retention time 21.7 minutes and 23.7 minutes. MS spectra of these compounds shows them to be the products **4** (Figure A5) and **5** (Figure A6 and A7).

peak #	R.T. min	first scan	max scan	last scan	PK TY	peak height	corr. area	corr. % max.	% of total
1	21.737	3248	3259	3280	BB	4278075	79840296	100.00%	97.276%
2	23.655	3587	3595	3611	BB	112818	2235505	2.80%	2.724%

Sum of corrected areas: 82075800

GBA_20170925.M Wed Jun 27 01:53:17 2018

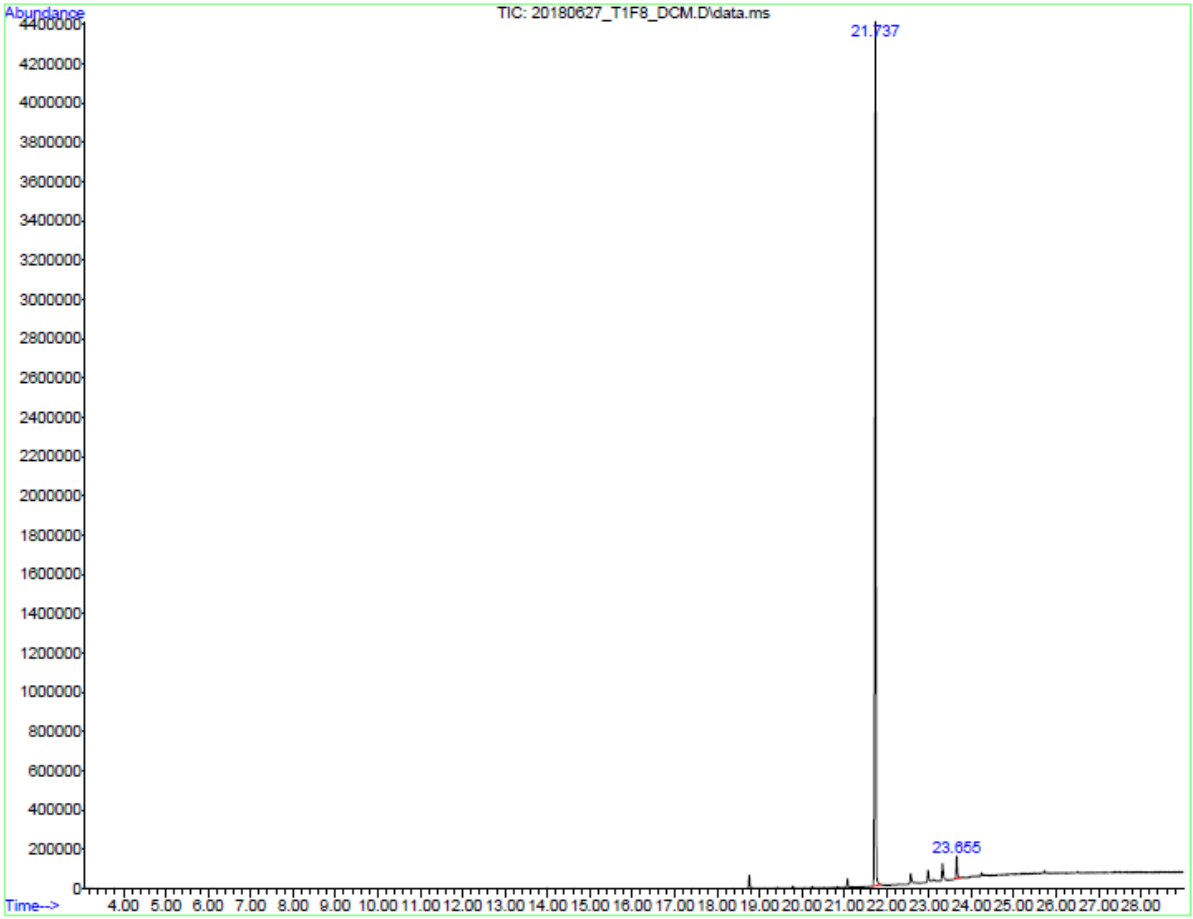

Figure A15: GC spectrum of product in the CH_2Cl_2-phase from reaction 8 in the synthesis of 1-((1H-indol-4-yl)oxy)-3-chloropropan-2-ol (**5**) from 1H-indol-4-ol (**3**).

8. MS analysis of black precipitate produced in the synthesis of 1-((1H-indol-4-yl)oxy)-3-chloropropan-2-ol (**5**) from 1H-indol-4-ol (**3**)

MS spectrum of black precipitate (Figure A16) shows several different peaks, indicating that the precipitate is composed of several different compounds.

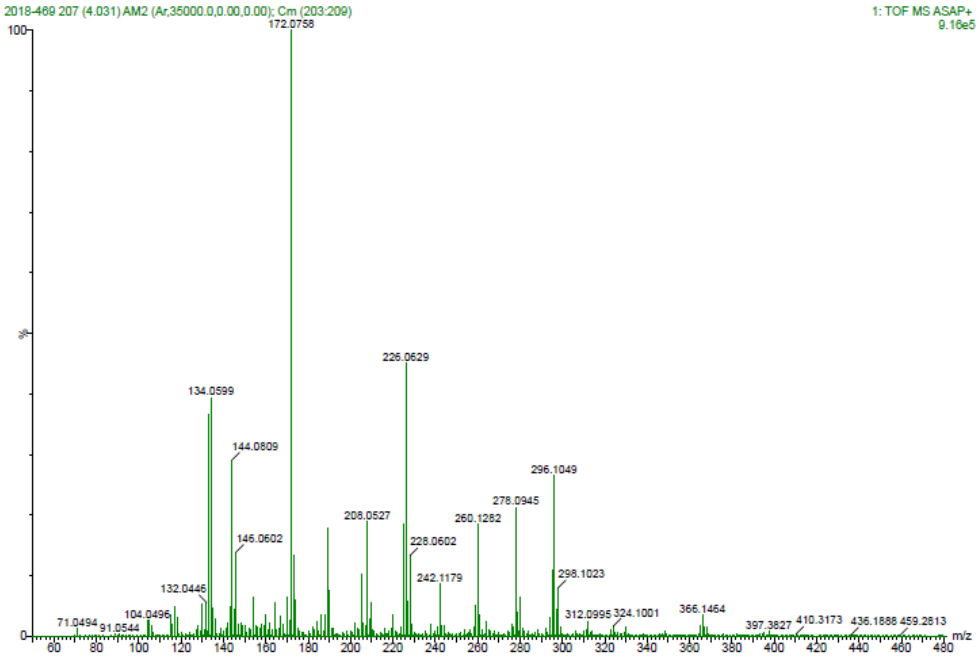

Figure A16: MS spectrum of black precipitate produced in the synthesis of 1-((1H-indol-4-yl)oxy)-3-chloropropan-2-ol (**5**) from 1H-indol-4-ol (**3**). Ions observed can be [M+H] or [M•].

9. GC-MS analysis of the product from reaction 2 in the opening of epoxide on 4-(oxiran-2-ylmethoxy)-1H-indole (**4**) forming 1-((1H-indol-4-yl)oxy)-3-chloropropan-2-ol (**5**)

The GC-chromatogram of this reaction (Figure A17) shows two compounds in the product at retention times 21.8 and 23.7 minutes, earlier shown to be compounds **4** and **5** respectively (Figure A5-8).

peak #	R.T. min	first scan	max scan	last scan	PK TY	peak height	corr. area	corr. % max.	% of total
1	21.728	3230	3258	3273	PV	450118	8104313	40.87%	29.011%
2	23.663	3524	3596	3616	BV	961906	19830647	100.00%	70.989%

Sum of corrected areas: 27934960

GBA_20170925.M Thu May 31 22:53:08 2018

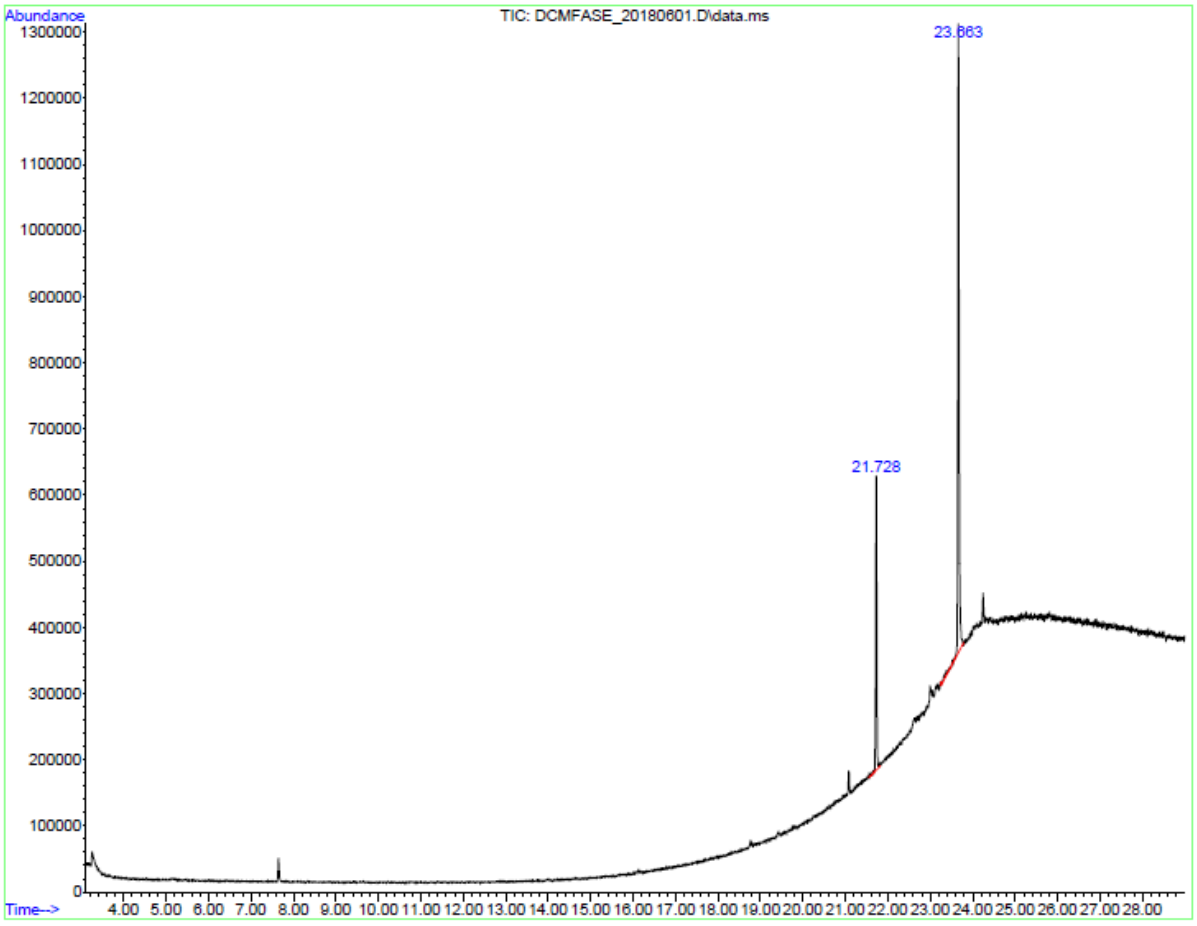

Figure A17: GC spectrum of product in the CH_2Cl_2-phase from reaction 2 in the opening of epoxide on 4-(oxiran-2-ylmethoxy)-1H-indole (**4**) forming 1-((1H-indol-4-yl)oxy)-3-chloropropan-2-ol (**5**).

10. GC-MS analysis of the product from reaction 3 in the opening of epoxide on 4-(oxiran-2-ylmethoxy)-1H-indole (**4**) forming 1-((1H-indol-4-yl)oxy)-3-chloropropan-2-ol (**5**)

The GC-chromatogram of this reaction (Figure A18) shows two compounds in the product at retention times 21.8 and 23.7 minutes, earlier shown to be compounds **4** and **5** respectively (Figure A5-8).

peak #	R.T. min	first scan	max scan	last scan	PK TY	peak height	corr. area	corr. % max.	% of total
1	21.728	3227	3258	3271	BB	808471	13806599	32.51%	24.534%
2	23.664	3553	3596	3631	VV	1972215	42468391	100.00%	75.466%

Sum of corrected areas: 56274990

GBA_20170925.M Thu Jun 07 22:06:24 2018

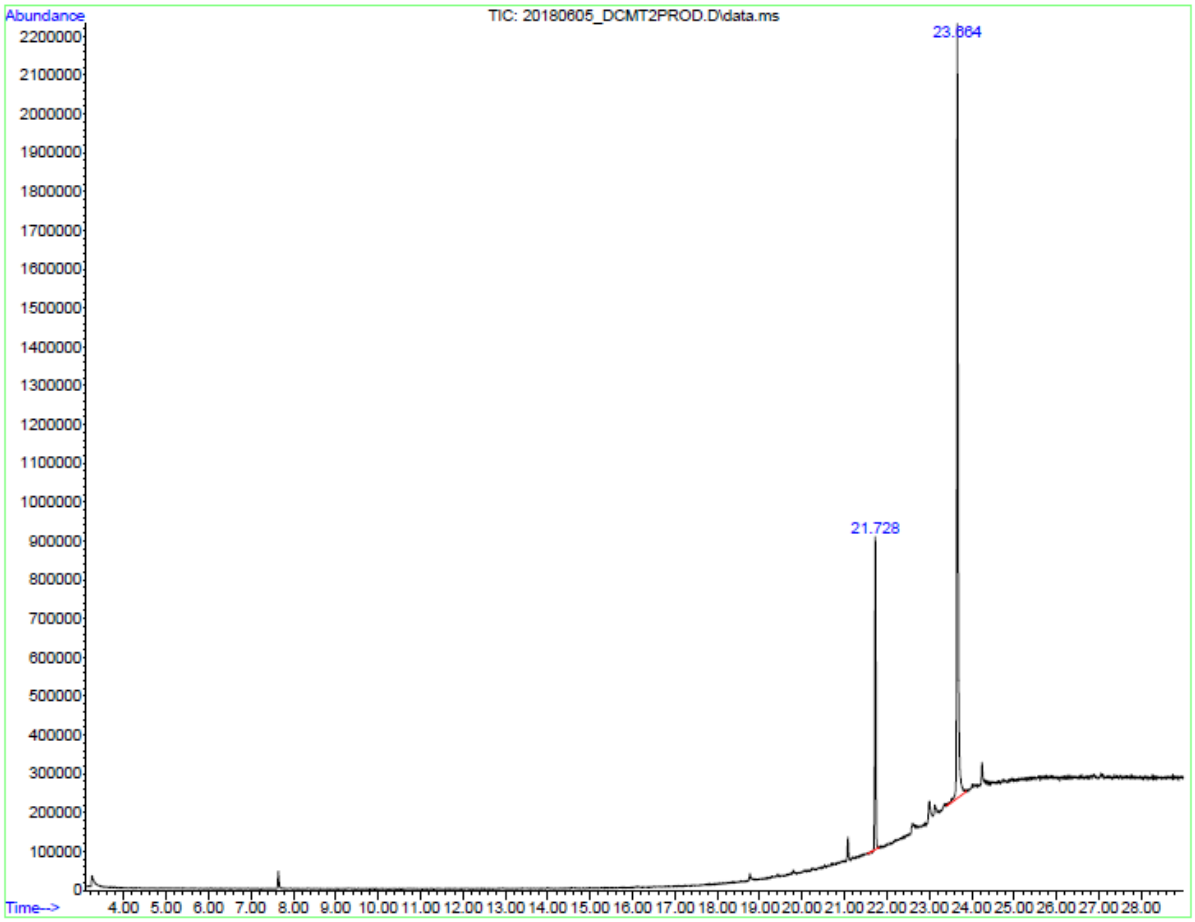

Figure A18: GC spectrum of product in the CH_2Cl_2-phase from reaction 3 in the opening of epoxide on 4-(oxiran-2-ylmethoxy)-1H-indole (**4**) forming 1-((1H-indol-4-yl)oxy)-3-chloropropan-2-ol (**5**).

11. GC-MS analysis of the product from reaction 4 in the opening of epoxide on 4-(oxiran-2-ylmethoxy)-1H-indole (**4**) forming 1-((1H-indol-4-yl)oxy)-3-chloropropan-2-ol (**5**)

The GC-chromatogram of this reaction (Figure A19) shows two compounds in the product at retention times 21.8 and 23.7 minutes, earlier shown to be compounds **4** and **5** respectively (Figure A5-8).

peak #	R.T. min	first scan	max scan	last scan	PK TY	peak height	corr. area	corr. % max.	% of total
1	21.727	3246	3258	3266	BV	81553	1438982	8.80%	7.802%
2	23.664	3579	3596	3616	VV	702882	16359996	100.00%	88.700%
3	24.245	3692	3698	3703	PV 2	36797	645157	3.94%	3.498%

Sum of corrected areas: 18444135

GBA_20170925.M Fri Jul 13 23:18:52 2018

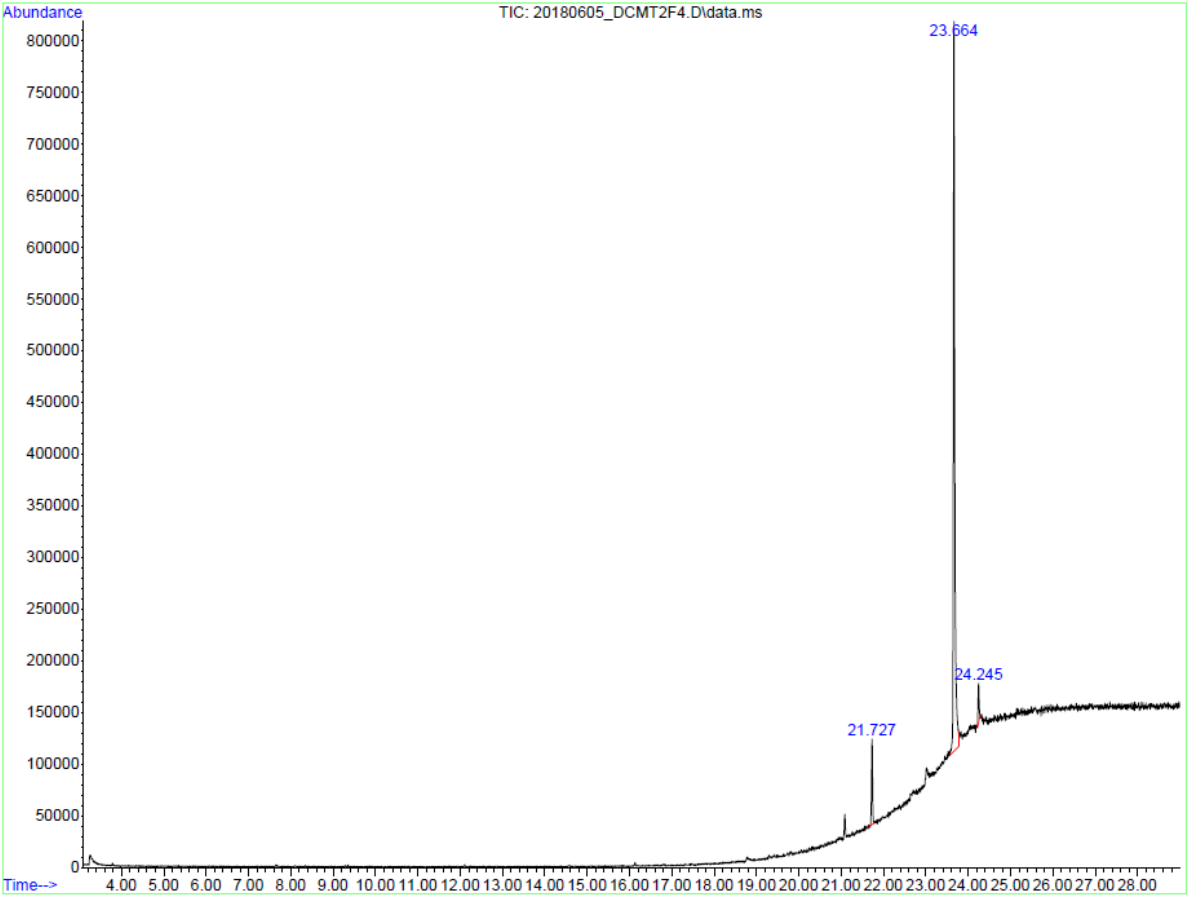

Figure A19: GC spectrum of product in the CH_2Cl_2-phase from reaction 4 in the opening of epoxide on 4-(oxiran-2-ylmethoxy)-1H-indole (**4**) forming 1-((1H-indol-4-yl)oxy)-3-chloropropan-2-ol (**5**).

12. GC-MS analysis of the product from reaction 5 in the opening of epoxide on 4-(oxiran-2-ylmethoxy)-1H-indole (**4**) forming 1-((1H-indol-4-yl)oxy)-3-chloropropan-2-ol (**5**)

The GC-chromatogram of this reaction (Figure A20) shows two compounds in the product at retention times 21.8 and 23.7 minutes, earlier shown to be compounds **4** and **5** respectively (Figure A5-8). There is also a large solvent peak at 3.2 minutes.

peak #	R.T. min	first scan	max scan	last scan	PK TY	peak height	corr. area	corr. % max.	% of total
1	3.193	13	18	68	BB	1315829	37420042	82.66%	33.823%
2	21.729	3247	3258	3274	BB	1623384	27944509	61.73%	25.258%
3	23.664	3563	3596	3639	BB	1990747	45270567	100.00%	40.919%

Sum of corrected areas: 110635118

GBA_20170925.M Tue Jun 26 03:11:34 2018

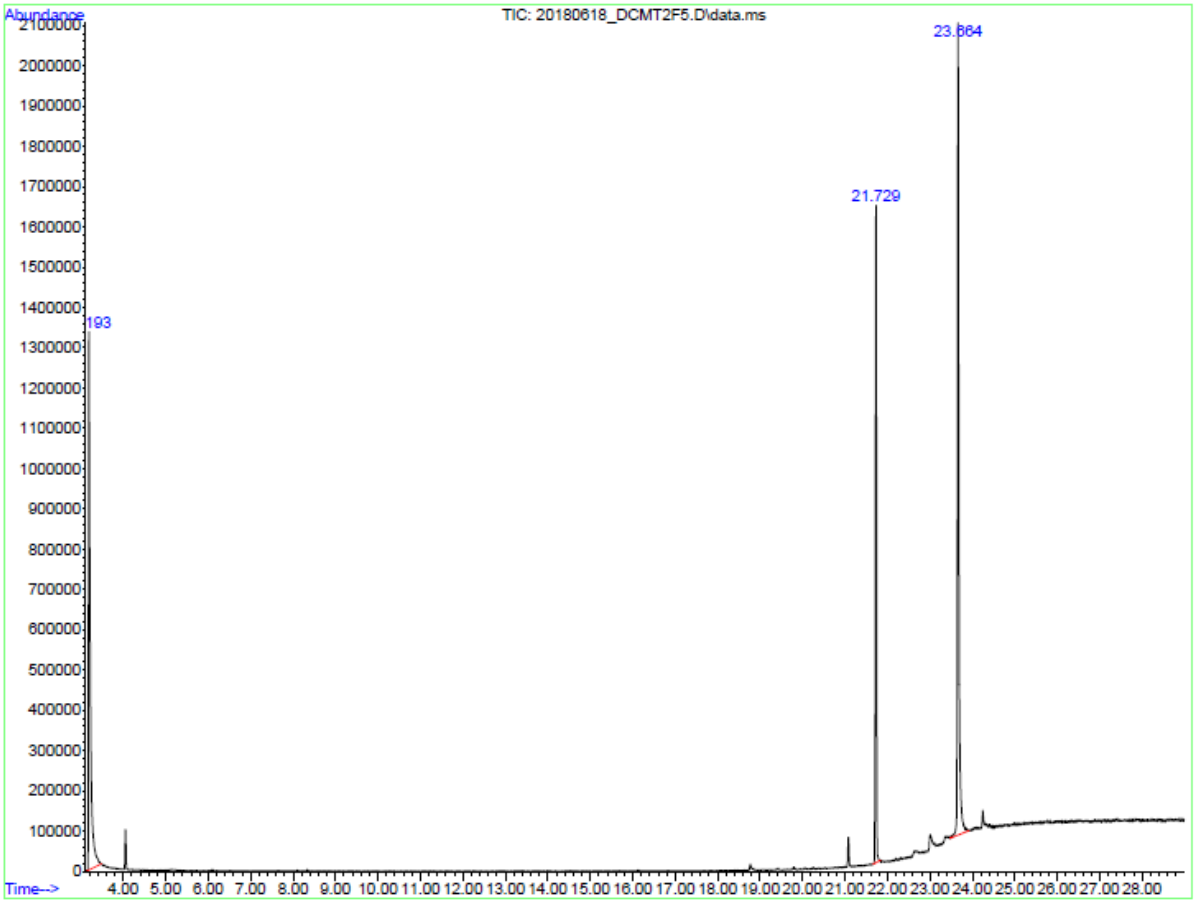

Figure A20: GC spectrum of product in the CH_2Cl_2-phase from reaction 5 in the opening of epoxide on 4-(oxiran-2-ylmethoxy)-1H-indole (**4**) forming 1-((1H-indol-4-yl)oxy)-3-chloropropan-2-ol (**5**).

13. GC-MS analysis of the product from reaction S1 in the opening of epoxide on 4-(oxiran-2-ylmethoxy)-1H-indole (**4**) forming 1-((1H-indol-4-yl)oxy)-3-chloropropan-2-ol (**5**)

The GC-chromatogram of reaction S1 after purification by flash-chromatography (Figure A21) shows a major peak at 23.7 minutes, earlier shown to be compound **5** (Figure A5, 7-8).

peak #	R.T. min	first scan	max scan	last scan	PK TY	peak height	corr. area	corr. % max.	% of total
1	14.633	2011	2018	2027	BB	75878	1127468	3.78%	3.361%
2	21.724	3242	3257	3269	BB	92200	1586132	5.31%	4.729%
3	22.979	3431	3476	3489	BB	55101	972353	3.26%	2.899%
4	23.658	3541	3595	3616	PV	1583535	29856222	100.00%	89.011%

Sum of corrected areas: 33542174

GBA_20170925.M Sat Jul 14 01:11:40 2018

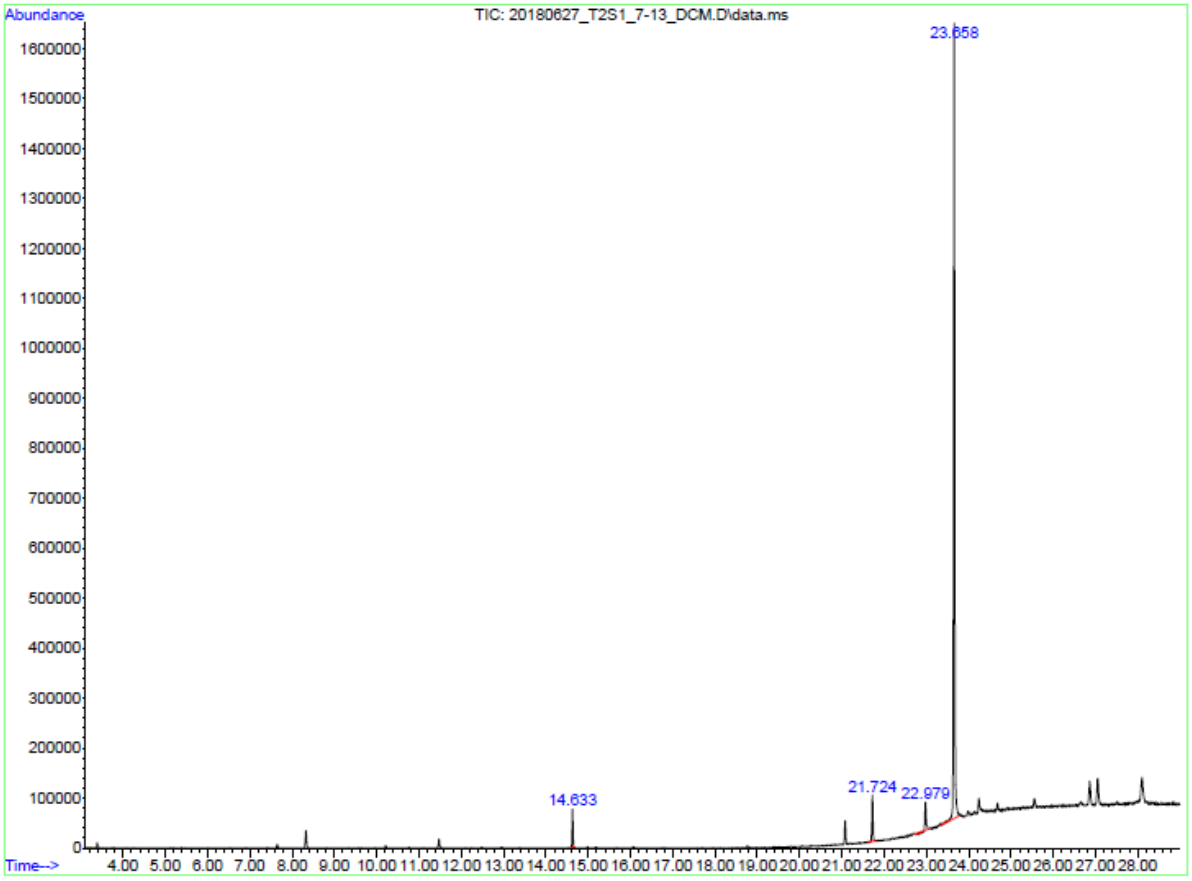

Figure A21: GC spectrum of product from reaction S1 in the opening of epoxide on 4-(oxiran-2-ylmethoxy)-1H-indole (**4**) forming 1-((1H-indol-4-yl)oxy)-3-chloropropan-2-ol (**5**).

14. GC-MS analysis of the product from reaction S1 in the opening of epoxide on 4-(oxiran-2-ylmethoxy)-1H-indole (**4**) forming 1-((1H-indol-4-yl)oxy)-3-chloropropan-2-ol (**5**)

The GC-chromatogram of a red impurity separated from the S1 product by flash-chromatography (Figure A22) shows two peaks. One peak is from the solvent 1,4-dioxane at 3.3 minutes and one peak at 14.6 minutes is an unknown impurity.

peak #	R.T. min	first scan	max scan	last scan	PK TY	peak height	corr. area	corr. % max.	% of total
1	3.361	41	48	65	BB	2757751	41768311	100.00%	70.675%
2	14.633	2009	2018	2030	BB	1137145	17331011	41.49%	29.325%

Sum of corrected areas: 59099322

GBA_20170925.M Tue Jun 26 03:19:06 2018

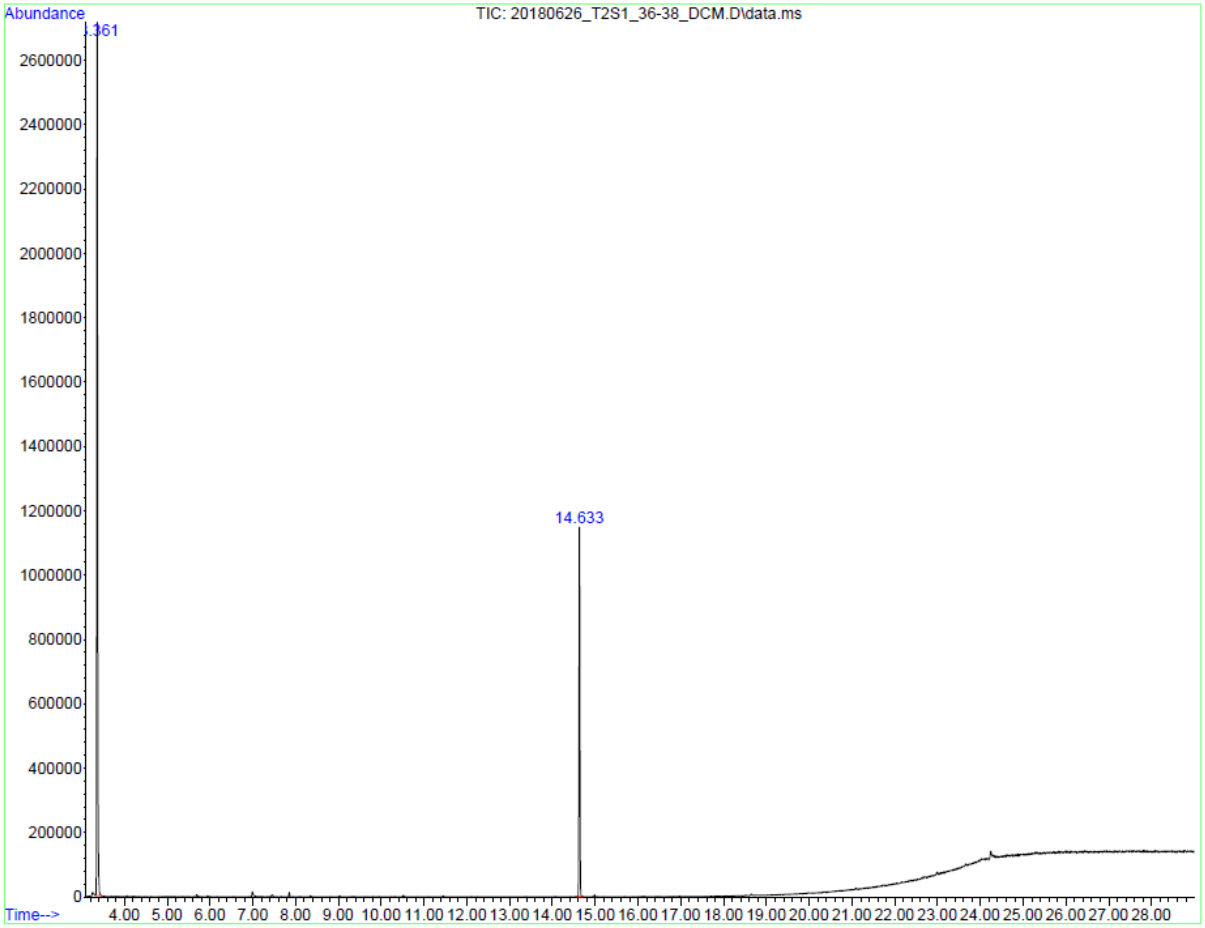

Figure A22: GC spectrum of by-product from reaction S1 in the opening of epoxide on 4-(oxiran-2-ylmethoxy)-1H-indole (**4**) forming 1-((1H-indol-4-yl)oxy)-3-chloropropan-2-ol (**5**).

The MS spectrum of the red by-product from reaction S1 can be seen in Figure A23.

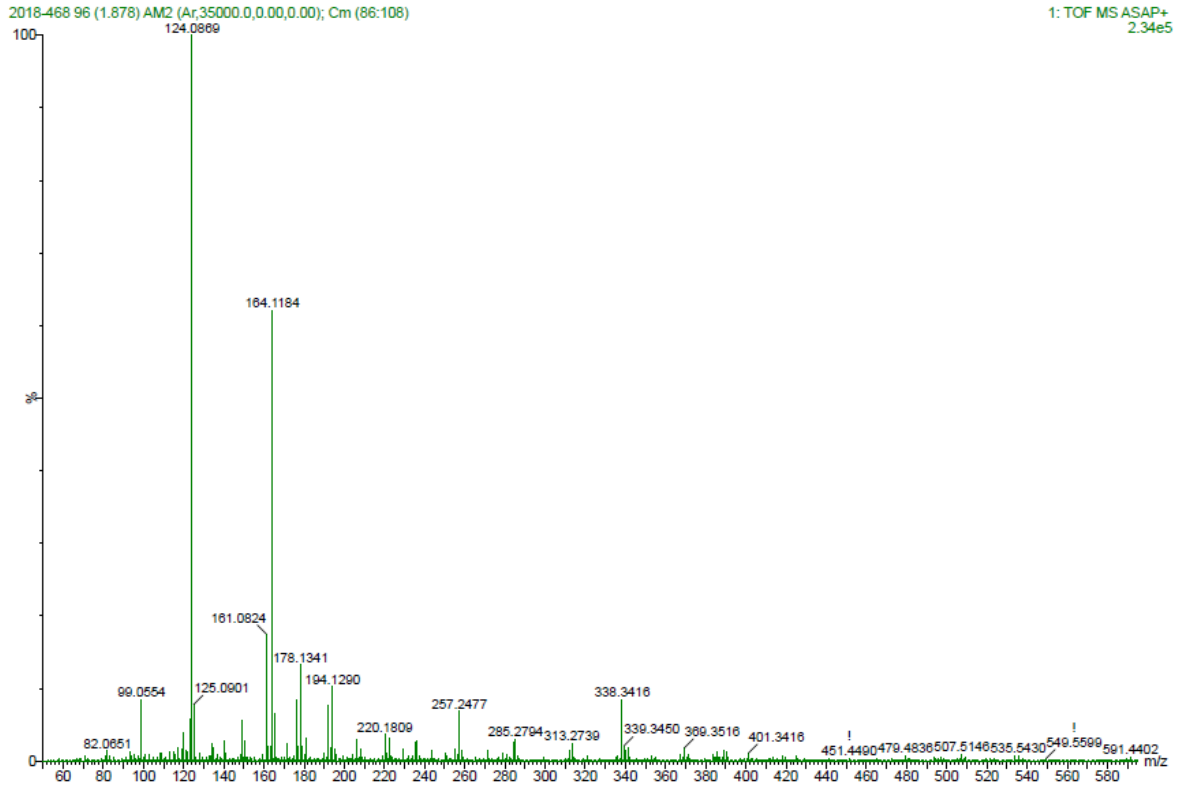

Figure A23: MS spectrum red by-product produced in the opening of the epoxide on 4-(oxiran-2-ylmethoxy)-1H-indole (**4**) forming 1-((1H-indol-4-yl)oxy)-3-chloropropan-2-ol (**5**). Ions observed can be [M+H] or [M•].

15. Chromatogram from chiral HPLC analysis at 24 hours reaction time in the synthesis of racemic ester 1-((1H-indol-4-yl)oxy)-3-chloropropan-2-yl butyrate (**6**) from 1-((1H-indol-4-yl)oxy)-3-chloropropan-2-ol (**5**)

Chiral HPLC analysis showing 77,5% starting material left in the synthesis of racemic ester 1-((1H-indol-4-yl)oxy)-3-chloropropan-2-yl butyrate (**6**) from 1-((1H-indol-4-yl)oxy)-3-chloropropan-2-ol (**5**) can be seen in Figure A24.

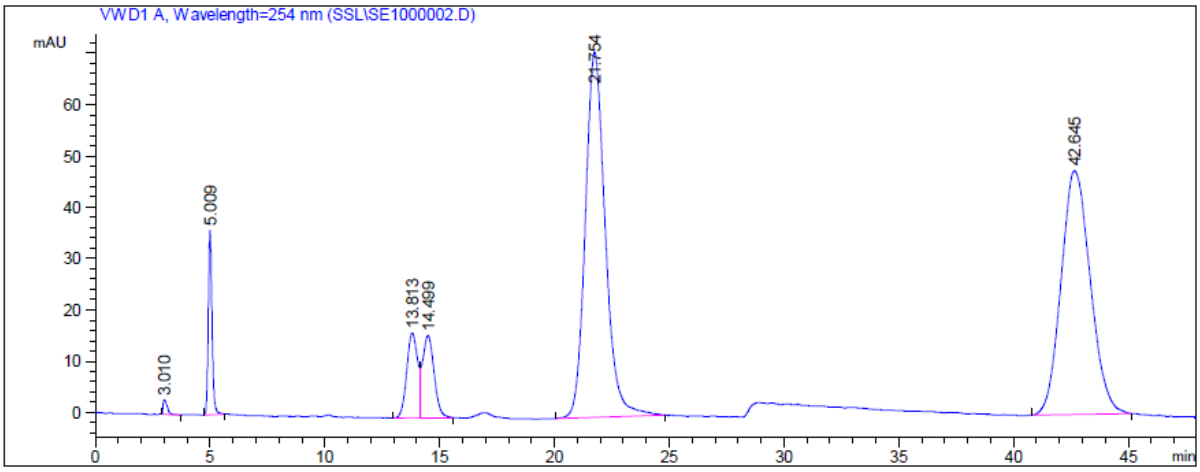


```
=====================================================================
                    Area Percent Report
=====================================================================

Sorted By             :      Signal
Multiplier:                   :      1.0000
Dilution:                     :      1.0000
Use Multiplier & Dilution Factor with ISTDs


Signal 1: VWD1 A, Wavelength=254 nm

Peak RetTime Type  Width     Area      Height     Area
  #   [min]        [min]  mAU   *s   [mAU   ]      %
----|-------|----|-------|----------|----------|--------|
   1   3.010 BB    0.1731   36.35133    2.80337   0.3614
   2   5.009 BB    0.1731  408.01199   35.97292   4.0559
   3  13.813 BV    0.5012  542.75885   16.52206   5.3953
   4  14.499 VB    0.5277  562.81689   16.02350   5.5947
   5  21.754 BB    0.9259 4305.72852   71.14944  42.8013
   6  42.645 BB    1.3152 4204.13281   47.49442  41.7914

Totals :                  1.00598e4   189.96571
```

Figure A24: Chiral HPLC chromatogram at 24 hours reaction time in the synthesis of **6.** (*R*)-**5** has t_R=42.6 minutes and (*S*)-**5** has t_R=21.8 minutes. (*S*)-**6** has t_R=15.5minutes and (*R*)-**6** has t_R=13.8 minutes. (Chiralcel OD-H column and hexane:2-propanol (80:20), 1 mL/min flow for 27 min, then hexane:2-propanol (70:30)).

16. Chromatogram from chiral HPLC analysis at 50% conversion of reaction 1 in the transesterification of 1-((1H-indol-4-yl)oxy)-3-chloropropan-2-ol (**5**) using CALB

Figure A25 shows the chromatogram from the chiral HPLC analysis of reaction 1 after 321 hours.

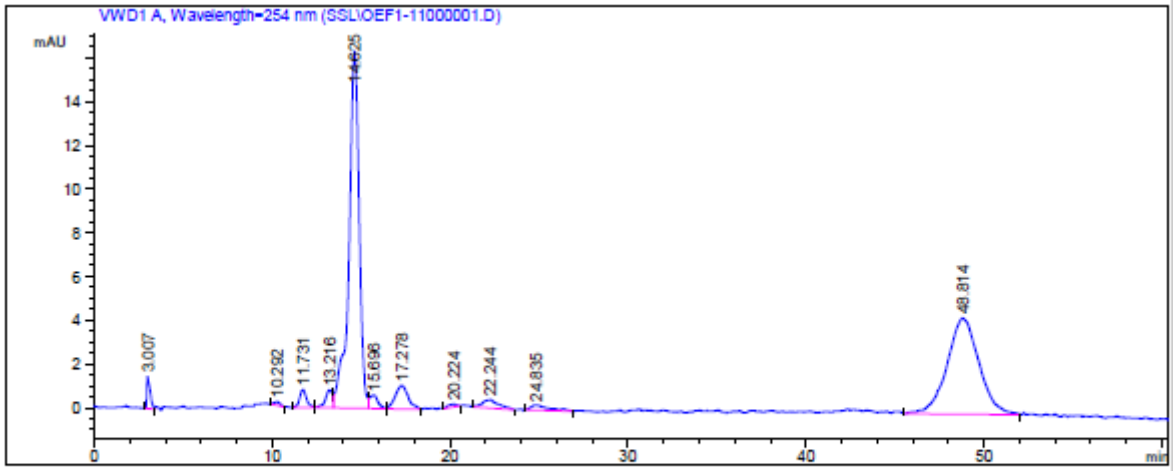


```
================================================================================
                          Area Percent Report
================================================================================

Sorted By             :      Signal
Multiplier:                   :      1.0000
Dilution:                     :      1.0000
Use Multiplier & Dilution Factor with ISTDs


Signal 1: VWD1 A, Wavelength=254 nm

Peak RetTime Type  Width     Area      Height     Area
  #   [min]        [min]  mAU   *s   [mAU   ]      %
----|-------|----|-------|----------|----------|--------|
   1   3.007 BV    0.1816   18.88246    1.44465   1.3638
   2  10.292 BB    0.3371    4.14883 1.73599e-1   0.2996
   3  11.731 BB    0.4052   22.08223 8.25769e-1   1.5948
   4  13.216 BV    0.4094   22.33854 8.09254e-1   1.6134
   5  14.625 VV    0.5936  650.41443   16.30219  46.9750
   6  15.696 VB    0.4688   19.38803 6.11669e-1   1.4003
   7  17.278 BB    0.7575   54.20830    1.07455   3.9151
   8  20.224 BB    0.4854    3.76384 1.04223e-1   0.2718
   9  22.244 BB    0.9053   24.73436 3.85771e-1   1.7864
```

Peak #	RetTime [min]	Type	Width [min]	Area mAU *s	Height [mAU]	Area %
10	24.835	BB	0.9062	17.00141	2.29204e-1	1.2279
11	48.814	BB	1.7484	547.63464	4.38444	39.5519
Totals :				1384.59708	26.34532	

*** End of Report ***

Figure A25: Chiral HPLC chromatogram at 50% conversion of reaction 1 in the transesterification of 1-((1H-indol-4-yl)oxy)-3-chloropropan-2-ol (**5**) using CALB (Chiralcel OD-H column and hexane:2-propanol (80:20), 1 mL/min flow).

17. Chromatogram from a chiral HPLC analysis at 50% conversion of reaction 2 in the transesterification of 1-((1H-indol-4-yl)oxy)-3-chloropropan-2-ol (**5**) using CALB

Figure A26 shows the chromatogram from the chiral HPLC analysis of reaction 2 after 98 hours.

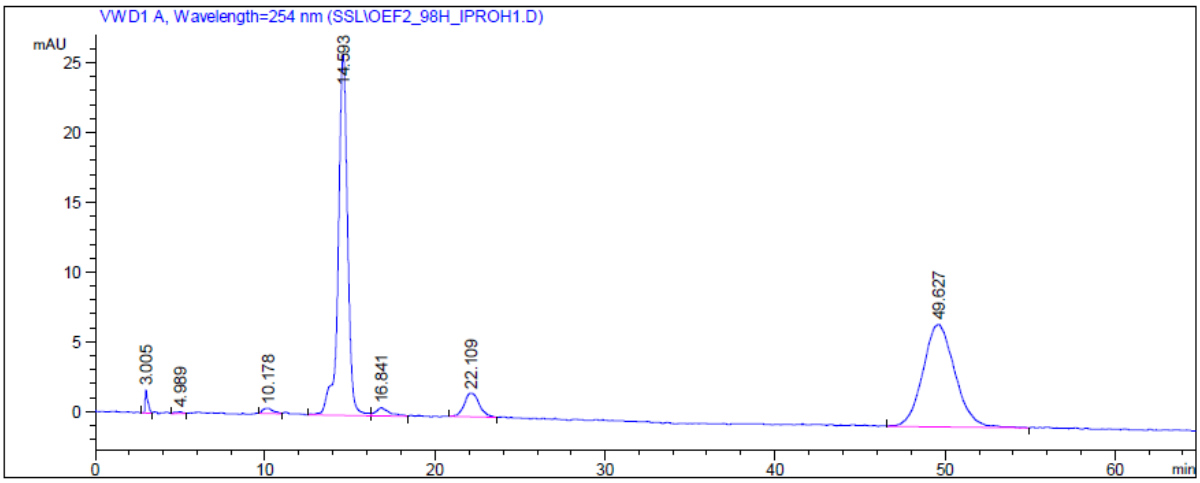


```
=====================================================================
                        Area Percent Report
=====================================================================

Sorted By             :      Signal
Multiplier:                   :      1.0000
Dilution:                     :      1.0000
Use Multiplier & Dilution Factor with ISTDs


Signal 1: VWD1 A, Wavelength=254 nm

Peak RetTime Type  Width     Area      Height     Area
  #   [min]        [min]  mAU   *s   [mAU   ]      %
----|-------|----|-------|----------|----------|--------|
   1   3.005 BV    0.1610   18.45449    1.63260   0.8651
   2   4.989 VB    0.3605    3.93866 1.43738e-1   0.1846
   3  10.178 BV    0.5442   16.91636 4.01273e-1   0.7930
   4  14.593 BV    0.5815  993.75037   25.90343  46.5864
   5  16.841 VV    0.7666   32.32598 5.74917e-1   1.5154
   6  22.109 BB    0.9450  105.28207    1.71099   4.9356
   7  49.627 BB    1.6081  962.46527    7.35560  45.1198

Totals :                  2133.13319   37.72256
```

Figure A26: Chiral HPLC chromatogram at 50% conversion of reaction 2 in the transesterification of 1-((1H-indol-4-yl)oxy)-3-chloropropan-2-ol (**5**) using CALB (Chiralcel OD-H column and hexane:2-propanol (80:20), 1 mL/min flow).

18. Chromatogram from chiral HPLC analysis at different degrees of conversion of reaction 3 in the transesterification of 1-((1H-indol-4-yl)oxy)-3-chloropropan-2-ol (**5**) using CALB

Three chromatograms were used in the calculation of ee_p, ee_s and c. The chromatograms are from samples taken after 4 hours, 26 hours and 30 hours (Figure A27, A28 and A29). The calculated ee_p, ee_s and c values are presented in Table A1.

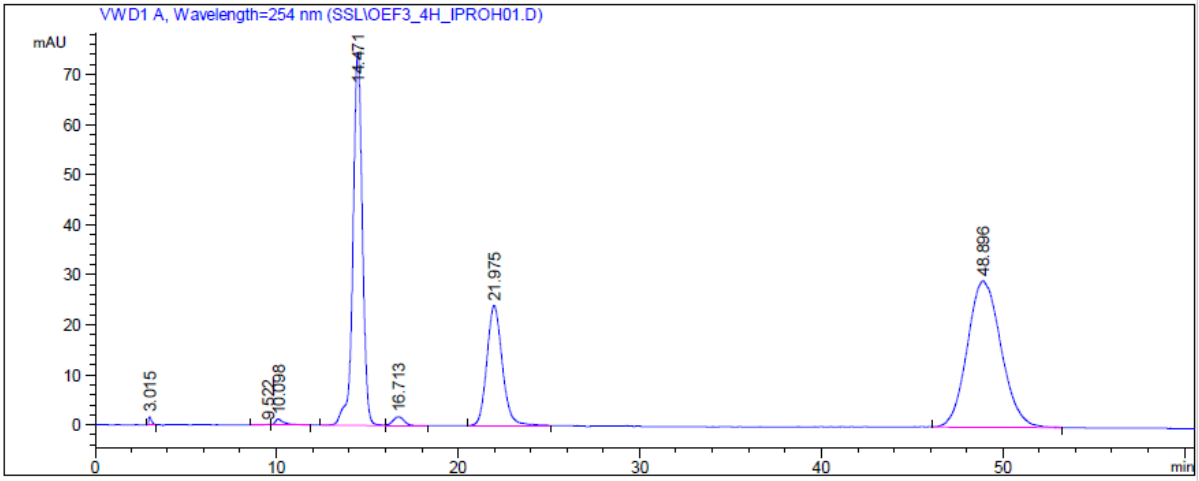


```
=====================================================================
                      Area Percent Report
=====================================================================

Sorted By             :      Signal
Multiplier:                   :      1.0000
Dilution:                     :      1.0000
Use Multiplier & Dilution Factor with ISTDs


Signal 1: VWD1 A, Wavelength=254 nm

Peak RetTime Type  Width     Area      Height     Area
  #   [min]        [min]  mAU   *s   [mAU   ]      %
----|-------|----|-------|----------|----------|--------|
   1   3.015 BV    0.1627   18.75426    1.71242   0.2333
   2   9.522 BV    0.3974    6.03875 1.97564e-1   0.0751
   3  10.098 VB    0.5521   47.88768    1.23302   0.5957
   4  14.471 VV    0.5547 2691.86304   74.64001  33.4878
   5  16.713 VB    0.6714   76.66808    1.75956   0.9538
   6  21.975 BB    0.9175 1419.50720   23.98991  17.6592
   7  48.896 BB    1.7643 3777.62305   29.33720  46.9951

Totals :                  8038.34205  132.86970
```

Figure A27: Chromatogram of samples taken after 4 hours reaction time in the acylation of **5** using CALB (Chiralcel OD-H column and hexane:2-propanol (80:20), 1 mL/min flow).

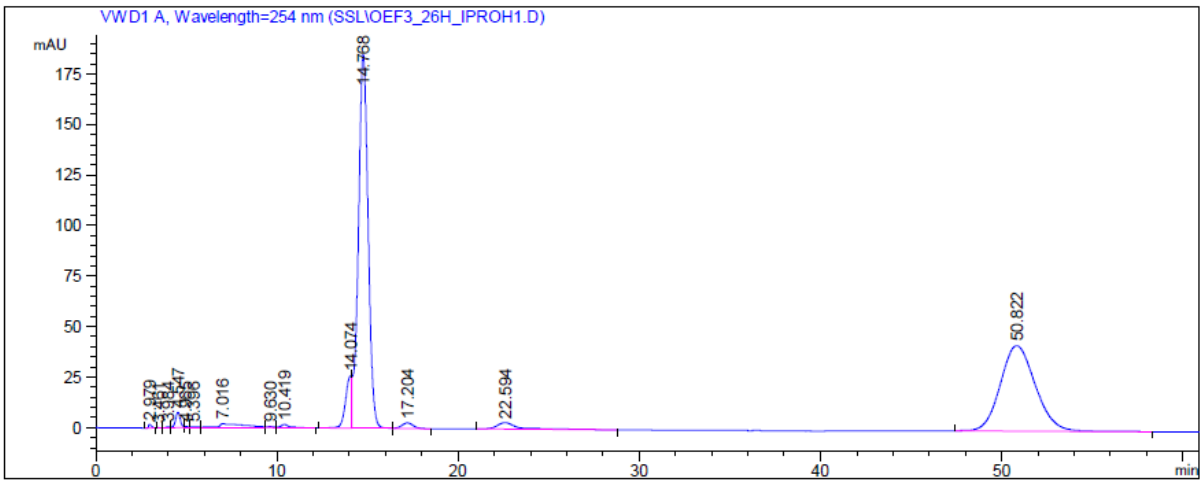


```
=====================================================================
                    Area Percent Report
=====================================================================

Sorted By             :      Signal
Multiplier:                   :      1.0000
Dilution:                     :      1.0000
Use Multiplier & Dilution Factor with ISTDs


Signal 1: VWD1 A, Wavelength=254 nm

Peak RetTime Type  Width     Area      Height     Area
  #   [min]        [min]  mAU   *s   [mAU   ]      %
----|-------|----|-------|----------|----------|--------|
   1   2.979 BB    0.1574   20.62699    1.96479   0.1473
   2   3.461 BB    0.1235    1.74127 2.22078e-1   0.0124
   3   3.984 BV    0.1996    7.09208 5.20883e-1   0.0506
   4   4.547 VV    0.2755  135.77895    7.59540   0.9693
   5   4.965 VV    0.1595    6.38497 5.71521e-1   0.0456
   6   5.396 VB    0.3373    5.62615 2.15012e-1   0.0402
   7   7.016 BV    1.2713  172.16670    1.66379   1.2291
   8   9.630 VV    0.4040   15.00724 5.33369e-1   0.1071
   9  10.419 VB    0.4856   56.03207    1.61772   0.4000

Peak RetTime Type  Width     Area      Height     Area
  #   [min]        [min]  mAU   *s   [mAU   ]      %
----|-------|----|-------|----------|----------|--------|
  10  14.074 BV    0.3596  599.22937   25.67692   4.2780
  11  14.768 VV    0.5773 6937.71387  184.98531  49.5294
  12  17.204 VB    0.6915  127.34466    2.81169   0.9091
  13  22.594 BB    1.2282  280.08994    3.20812   1.9996
  14  50.822 BB    2.0621 5642.43164   42.16298  40.2822

Totals :                  1.40073e4   273.74958
```

Figure A28: Chromatogram of samples taken after 26 hours reaction time in the acylation of **5** using CALB (Chiralcel OD-H column and hexane:2-propanol (80:20), 1 mL/min flow).

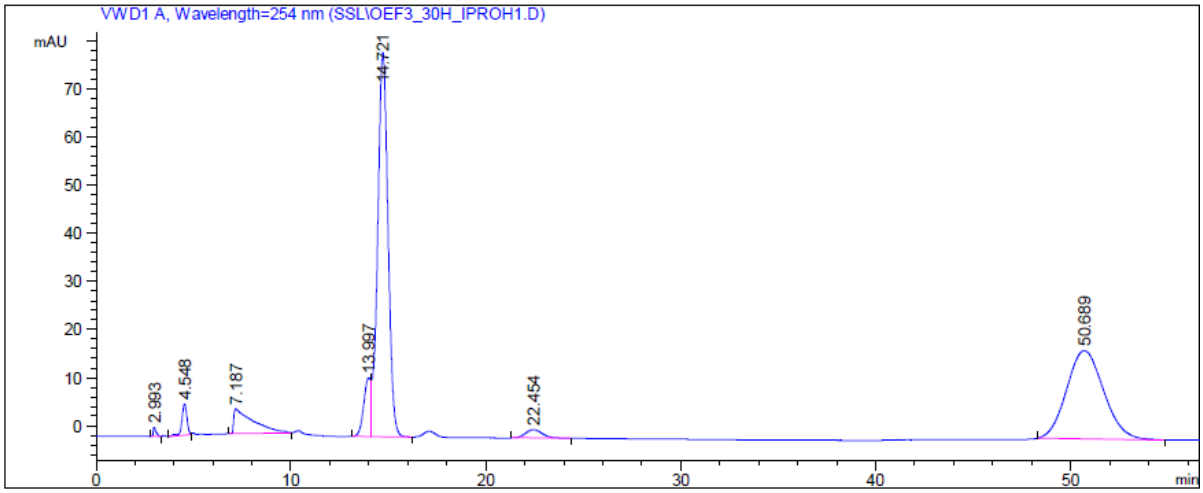


```
=====================================================================
                        Area Percent Report
=====================================================================

Sorted By             :      Signal
Multiplier:                   :      1.0000
Dilution:                     :      1.0000
Use Multiplier & Dilution Factor with ISTDs


Signal 1: VWD1 A, Wavelength=254 nm

Peak RetTime Type  Width     Area      Height     Area
  #   [min]        [min]  mAU   *s    [mAU   ]      %
----|-------|----|-------|----------|----------|--------|
   1   2.993 BB    0.1452   18.72581    1.88228   0.2992
   2   4.548 BV    0.2727  116.27277    6.54800   1.8577
   3   7.187 BB    0.8774  357.88852    5.10647   5.7182
   4  13.997 BV    0.3784  303.46234   12.22766   4.8486
   5  14.721 VB    0.5668 2939.89966   79.77852  46.9722
   6  22.454 BB    0.7080  101.39256    1.71305   1.6200
   7  50.689 BB    1.6539 2421.16162   18.32114  38.6841

Totals :                  6258.80327  125.57713
```

Figure A29: Chromatogram of samples taken after 30 hours reaction time in the acylation of **5** using CALB (Chiralcel OD-H column and hexane:2-propanol (80:20), 1 mL/min flow).

Table A1: Calculated ee_p, ee_s and c values for reaction 3 in the acylation of **5** using CALB. Chromatograms used in the calculations can be seen in Figure A27-29.

Prøvenr.	Timer	%R	%S	%P	%Q	c	ees	eep
1	4	47,1291	17,5757	32,3528	1,1033	0,328	45,674	93,404
3	26	40,2822	1,9996	49,5294	4,278	0,518	90,542	84,099
4	30	38,6841	1,62	46,9722	4,8486	0,531	91,961	81,287

19. Chromatogram from chiral HPLC analysis at 48 hours reaction time in the hydrolysis of **6**

In Figure A30 the chromatogram at 47% conversion in the hydrolysis of **6** is shown.

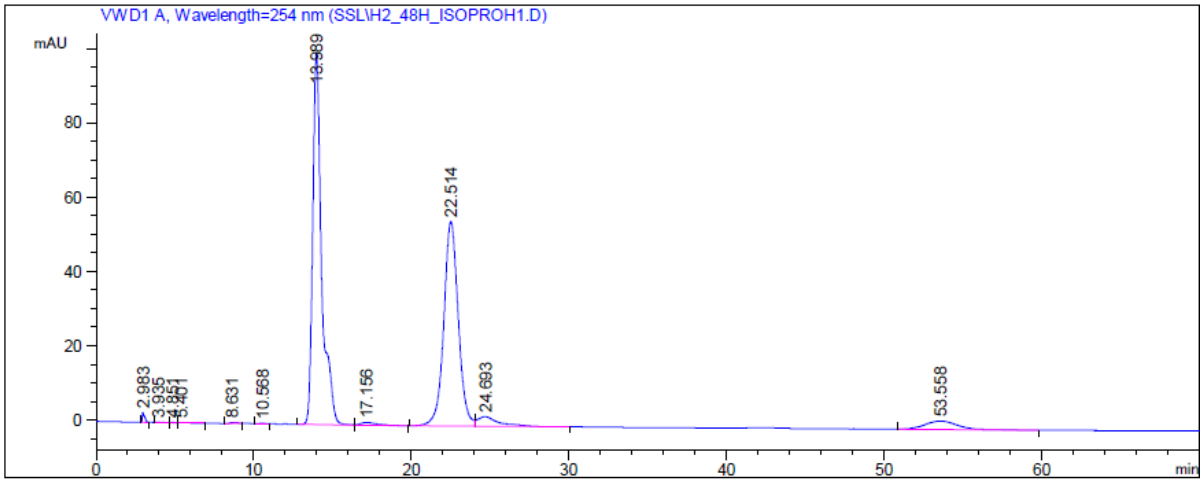


```
=====================================================================
                        Area Percent Report
=====================================================================

Sorted By             :      Signal
Multiplier:                   :      1.0000
Dilution:                     :      1.0000
Use Multiplier & Dilution Factor with ISTDs


Signal 1: VWD1 A, Wavelength=254 nm

Peak RetTime Type  Width     Area      Height     Area
  #   [min]        [min]  mAU   *s   [mAU   ]      %
----|-------|----|-------|----------|----------|--------|
   1   2.983 BV    0.1526   30.21248    2.72592   0.3719
   2   3.935 BV    0.4117    5.68256 1.78718e-1   0.0700
   3   4.851 VV    0.3391    3.55930 1.33943e-1   0.0438
   4   5.401 VB    0.5528    5.84567 1.27407e-1   0.0720
   5   8.631 BB    0.4600    6.72787 2.01183e-1   0.0828
   6  10.568 BB    0.3464    4.24282 1.91077e-1   0.0522
   7  13.989 BV    0.5818 3941.10205  100.05737  48.5140
   8  17.156 VB    0.8814   49.62782 7.13454e-1   0.6109
   9  22.514 BV    0.9694 3501.99780   55.04354  43.1088

Peak RetTime Type  Width     Area      Height     Area
  #   [min]        [min]  mAU   *s   [mAU   ]      %
----|-------|----|-------|----------|----------|--------|
  10  24.693 VB    1.3534  249.21632    2.56820   3.0678
  11  53.558 BB    1.8435  325.41669    2.28300   4.0058

Totals :                  8123.63139  164.22382
```

Figure A30: Chromatogram at 47% conversion in the hydrolysis of **6** is shown (Chiralcel OD-H column and hexane:2-propanol (80:20), 1 mL/min flow).

20. RF-HPLC chromatogram of **9**

In Figure A31 the RF-HPLC chromatogram of **9** can be seen.

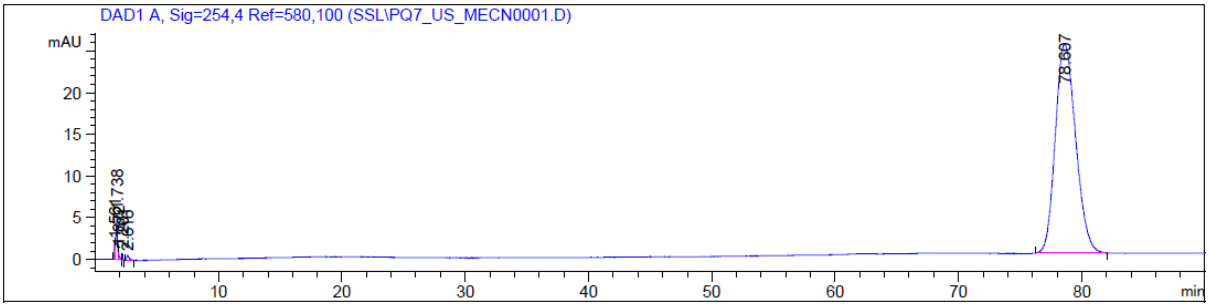

Peak #	RetTime [min]	Type	Width [min]	Area [mAU*s]	Height [mAU]	Area %
1	1.561	BV	0.0529	6.67903	1.95146	0.2268
2	1.738	VV	0.0973	40.04592	5.35150	1.3598
3	1.872	VB	0.0862	6.76058	1.09233	0.2296
4	2.201	BB	0.0680	3.60141	8.23404e-1	0.1223
5	2.616	BB	0.1955	10.27064	6.67534e-1	0.3487
6	78.607	BB	1.3532	2877.72144	25.06981	97.7129
Totals :				2945.07901	34.95603	

Figure A31: RF-HPLC chromatogram of **9 (**Eclipse XDB - C18 column, 100% MeCN, flow 1mL/min.).

21. RF-HPLC chromatogram of reactions 1-3 in the hydrolysis of **9**

In Figures A32, A33 and A34 the RF-HPLC chromatograms of reactions 1, 2 and 3 respectively can be seen.

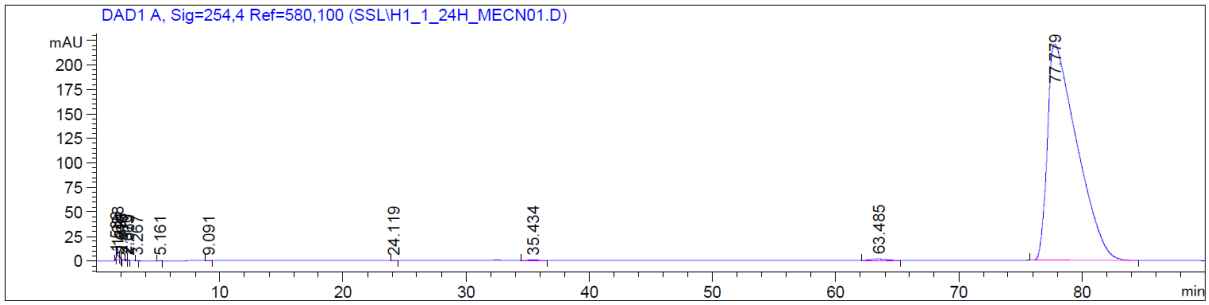

Peak #	RetTime [min]	Type	Width [min]	Area [mAU*s]	Height [mAU]	Area %
1	1.586	BV	0.0554	12.54076	3.29870	0.0341
2	1.688	VV	0.1154	69.05576	8.44449	0.1876
3	1.891	VB	0.0625	10.60717	2.50093	0.0288
4	2.015	BB	0.0471	1.57628	5.39285e-1	4.283e-3
5	2.376	BV	0.0672	3.86589	8.64177e-1	0.0105
6	2.563	VB	0.1274	4.27179	4.55351e-1	0.0116
7	3.267	BB	0.0885	3.23193	5.50735e-1	8.782e-3
8	5.161	BB	0.1352	3.09753	3.27942e-1	8.417e-3
9	9.091	BB	0.1698	2.53619	1.79529e-1	6.892e-3
10	24.119	BB	0.1822	2.01595	1.33454e-1	5.478e-3
11	35.434	BB	0.6469	33.73986	6.12300e-1	0.0917
12	63.485	BB	0.9827	105.69494	1.25994	0.2872
13	77.779	BB	2.1549	3.65482e4	220.02904	99.3146
Totals :				3.68005e4	239.19588	

Figure A32: RF-HPLC chromatogram of reaction 1 **(**Eclipse XDB - C18 column, 100% MeCN, flow 1mL/min).

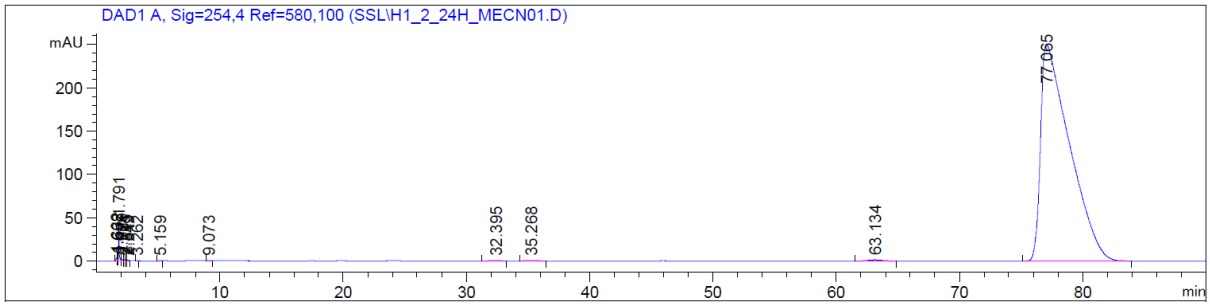

Peak #	RetTime [min]	Type	Width [min]	Area [mAU*s]	Height [mAU]	Area %
1	1.632	BV	0.0855	19.42873	3.00420	0.0472
2	1.698	VV	0.0441	7.08072	2.35112	0.0172
3	1.791	VV	0.0518	156.71562	44.78801	0.3809
4	2.020	VB	0.0690	5.50884	1.12844	0.0134
5	2.201	BB	0.0594	2.16030	5.67605e-1	5.250e-3
6	2.375	BV	0.0628	3.48176	8.68585e-1	8.462e-3
7	2.549	VB	0.1326	4.01874	4.35837e-1	9.767e-3
8	3.262	BB	0.0842	3.12062	5.94931e-1	7.584e-3
9	5.159	BB	0.1239	3.53683	3.97172e-1	8.596e-3
10	9.073	BB	0.1647	2.47478	1.79712e-1	6.015e-3
11	32.395	BB	0.6402	31.02929	5.70796e-1	0.0754
12	35.268	BB	0.6548	36.30016	6.51762e-1	0.0882
13	63.134	BB	0.9690	124.68269	1.51050	0.3030
14	77.065	BB	2.1121	4.07466e4	249.92014	99.0290
Totals :				4.11461e4	306.96881	

Figure A33: RF-HPLC chromatogram of reaction 2 **(**Eclipse XDB - C18 column, 100% MeCN, flow 1mL/min).

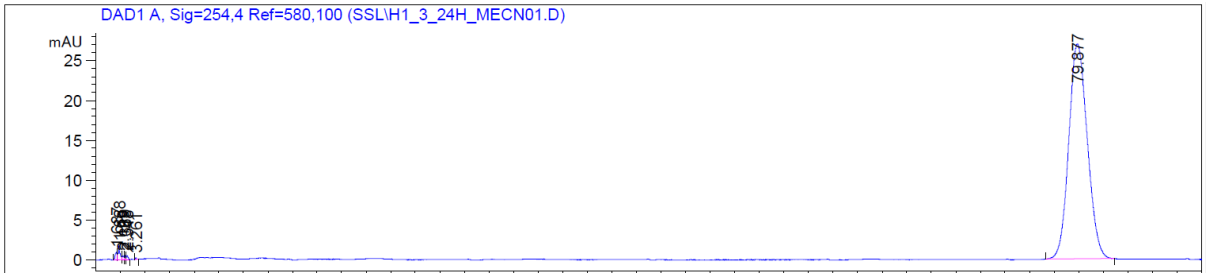

Peak #	RetTime [min]	Type	Width [min]	Area [mAU*s]	Height [mAU]	Area %
1	1.687	BV	0.1345	10.05297	9.57556e-1	0.3499
2	1.888	VV	0.1332	17.98175	1.74516	0.6259
3	2.199	VV	0.1095	4.15788	5.02509e-1	0.1447
4	2.369	VV	0.0777	3.06451	5.52451e-1	0.1067
5	2.548	VB	0.1346	4.68608	4.90076e-1	0.1631
6	3.261	BB	0.0925	1.27711	2.08391e-1	0.0445
7	79.877	BB	1.2321	2831.57520	26.94229	98.5652
Totals :				2872.79549	31.39844	

Figure A34: RF-HPLC chromatogram of reaction 3 **(**Eclipse XDB - C18 column, 100% MeCN, flow 1mL/min).

22. RF-HPLC chromatogram of reactions 4-6 in the hydrolysis of **9**

In Figures A35, A36 and A37, the RF-HPLC chromatograms of reactions 4, 5 and 6 respectively can be seen.

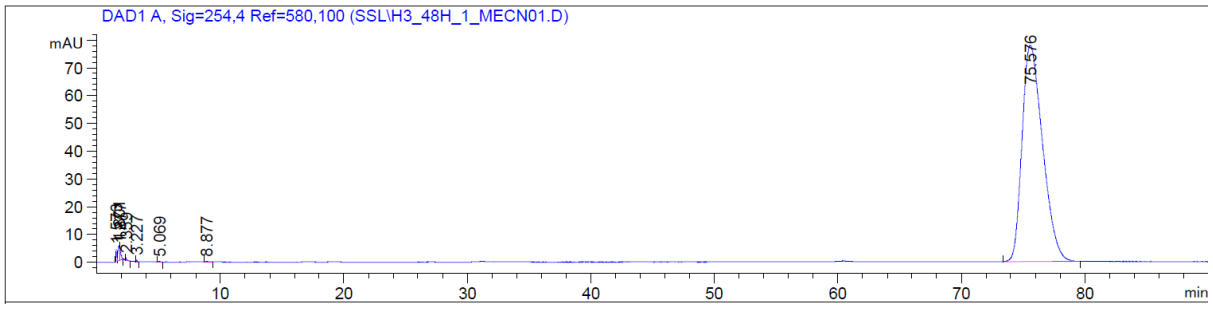

Peak #	RetTime [min]	Type	Width [min]	Area [mAU*s]	Height [mAU]	Area %
1	1.573	BV	0.0609	18.87289	4.59585	0.2074
2	1.801	VV	0.1390	51.64273	5.42631	0.5675
3	1.877	VB	0.0900	29.31174	4.44297	0.3221
4	2.359	BB	0.0826	4.67144	8.06708e-1	0.0513
5	3.227	BB	0.0880	2.88570	5.09734e-1	0.0317
6	5.069	BB	0.1304	2.76200	3.00044e-1	0.0303
7	8.877	BB	0.1936	2.46589	1.57540e-1	0.0271
8	75.576	BB	1.4137	8987.93848	77.86452	98.7626
Totals :				9100.55087	94.10368	

Figure A35: RF-HPLC chromatogram of reaction 4 **(**Eclipse XDB - C18 column, 100% MeCN, flow 1mL/min).

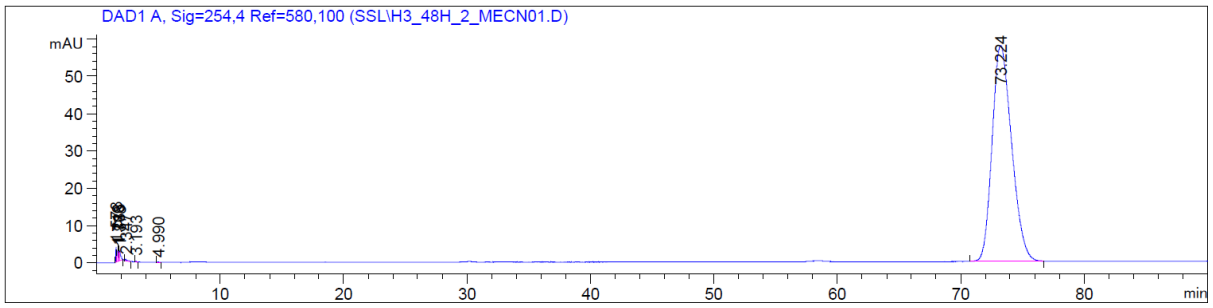

Peak #	RetTime [min]	Type	Width [min]	Area [mAU*s]	Height [mAU]	Area %
1	1.573	BV	0.0606	17.15837	4.11477	0.2670
2	1.716	VV	0.0835	17.20944	3.06696	0.2677
3	1.788	VV	0.0770	16.28167	3.06129	0.2533
4	1.878	VB	0.0957	18.90133	2.69774	0.2941
5	2.347	BB	0.1116	4.00916	4.84270e-1	0.0624
6	3.193	BB	0.0878	1.49011	2.60130e-1	0.0232
7	4.990	BB	0.1125	1.52318	1.66805e-1	0.0237
8	73.224	BB	1.4081	6350.88037	57.83767	98.8087
Totals :				6427.45363	71.68964	

Figure A36: RF-HPLC chromatogram of reaction 5 **(**Eclipse XDB - C18 column, 100% MeCN, flow 1mL/min).

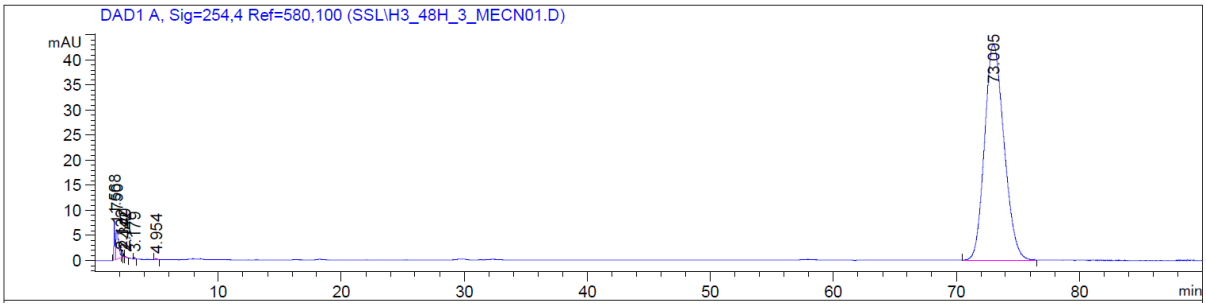

Peak #	RetTime [min]	Type	Width [min]	Area [mAU*s]	Height [mAU]	Area %
1	1.568	BV	0.0748	43.30465	8.05063	0.8893
2	1.750	VV	0.2087	86.08399	5.91683	1.7677
3	2.132	VB	0.0815	2.87844	5.08494e-1	0.0591
4	2.340	BV	0.0644	2.61238	6.29688e-1	0.0536
5	2.442	VB	0.1000	1.30166	1.76596e-1	0.0267
6	3.179	BB	0.0923	1.97898	3.48233e-1	0.0406
7	4.954	BB	0.1216	2.02486	2.19491e-1	0.0416
8	73.005	BB	1.3530	4729.52637	43.00559	97.1213
Totals :				4869.71131	58.85555	

Figure A37: RF-HPLC chromatogram of reaction 6 **(**Eclipse XDB - C18 column, 100% MeCN, flow 1mL/min**)**.

23. RF-HPLC chromatogram of reactions 7-9 in the hydrolysis of **9**

In Figures A38, A39 and A40 the RF-HPLC chromatograms of reactions 7 - 9 can be seen.

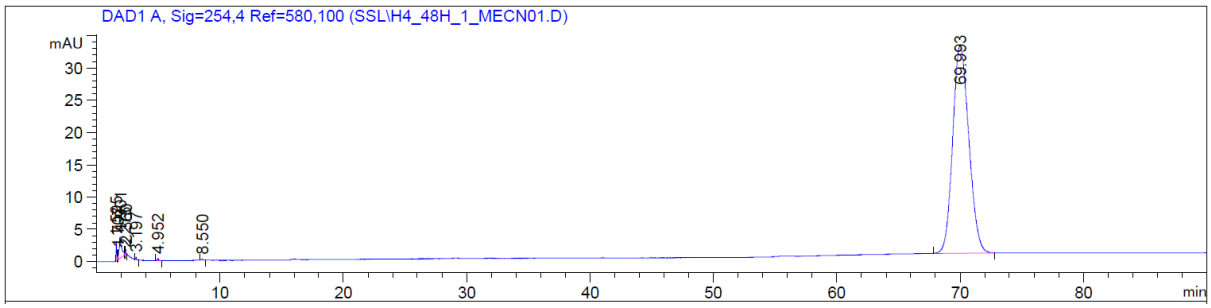

Peak #	RetTime [min]	Type	Width [min]	Area [mAU*s]	Height [mAU]	Area %
1	1.595	BV	0.0549	10.98648	2.98472	0.3667
2	1.707	VV	0.0537	4.23402	1.12943	0.1413
3	1.901	VV	0.1581	42.34180	3.42693	1.4131
4	2.275	VV	0.0607	2.27776	4.95092e-1	0.0760
5	2.360	VB	0.0625	3.66575	8.81333e-1	0.1223
6	3.197	BB	0.0799	2.15329	4.12811e-1	0.0719
7	4.952	BB	0.1094	2.40525	2.76866e-1	0.0803
8	8.550	BB	0.1526	1.93230	1.55872e-1	0.0645
9	69.993	BB	1.0649	2926.36572	32.21078	97.6639
Totals :				2996.36239	41.97384	

Figure A38: RF-HPLC chromatogram of reaction 7 **(**Eclipse XDB - C18 column, 100% MeCN, flow 1mL/min**)**.

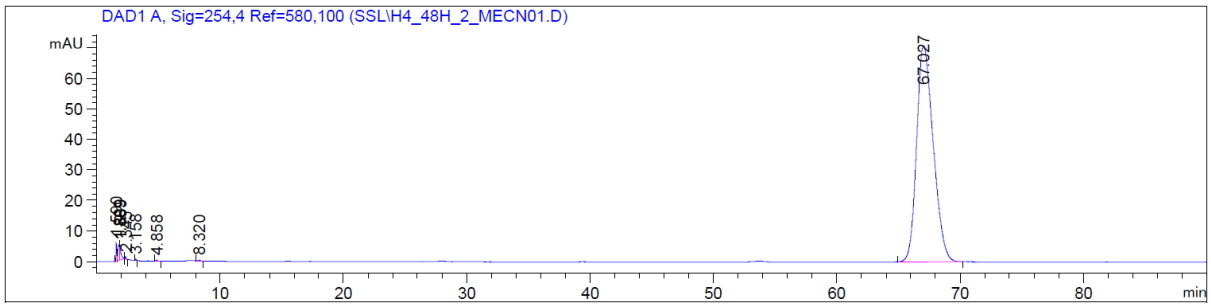

Peak #	RetTime [min]	Type	Width [min]	Area [mAU*s]	Height [mAU]	Area %
1	1.590	BV	0.0571	25.45739	6.30475	0.3772
2	1.809	VV	0.1346	42.29357	5.05624	0.6267
3	1.889	VB	0.1018	38.74585	5.03154	0.5741
4	2.345	BB	0.0561	3.33236	9.02095e-1	0.0494
5	3.158	BB	0.0767	3.06917	6.20654e-1	0.0455
6	4.858	BB	0.1201	3.05066	3.78377e-1	0.0452
7	8.320	BB	0.1635	2.84928	2.13802e-1	0.0422
8	67.027	BB	1.0949	6629.75342	70.96799	98.2396
Totals :				6748.55169	89.47546	

Figure A39: RF-HPLC chromatogram of reaction 8 **(**Eclipse XDB - C18 column, 100% MeCN, flow 1mL/min**)**.

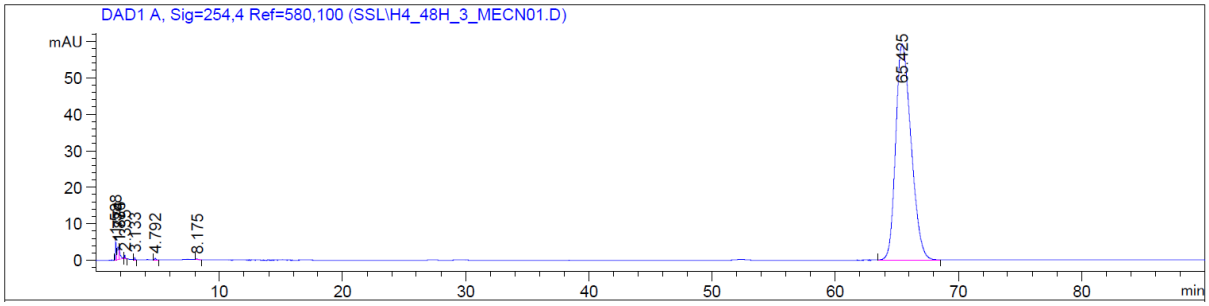

Peak #	RetTime [min]	Type	Width [min]	Area [mAU*s]	Height [mAU]	Area %
1	1.588	BV	0.0575	22.46458	5.52048	0.4301
2	1.774	VV	0.1281	28.40325	3.44746	0.5438
3	1.886	VB	0.0962	23.53728	3.25972	0.4507
4	2.335	BB	0.0566	3.33718	9.13555e-1	0.0639
5	3.133	BB	0.0758	3.11126	6.06511e-1	0.0596
6	4.792	BB	0.1106	3.06630	3.82230e-1	0.0587
7	8.175	BB	0.1510	2.54059	2.05840e-1	0.0486
8	65.425	BB	1.0175	5136.19092	59.18140	98.3445
Totals :				5222.65137	73.51719	

Figure A38: RF-HPLC chromatogram of reaction 9 **(**Eclipse XDB - C18 column, 100% MeCN, flow 1mL/min**)**.

24. MS analysis of crystals produced in the hydrolysis of **9**

In Figure A39 the MS spectrum of the crystals produced in reaction 9, 10 and 11 in the hydrolysis of **9**.

Elemental Composition Report **Page 1**

Single Mass Analysis
Tolerance = 5.0 PPM / DBE: min = -2.0, max = 50.0
Element prediction: Off
Number of isotope peaks used for i-FIT = 2

Monoisotopic Mass, Odd and Even Electron Ions
428 formula(e) evaluated with 4 results within limits (all results (up to 1000) for each mass)
Elements Used:
C: 0-100 H: 0-500 O: 0-20 P: 0-2
2018-464 125 (2.447) AM2 (Ar,35000.0,0.00,0.00); Cm (119:128)
1: TOF MS ASAP+

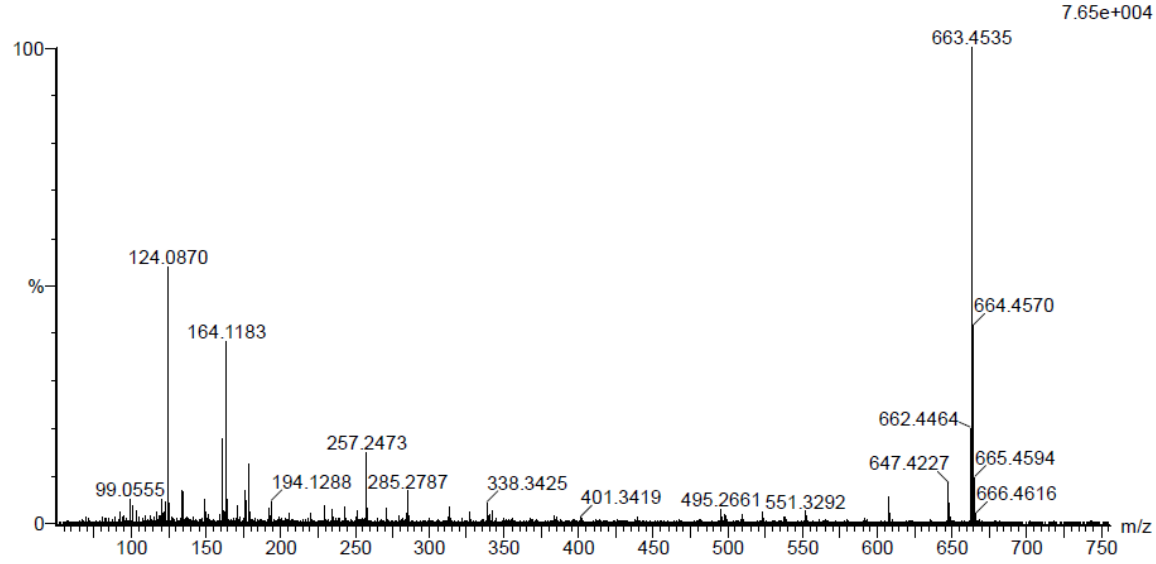

Mass	Calc. Mass	mDa	PPM	DBE	i-FIT	Norm	Conf(%)	Formula
Minimum:				-2.0				
Maximum:		5.0	5.0	50.0				
663.4535	663.4531	0.4	0.6	-1.5	358.3	2.504	8.18	C31 H67 O14
	663.4542	-0.7	-1.1	11.5	357.4	1.601	20.17	C42 H64 O4 P
	663.4519	1.6	2.4	2.5	356.1	0.336	71.48	C35 H69 O7 P2
	663.4566	-3.1	-4.7	20.5	362.1	6.380	0.17	C49 H59 O

Figure A39: MS spectrum of the crystals produced in reaction 9, 10 and 11 in the hydrolysis of **9.** Ions observed could be [M+H] or [M•].

25. MS analysis of **9**

In Figure 39 the MS spectrum of **9** can be seen.

Elemental Composition Report **Page 1**

Single Mass Analysis
Tolerance = 3.0 PPM / DBE: min = -2.0, max = 50.0
Element prediction: Off
Number of isotope peaks used for i-FIT = 2

Monoisotopic Mass, Even Electron Ions
1805 formula(e) evaluated with 4 results within limits (all results (up to 1000) for each mass)
Elements Used:
C: 0-100 H: 0-500 N: 0-10 O: 0-20
2018-472 229 (4.463) AM2 (Ar,35000.0,0.00,0.00); Cm (225:229)
1: TOF MS ASAP+

2.57e+006

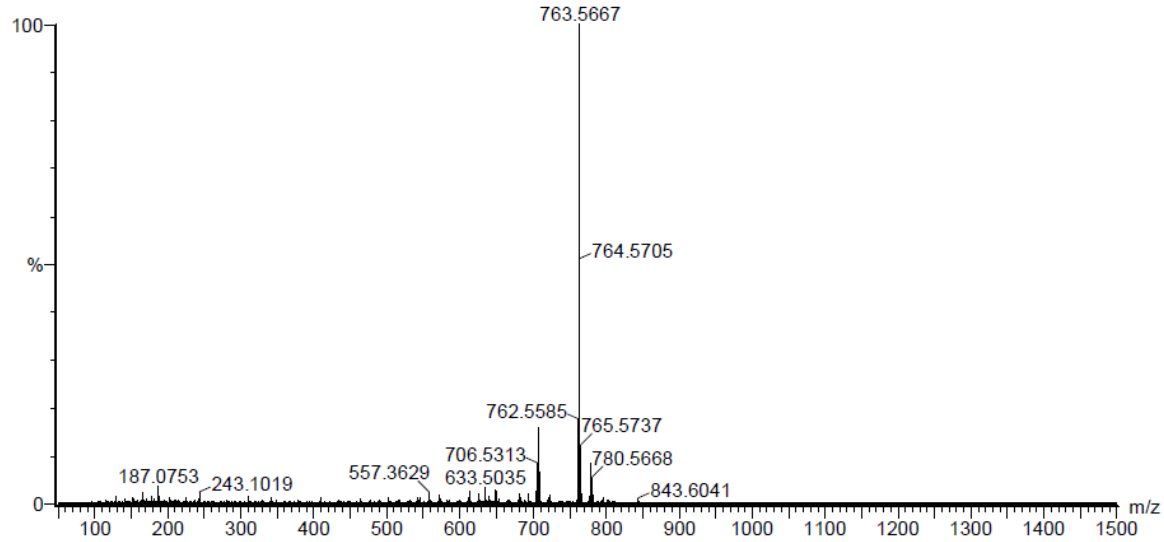

Minimum:				-2.0				
Maximum:		5.0	3.0	50.0				
Mass	Calc. Mass	mDa	PPM	DBE	i-FIT	Norm	Conf(%)	Formula
763.5667	763.5665	0.2	0.3	15.5	464.9	0.637	52.87	C52 H75 O4
	763.5657	1.0	1.3	3.5	466.9	2.623	7.26	C36 H75 N8 O9
	763.5679	-1.2	-1.6	20.5	466.2	1.992	13.64	C53 H71 N4
	763.5684	-1.7	-2.2	2.5	465.6	1.338	26.23	C40 H79 N2 O11

Figure A39: MS spectrum of **9.** Ions observed are [M+H].